NUMERICAL SIMULATION OF TWO PHASE FLOW USING THE HOMOGENEOUS FLOW MODEL

by

Murat DAL

B.S. in M.E., Boğaziçi University, 1995

Submitted to the Institute for Graduate Studies in Science and Engineering in partial fulfilment of the requirements for the degree of

Master of Science

in

Mechanical Engineering

Boğaziçi University

1999

ACKNOWLEDGEMENTS

I would like to express my gratitude to Assistant Prof. Dr. Ali ECDER, Mechanical Engineering Department, Boğaziçi University, who kindly accepted to supervise this thesis.

I would like to thank to Prof. Dr. Akın TEZEL and Prof. Dr. Vural ALTIN for their comments.

I would like to express my appreciation to Arçelik R&D Center, Heat Transfer and Fluid Dynamics Group, especially Engin DİRİK, research specialist, for their invaluable help and contributions in this work.

I would like to thank to my family and my friends for their support and encouragement during this work.

ABSTRACT

The objective of this study is to understand physical and numerical modelling aspects of two phase flow occurring in heat exchangers used in domestic refrigerators, and to construct a computer model to simulate one dimensional two phase flow using the homogeneous flow model.

This study is mainly composed in two parts. First part focuses on the two phase flow characteristics of refrigerants in tube: Flow regimes, pressure drop, void fraction and heat transfer correlations are investigated. Empirical correlations are evaluated and compared for a typical evaporator condition.

Second part, introduces governing equations for 1-D two phase flow and describes the development of a finite difference type numerical scheme for a simulation of the transient behaviour of two phase flow in heat exchangers. A second order accurate numerical method, namely MacCormack, is applied for solving the equations.

Simulation results are compared with the literature and similar flow characteristics are found. Although the presented model is second order accurate and easy to apply, it is too slow for use in an overall refrigeration system simulation. Also, it requires small CFL number and fine grid for some applications which means more execution time.

Homogeneous flow model was the simplest model. An improved model, at least including slip effects should be preferred. For a complete system simulation, a simplified system of equation should be taken with an advanced implicit method.

ÖZET

Bu yüksek lisans tez çalışmasının amacı ev tipi buzdolaplarında kullanılan ısı değiştiricilerinde oluşan iki fazlı akışın fiziksel ve sayısal modelleme yönlerini anlamak ve iki fazlı akış denklemlerini homojen akış modeli kullanarak bir boyutta çözen bir bilgisayar modeli geliştirmektir.

Bu çalışma iki ana bölümden oluşmaktadır. Birinci bölüm boru içinde soğutkanın iki fazlı akışının özelliklerine odaklanmıştır. Akış tipleri, basınç kaybı, boşluk oranı ve ısı geçişi korelasyonları incelenmiştir. Deneysel korelasyonlar tipik bir soğutma sistemindeki buharlaştırıcı şartları için hesaplanmış ve karşılaştırılmıştır.

İkinci bölümde ise bir boyutlu iki fazlı akış denklemleri tanıtılmış ve ısı değiştiricilerindeki iki fazlı akışı zamana bağlı olarak simüle eden bir sonlu farklar yöntemi anlatılmıştır. İkinci dereceden doğru bir sayısal yöntem olan MacCormak metodu denklemlerin çözümünde kullanılmıştır.

Sayısal çalışmaların sonuçları literatürdeki bir çalışma ile karşılaştırılmış ve benzer akış karakteristikleri bulunmuştur. Bu sayısal metod ikinci dereceden doğru ve uygulaması kolay olmasına rağmen, komple bir soğutma sistemi simülasyonu için oldukça yavaştır. Ayrıca bazı uygulamalarda küçük CFL sayısı ve sık ağ yapısı gerektirdiğinden simülasyon süresi daha da artmaktadır.

Homojen akış modeli yerine daha gelişmiş, en azından kayma etkisini içeren bir model tercih edilmelidir. Komple bir soğutma çevrimi modellenmesi durumunda basitleştirilmiş denklem sistemi, ileri bir kapalı sayısal metodla çözülmelidir.

LIST OF FIGURES

LIST OF TABLES

LIST OF SYMBOLS

a	Speed of Sound
av, w	Numerical Artificial Viscosity Constant, dimensionless
A_c	Total Inside Cross Sectional Area of Tube, m^2
A_g	Cross Sectional Area Occupied by Vapour, m^2
A_f	Cross Sectional Area Occupied by Liquid, m^2
c_p	Specific Heat at Constant Pressure, J/kg·K
c_v	Specific Heat at Constant Volume, J/kg·K
d, D	Tube Diameter, m
e	Internal energy, kJ/kg
f	Function of
f	Overall Friction Factor for the Heat Exchanger, dimensionless
F	Two Phase Convective Multiplier, dimensionless
G	Mass Flow rate per Area, $kg/m^2 \cdot s$
h	Convection Coefficient, $W/m^2 \cdot K$
h	Enthalpy, kJ/kg
k	Thermal Conductivity, $W/m^2 \cdot K$
L	Total Length of Heat Exchanger Tubes, m
m	Mass Flow rate, kg/s
M	Molecular Weight, kg

P_r	Reduced Pressure, dimensionless, $\frac{P_{sat}}{P_{crit}}$
q"	Heat Transfer Rate, W
S	suppression factor, dimensionless
S	Slip Ratio, dimensionless
T	Temperature, K
Xtt, X	The Lockhart Martinelli Parameter, dimensionless
x	Mass Quality, dimensionless

Greek Symbols

α	Void Fraction
β	Two Phase Flow Factor, dimensionless
θ	Liquid/Vapour Gradient Ratio, dimensionless
μ	Dynamic Viscosity Coefficient, kg/ms
v	specific volume, m^3/kg
ρ	Density, kg/m^3
σ	Surface Tension of Refrigerant
τ	Shear (viscous) Stress, N/m^2
ϕ	Two phase flow frictional multiplier, dimensionless

Dimensionless Groups

Bo	Boiling Number, dimensionless, $Bo = \frac{q''}{G * h_{fg}}$,
Co	Convection Number, dimensionless, $Co = \left(\frac{1-x}{x}\right)^{0.8}\left(\frac{\rho_g}{\rho_f}\right)^{0.5}$
Fr	Froude Number, dimensionless $\frac{G^2}{\rho^2 g D}$
Nu	Nusselt Number, dimensionless, $Nu = \frac{hd}{k}$
Pr	Prandtl Number, dimensionless, $\Pr = \frac{c_p \mu}{k}$
Re	Reynolds Number, dimensionless, $\frac{Gd_i}{\mu}$
We	Weber Number, dimensionless, $\frac{G^2 d_i}{\sigma \rho_l g_c}$

Subscripts

a	Refers to Air Side
b	Refers to Bend
cb	Refers to Convective Boiling
hx	Refers to Heat Exchanger
i	Refers to Inside Surface
l	Refers to Liquid
mix	Refers to mixture
nb	Refers to Nucleate Boiling
o	Refers to Outside Surface
pool	Refers to Pool Boiling
r	Refers to Refrigerant
sat	Refers to Saturation
v, g	Refers to Vapour, Gas

TABLE OF CONTENTS

1. INTRODUCTION

Two phase flow occurs in many industrial applications. One such industry is air conditioning, heating and refrigerating industry. In refrigerating industry two phase flow exists in condenser, evaporator and capillary tube. The aim of this study is to give a literature review and to model numerically two phase flow heat transfer in evaporator and condenser.

The technological importance of two phase gas-liquid flow is immense when one considers the amount of the capital invested in equipment in which such flow is occurring. At current energy prices, unit selection has to be based on the real life cost analysis. In order to arrive to a better understanding of the refrigerator operation and higher efficiency rates under transient conditions experimental and theoretical work should be done.

1.1. What is Two Phase Flow

A phase is one of the states of matter, it can be either a gas, a liquid or a solid. Multiphase flow is the simultaneous flow of several phases. Two phase flow is the simplest case of multiphase flow.

The term two component is used to describe flows in which the phases do not consist of the same chemical substance. For example, steam water flows are two phase, while air water flows are two component. In some literature [1], some two component flows (mostly immiscible liquid-liquid) consist of a single phase but are often called two phase.

Gas-liquid type of two phase flow is important for heat transfer type of application, e.g. boiling and condensation. Liquid-liquid and gas-solid type of two phase flow is important for combustion type of application, e.g. fluidised beds, exhaust. Liquid-solid type of two phase flow is important for environmentalist, e.g. coal-water slurries, suspensions in rivers

1.2. Two Phase Flow Regimes and Flow Patterns

In gas-liquid flow systems where the interface between the phases can have very complex forms, it is very difficult to achieve a completely satisfactory theoretical model. However, considerable progress can be made in modelling such flow if some constraints are introduced in describing the flow configuration and hence the geometric form of the interface. It is useful in many applications to introduce the concept of *flow patterns* or *flow regimes*. Yılmaz [2] regarded this as a convenient classification of the various types of interface distribution in practice.

The particular flow pattern depends on the condition of pressure, flow, heat flux and channel geometry. In the design of a heat exchanger it is desirable to know what the flow pattern or successive flow pattern is, so that a hydrodynamic or heat transfer theory appropriate to that pattern can be chosen. The gas and liquid phases may assume different geometrical configurations when flowing simultaneously. One phase may be dispersed while the other is continuous, or both phases may be stratified. Such flow configurations are usually termed two phase flow pattern or flow regimes. A change of flow pattern means a change in the mode of transport of momentum or heat.

In a transparent channel one can apparently see what is going on. When the flow is rapid, it is an easy matter to take high speed films and this extends the range of visual observation and interpretation. There is considerable disparity in the description of visual observations given by different authors. Some of the names that have been given to regimes in gas-liquid co-current flow based of visual observations are: *bubbly, gas dispersed, gas piston, liquid slug, annular, liquid dispersed, froth slugging, mixed frothy, wall film, mist, aerated, piston, churn, wave entrainment, drop entrainment, semi annular, stratified, wavy,* and there are many more.

In this study the classification is made in terms of the most commonly accepted terms and descriptions. It is necessary to define the flow regimes independently for vertical and horizontal flow. The flow patterns in vertical and horizontal tubes are given in Figure 1.1

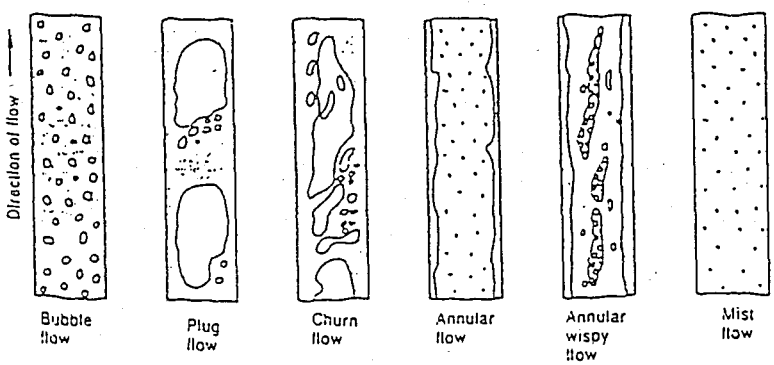

a.) Flow patterns for upward flow in vertical tubes

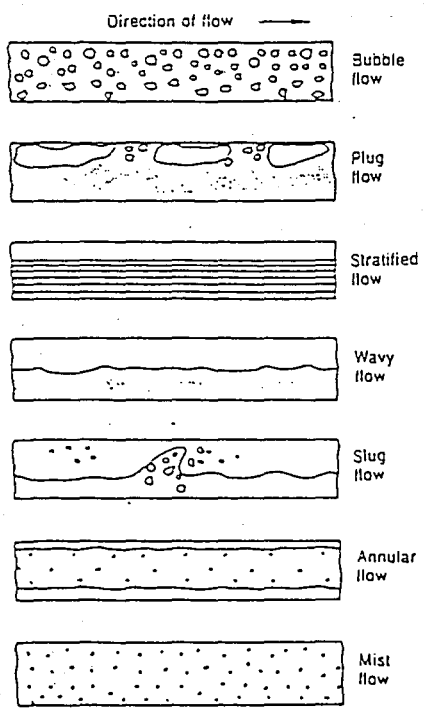

b.) Flow patterns in horizontal tubes

FIGURE 1.1. Flow patterns in two phase flow [3]

In condensers and evaporators several flow patterns may not occur simultaneously in a given tube as is shown in Figure 1.2

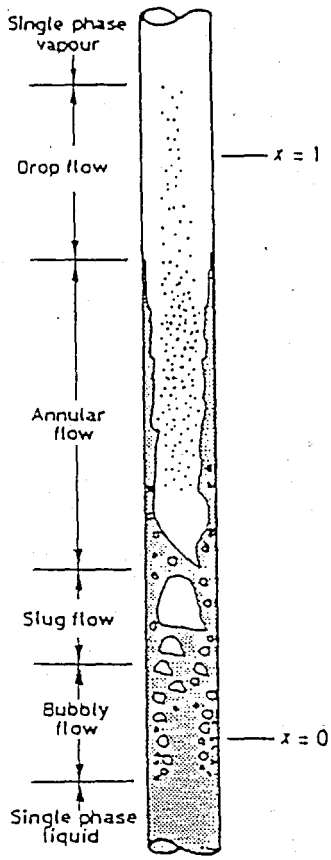

a.) Flow patterns for upward flow in vertical tubes

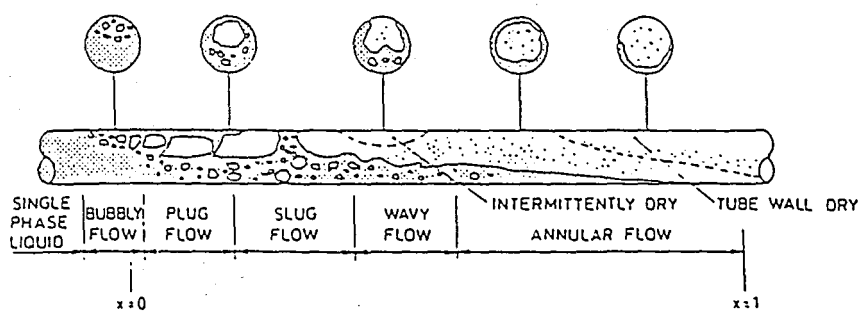

b.) Flow patterns in horizontal tubes

FIGURE 1.2. Approximate sequence of flow patterns [4]

The characteristics of these flow patterns are:

- In Bubbly Flow, Gas bubbles are approximately same and uniform size. In horizontal tube bubbles tend to go to the top of the tube due to gravity
- In Plug Flow increased liquid flow instead of gas flow results in an intermittent flow pattern. Individual gas bubbles came together to produce long plugs.
- In Stratified Flow, (in horizontal tube) the separation of the liquid and gas phases is complete, the liquid flowing at the bottom of the tube and the gas at the top. The two phases have a relatively smooth interface
- In Wavy Flow, one can see large surface waves. These waves develop from the stratified flow when the gas velocity is increased.
- In Slug Flow, (in horizontal tube) wave amplitude is so large that the wave touches to top of the tube. It can be seen by further increasing of the gas velocity in the wavy flow regime.
- In Churn Flow, (in vertical tube) large gas bubbles in slug flow breakdown. This is highly unstable flow of oscillatory nature. Liquid near the tube wall continuously displaces up and down.
- In Annular Flow, higher gas flow causes a liquid film to develop on the wall and the gas to flow in the core with entrained liquid droplets; liquid film approaches to the wall as time goes until the liquid is all vaporised. In horizontal tube the liquid film is thinner at the top and ticker at the bottom due to gravity.

  The annular flow occurs when the ratio of the tube cross section filled with vapour to the total cross section is approximately 85 per cent. [5]
- Dispersed Bubble Flow exhibits small gas bubbles dispersed in a liquid matrix with bubbles tending to flow in the upper part of the tube
- Mist Flow exhibits small liquid droplets dispersed in a gas matrix.

1.2.1. Flow Regimes in Horizontal Two Phase Flow

For horizontal concurrent flow with evaporation; starting with subcooled liquid, the vaporisation process may begin with boiling being initiated before the bulk liquid reaches saturation temperature. With the void fraction being low, bubbles begin to form and collect at the top of the tube due to buoyancy. Both vapour and liquid superficial velocities increase as the boiling process continues, changing flow regime from bubble flow to plug flow. Again the plugs of vapour remain at the top of the tube due to buoyancy effects. For low mass fluxes and, hence, low superficial liquid and vapour velocities, stratified flow ultimately results. The liquid flowing at the bottom of the tube is separated from the vapour in the upper portion of the tube by a smooth interface.

At higher mass fluxes, both superficial liquid and vapour velocities increase and waves begin to form at the liquid-vapour interface. Under certain conditions, these interfacial waves grow to encompass the entire tube cross section, resulting in the formation of liquid slugs that continues down the tube. The vapour separating these liquid slugs again remains near the top of the tube due to buoyancy effects. This flow regime is called slug flow. Slug and plug flow can also be called intermittent flow.

At higher qualities, the liquid is swept around the tube wall and annular flow occurs. In this flow, an annular liquid ring forms around the tube periphery with a high velocity vapour core moving through the center of the tube. For moderately high mass fluxes, the liquid ring is asymmetric with buoyancy effects thinning the liquid at the top of the tube and thickening it at the bottom of the tube. At high mass fluxes, the liquid flow becomes completely turbulent and strong lateral Reynolds stresses and shear resulting from secondary flows tend to distribute the liquid more evenly around the perimeter. Interfacial waves are ripped off the annular ring and form droplets that are entrained in the vapour core. The annular ring is vaporised as quality increases, leaving only mist flow (also called dispersed or spray flow) with liquid droplets entrained in the vapour core. [6]

1.2.2. Flow Regime Maps

Despite the present deficiencies in the understanding of the various flow patterns and the transitions from one pattern to another, there is a need for simple methods to give some idea of the particular pattern likely occur for a given set of local flow parameters. One method of representing the various transitions is in the form of a flow pattern map. The respective pattern may be presented as areas on a graph.

Flow maps to identify the flow regime with respect to parameters such as superficial gas and fluid velocity, Lockhart-Martinelli parameter and Froude number are found in literature. Wattelet at al.[6] gives some of them, such as Baker map, Mandhane map and Taitel and Dukler map.

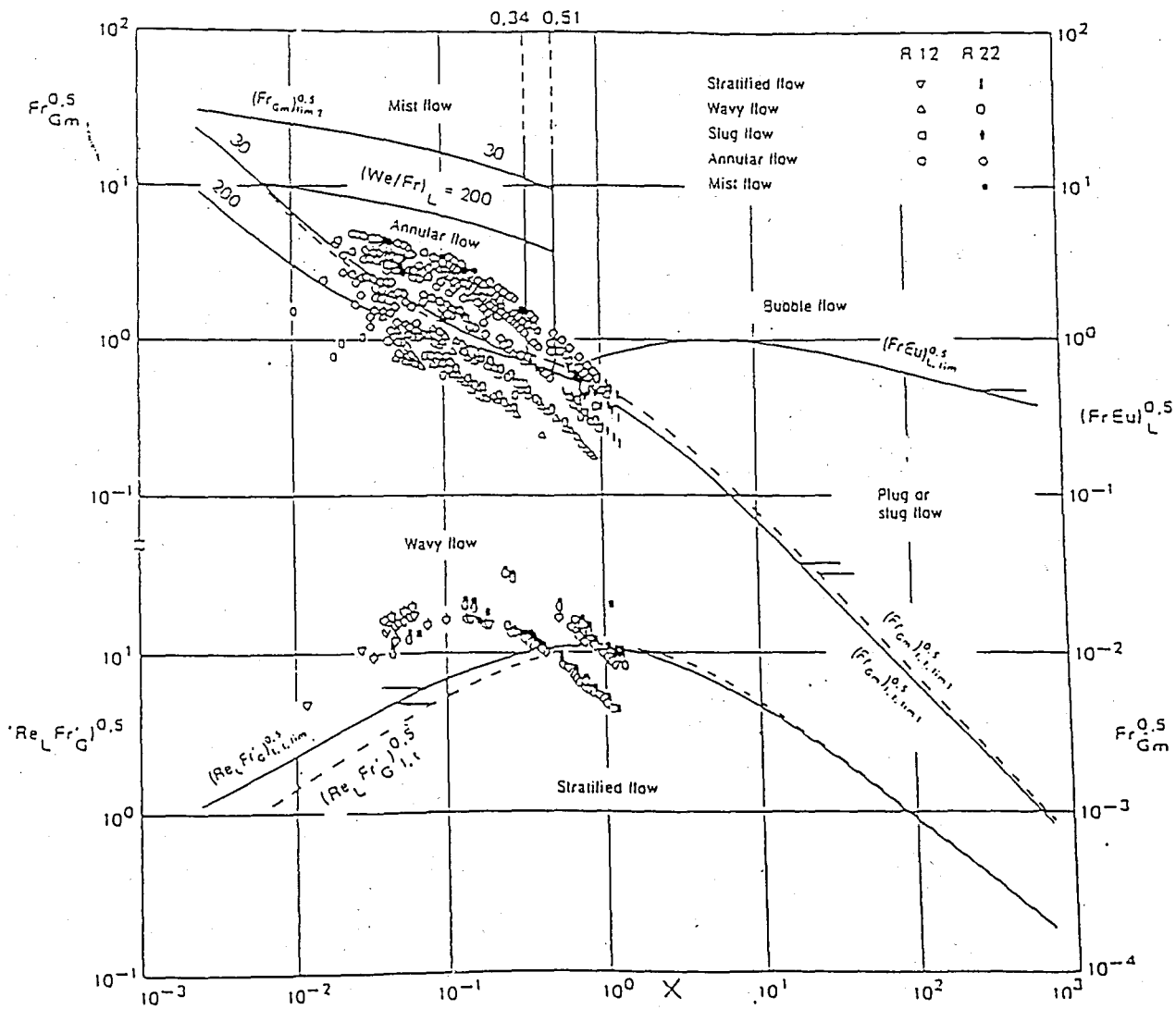

FIGURE 1.3. Flow pattern map for horizontal pipe flow (R12 and R22 data) [3]

VDI Heat Atlas [3] gives a flow map where Steiner adopted a publication by Taitel and Dukler as a basis revising the regime transitions for wavy flow into slug, plug, and annular flow regimes and checking them against measured R-12 and R-22 data.

1.2.3. Flow Pattern Determination

The identification of the flow regimes made by two ways. First is visual observations, it is simple but the accuracy is limited; second is based on the statistical and spectral properties of the void fraction, pressure signal, or pressure drop signal.

Three methods will be explained in the following paragraphs; Statistical methods, Spectral methods and methods using pressure traces and records.

Statistical methods:

The flow regimes were classified by the statistical properties of fluctuations. Identification of the flow regimes was made from the configuration of probability density functions, the order of variance, and the average value of the differential pressure drop.

Jones and Zuber,[7] used a linearised X-ray void measurement system to obtain statistical measurement in normally fluctuating air-water flow in a rectangular channel. They showed that probability density function (PDF) of the fluctuations in void fraction may be used as a flow pattern discriminator for the three dominant patterns of bubbly, slug, and annular flow.

Spectral methods:

The spectral distribution of wall pressure fluctuations is used to characterise the flow regimes for horizontal air-water two phase flow. Flow regimes were grouped into three general areas: separated flow (stratified, wavy, or annular flow), intermittent flow (slug or plug flow), and dispersed flow (bubble or mist flow). Separated flow had spectra with distributions centred about zero frequency with amplitude dropping off rapidly with increasing frequency. Intermittent flow had spectra with sharp peaks at frequencies other than zero. Dispersed flow had more uniform distributions of power over the entire frequency spectrum.[6]

Pressure traces and records:

A simple criteria bases on oscilloscope traces of the pressure drop for air water flow in a horizontal tube is developed.

Stratified flow showed no pressure fluctuations at all. This can be clearly distinguished from the wavy flow, whose pressure fluctuations increased as the gas flow rate increased. Slug flow was characterised by distinctive pressure peaks at regularly spaced intervals. Annular flow was characterised by increases in the amplitude of the pressure peaks and may be distinguished from wavy flow using this criterion. Dispersed flow(or mist flow) fluctuations were large in amplitude compared both wavy and annular flows. Again, the amplitude criterion may be used to distinguish between these flow patterns.[6]

1.3. Two Phase Flow Models

The two most important flow models of two phase gas-liquid flow are : [1,8,9]

1.3.1. Homogenous Flow Model

It provides the simplest technique for analysing two phase flow. Suitable average properties are determined and the mixture is treated as a pseudo fluid that obeys the usual equations of single phase flow. All the standard methods of fluid mechanics can then be applied.

The average quantities which are required are velocity, thermodynamic properties and transport properties. The pseudo properties are weighted averages. Indeed there still remains the problem of calculating meaningful average physical properties of the two phase system, particularly in respect to viscosity. The mean velocities of both phases are supposed to be equal (no slip), a condition very seldom encountered in practice.

The homogenous model is usually treated as the reference one because of the relative ease with which it can be studied analytically. However, in some cases the use of

this model is obviously inappropriate. For example, counter current vertical flows can not be described by this model.

1.3.2. Separated Flow Model

This model considers the phases to be artificially segregated into two streams; one of liquid and one of gas. In the model's simplest form each stream is assumed to travel at a mean velocity. It assumes constant but not necessarily equal gas and liquid velocities. For the case where the mean velocities of the two phases are equal the equations reduce to those of homogenous model. The separated flow model has been continuously developed since 1944 when Lockhart and Martinelli published their classic papers on two phase gas-liquid flow.

In the most sophisticated version of the analytical treatment, two sets of basic equations are written, one for each phase, and these six equations are solved simultaneously together with rate equations which describe how the two phases interact with each other and with the walls of the duct. The latter information is obtained from additional separate relationships in which the void fraction or the velocity ratio (slip) and the wall shear stress are related to the primary variables of the flow system.

From the consideration of the various flow pattern, it would be expected that this model would be most valid for the annular and stratified flow patterns.

1.4. Pressure Drop in a Tube

When a flow is flowing, the total pressure drop experienced by it results from pressure drops due to friction, momentum change (or acceleration), and gravity, i.e.,

$$\Delta P_{total} = \Delta P_{friction} + \Delta P_{acceleration} + \Delta P_{gravity} \qquad (1.1)$$

In most of the heat exchanger applications pressure drop due to acceleration and gravity are negligible. Therefore only pressure drop due to friction will be considered.

1.4.1. Single Phase Flow

Frictional pressure drop for a single phase in a tube can be calculated by the following equation[3]:

$$\Delta P = f \frac{L}{d_i} \frac{G^2}{2\rho} \qquad (1.2)$$

For laminar flow $\mathrm{Re}_i < 2000$

$$f = \frac{64}{\mathrm{Re}_i} \qquad (1.3)$$

The friction coefficient f, in the $\mathrm{Re}_i \approx 3000$ to $\mathrm{Re}_i \approx 100\,000$ range is:

$$f = 0.3164\,\mathrm{Re}_i^{-0.25} \qquad (1.4)$$

where

$$\mathrm{Re}_i = \frac{G d_i}{\mu} \qquad (1.5)$$

1.4.2. Two Phase Flow

According to the flow model assumed, different correlations are proposed:

Homogeneous flow approach:

In homogeneous flow approach, the friction factor is evaluated using Re_{mix} calculated by a mean two phase viscosity $\bar{\mu}$ in the normal friction factor relationship. i.e. :

$$\mathrm{Re}_{mix} = \frac{G d_i}{\bar{\mu}} \qquad (1.6)$$

The form of the relationship between $\bar{\mu}$ and quality x must be chosen to satisfy the following limiting conditions:

$$at\ x = 0, \bar{\mu} = \mu_f \quad at\ x = 1, \bar{\mu} = \mu_g \tag{1.7}$$

Collier and Thome,[10] in their textbook, mentioned some suggested type of equations for the mixture viscosity: such as McAdams, Cicchitti and Dukler. .

Wakeland,[11] uses friction factor correlations for two phase using the homogeneous flow approach with Dukler viscosity correlation.

Separated flow approach

Another approach relates the two phase flow pressure drops to corresponding single phase pressure drops. The basic idea is to correct the single phase pressure drop using a so called two phase flow multiplier, i.e.,

$$\left(\frac{dp}{dz}\right)_{tp} = \phi^2 \left(\frac{dp}{dz}\right) \tag{1.8}$$

Using the liquid phase, the two phase flow frictional multiplier is defined as: [1]

$$\phi_l^2 = \frac{\left(\frac{dp}{dz}\right)_{tp}}{\left(\frac{dp}{dz}\right)_l} \tag{1.9}$$

Here,

$\left(\frac{dp}{dz}\right)_{tp}$: refer to two phase friction drop

$\left(\frac{dp}{dz}\right)_l$: refer to pressure drop that would result if the liquid phase flowed alone in the tube

ϕ_l^2 : refer to two phase multiplier of the liquid alone phase

The frictional pressure drop of the liquid phase

$$\left(\frac{dp}{dz}\right)_l = \frac{f}{2} \frac{G^2(1-x)^2}{d_i \rho_l} \tag{1.10}$$

Therefore frictional pressure drop of two phase flow is :

$$\left(\frac{dp}{dz}\right)_{tp} = \phi_l^2 \frac{f}{2} \frac{G^2(1-x)^2}{d_i \rho_l} \qquad (1.11)$$

Lockhart and Martinelli defined a dimensionless parameter that indicates the relative effects of the phases as follows:

$$X^2 = \frac{\phi_g^2}{\phi_l^2} = \frac{\left(\frac{dp}{dz}\right)_l}{\left(\frac{dp}{dz}\right)_g} \qquad (1.12)$$

X^2 gives a measure of the degree to which the two phase mixture behaves as the liquid rather than as the gas.[1]

Lockhart and Martinelli, after their experimental work with air water flow, gives correlations for friction multipliers (ϕ_g^2, ϕ_l^2) as a function of their parameter.[1]. These correlations are then proofed by several researchers for refrigerants. In literature, correlations given by Chisholm is widely used [6,8,9].Chisholm's correlation for liquid phase is:

$$\phi_l^2 = 1 + \frac{C}{X} + \frac{1}{X^2} \qquad (1.13)$$

The constant C, takes different values for different cases of flow encountered for the liquid and gas: turbulent-turbulent, viscous-turbulent, turbulent-viscous, and viscous-viscous. Table 1.1. gives these values of constant C,

TABLE 1.1 Values of the constant for the Lockhart-Martinelli two phase multiplier correlation[6]

LIQUID	VAPOUR	SUBSCRIPT	*C*
Turbulent	Turbulent	tt	20
Turbulent	Viscous	tv	10
Viscous	Turbulent	vt	12
Viscous	Viscous	vv	5

The Lockhart-Martinelli parameter is possibly the most important parameter in two phase flow, both from a pressure drop and convective heat transfer point of view. X_{tt} is a function of quality, vapour to liquid density ratio, and liquid to vapour viscosity ratio.

$$X_{tt} = \left[\frac{1-x}{x}\right]^{0.9}\left[\frac{\mu_l}{\mu_g}\right]^{0.1}\left[\frac{\rho_g}{\rho_l}\right]^{0.5} \qquad (1.14)$$

Some of the other studies on pressure drop occurring in two phase flow done by Paliwoda[12], Wattelet et al. [6]. Although it is not considered in this study, the pressure drop estimation due to momentum change is given in Appendix A.

For two phase pressure drop in tees and bends Paliwoda developed a model.[14]. Karatas [15] in his master thesis convert Paliwoda's correlations in a more applicable form.

In this work, pressure losses are calculated using Chisholm correlations. In a domestic evaporator, liquid refrigerant is laminar whereas vapour refrigerant is turbulent. Therefore, the C constant takes the value 12. The pressure losses in bends are neglected. Results for selected correlation is given in Section 5.2. Other pressure drop correlations are summarised and calculations based on these correlations are given in Appendix A

1.5. Void Fraction Models and Refrigerant Charge Inventory Prediction

Analytical prediction of the refrigerant charge inventory in a refrigerator is important in system design. Refrigeration systems are charge-sensitive in the sense that their performance is determined by the amount of total charge in the unit.

The capability of predicting optimum refrigerant charge provides a tool for determining ways to minimise total system refrigerant charge. Also reductions in total charge should improve system cycling performance.[16]

The refrigerant charge inventory analysis includes the proper prediction of the refrigerant mass in the two phase regions of the condenser and the evaporator. However, the degree of vapour to liquid slip (velocity difference) at each cross section in the two phase region, and the variation of the refrigerant quality with length through the two phase

region includes uncertainties. The purpose of void fraction model is to account for the slip effect.

In literature, three methods are used to determine the void fraction;

1. Empirical methods: for example, Hancox's correlation mentioned in Wang and Touber's study[17],
2. Analytical methods: Rice[16] reviewed existing analytical correlations, classified them and evaluated them for their effect on refrigerant charge inventory prediction
3. Numerical methods: Wang and Touber[17], based on their numerical solutions, curve fitted a function between u_g/u_l and α using the least square method and obtained following polynomial equation:

$$\frac{u_g}{u_f} = \sum_{i=0}^{10} B_i \alpha^i \qquad (1.15)$$

The two phase refrigerant mass contained in a length of tubing is obtained by summing the gas *g* and liquid *l* contributions occupying each cross sectional area over the length of the region. These contributions are given separately by:[16]

$$m_g = \int_0^L \rho_g \cdot dV_g = \rho_g \int_0^L A_g \cdot dl \qquad (1.16)$$

$$m_l = \int_0^L \rho_l \cdot dV_l = \rho_l \int_0^L A_l \cdot dl \qquad (1.17)$$

where

A_g cross sectional area occupied by vapour

A_l cross sectional area occupied by liquid

Then at each cross section $A_c = A_g + A_l$. Introducing the void fraction $\alpha = \frac{A_g}{A_c}$, Equations 1.16 and 1.17 can be written as:

$$m_g = \rho_g A_c \int_0^L \alpha \cdot dl \qquad (1.18)$$

$$m_l = \rho_l A_c \int_0^L (1-\alpha) \cdot dl \qquad (1.19)$$

The total mass, m_t, in the two phase section can be obtained from Equations (1.18) and (1.19) in terms of tube volume V as:

$$m_t = V \cdot \left[\rho_g \int_0^L \alpha \cdot dl + \rho_l \int_0^L (1-\alpha) \cdot dl \right] \Big/ \int_0^L dl \qquad (1.20)$$

The void fraction, α, in equation (1.20) is generally represented as a function of mass quality, x.

$$\alpha = f_\alpha(x) \qquad (1.21)$$

Therefore, to evaluate m_t from equation (1.20) for a given void fraction equation. The tube length variable l, must be related to mass quality x, in some manner. This relationship obtained from an assumption regarding the heat flow variation, dQ with differential length, dl in the two phase region :

$$dQ = \dot{m}_r h_{fg} dx = f_Q(x) dl \qquad (1.22)$$

$$dl = \frac{\dot{m}_r h_{fg}}{f_Q(x)} dx \qquad (1.23)$$

where, $\dot{m}_r$ = refrigerant mass flow rate,

h_{fg} = enthalpy of vaporisation, and

$f_Q(x)$ = assumed heat flux equation (i.e., equation for local heat flow per differential length, dl)

assuming constant heat flux along the tube length, i.e.

$$f_Q(x) = q'' \pi D = const. \qquad (1.24)$$

following equality can be written,

$$\dot{m}_r h_{fg} = q'' \pi D L \tag{1.25}$$

equation (1.23) can be rewritten using equations (1.24) and (1.25)

$$dl = \frac{q'' \pi D L}{q'' \pi D} dx \quad \Rightarrow \quad dl = L dx \tag{1.26}$$

Then, for a constant heat flux problem equation (1.20) takes the form:

$$m_t = V\left[\rho_g \int_{x_i}^{x_o} \alpha dx + \rho_l \int_{x_i}^{x_o} (1-\alpha) dx\right] \tag{1.27}$$

where x_i and x_o are inlet and outlet refrigerant qualities.

Existing correlations for void fraction α, were classified by Rice[16] into four categories.

- homogeneous,
- slip-ratio correlated; Rigot and Ahrens/Thom, Zivi, Smith,
- X_{tt} correlated; Domanski and Didion [13], and
- mass-flux dependent; Tandon, Premoli, Hughmark

The homogeneous model is the most simplified. The model considers the two phases as a homogeneous mixture thereby travelling at the same velocity. In this model, the relationship between void fraction, α, and mass quality, x straightforwardly derived as:

$$\alpha = \frac{1}{1 + \left[\frac{1-x}{x}\right]\frac{\rho_g}{\rho_l}} \tag{1.28}$$

In this study, homogeneous void fraction model is used for its easiness. More involved models require additional iterations at each step. Rice[16] mentioned that many researchers have chosen homogeneous model: such as James, Daniels, Dhar, Stoecker, Bonne and MacArthur. Other void fraction models are important for a refrigerant charge prediction calculation, for an accurate prediction a more involved model, like a mass flux dependent model, should be chosen. Therefore a comparison and discussion for different models are given in Section 5.3. The complete correlations and figures obtained by evaluating them are also given in Appendix B for reference.

Rice[16] also concluded in his study, that the choice of heat flux assumption is insignificant for evaporators and secondary importance (after void fraction model) for condensers. Therefore, after Rice's conclusion and also for its simplicity constant heat flux assumption is used in our calculations.

1.6. Heat Transfer in Flow Boiling

To calculate total heat transfer coefficient of an evaporator, one of the coefficient needed is refrigerant side heat transfer coefficient. Since two phase flow is dominant in an evaporator, accurate estimation of the two phase flow boiling heat transfer coefficient is essential (When evaporation occurs at a solid-liquid interface, it is termed boiling). An accurate estimation of that coefficient usually offers considerable economic savings in the design and operation of evaporators.

In an evaporator tube, heat is transferred from the wall to liquid by three means:

1. nucleate boiling in the liquid adjacent to the wall,
2. convection from the wall to the liquid, followed by surface evaporation at the liquid-vapour interface, and
3. convection from the wall to the vapour.

The third term is usually quite small in comparison to 1. and 2. Therefore the heat transfer is by convective and nucleate boiling mechanisms.

Heat Transfer between the refrigerant and pipe wall in the two phase flow region is very complicated. Therefore the heat transfer coefficient is obtained with a combination of theories and experiments. In the literature many correlations can be found.

Initial methods for convective boiling heat transfer were based on the premise that the mechanism of heat transfer in forced convection was similar to single phase forced convection. It is shown that the ratio between the two-phase flow and the single phase liquid heat transfer coefficients can be correlated by the Lockhart-Martinelli parameter, X_{tt}

$$\frac{h_{TP}}{h_l} = f\left(\frac{1}{X_{tt}}\right) \qquad (1.29)$$

Using the form of Equation (1.29), several researchers developed correlations for forced-convective evaporation in both vertical and horizontal tubes[4,6]

Wakeland [11] and Wang and Touber [17] are used this kind of correlations for the refrigerant side film coefficient in their evaporator simulation work.

Three single phase heat transfer coefficients are reported by Wattelet et al.[6] which are generally used for turbulent flow inside tubes. These are Dittus-Boelter, Petukov and Gnielinski correlations

Incropera and Dewitt give the Dittus-Boelter equation:

$$Nu_D = 0.023\,\mathrm{Re}_D^{0.8}\,\mathrm{Pr}^n \qquad (1.30)$$

where n=0.4 for heating (evaporator condition) and 0.3 for cooling (condenser condition). Replacing Re_D and Pr number with their definitions, for evaporator applications:

$$h_l = 0.023\frac{k_l}{d_i}\left[\frac{Gd_i(1-x)}{\mu_l}\right]^{0.8}\left(\frac{\mu_l C_{p_l}}{k_l}\right)^{0.4} \qquad (1.31)$$

The equation has been confirmed experimentally for the range of conditions:[18]

$$0.7 \le \mathrm{Pr} \le 160$$

$$\mathrm{Re}_D \ge 10000$$

$$\frac{L}{D} \ge 10$$

Hambraeus[19] gives Pierre's correlation based on experimental work with three refrigerants, gives the heat transfer coefficient independent of quality:

$$h_{tp} = 0.0011\frac{k_l G_r}{\mu_l}\left(K_f\right)^{0.5} \qquad (1.32)$$

where K_f is the Pierre boiling number :

$$K_f = \frac{\Delta x h_{fg}}{gL} \qquad (1.33)$$

here Δx is the quality difference in the evaporator.

Other studies surveyed in the literature about heat transfer coefficient; Kandlikar [20] and Güngör andWinterton [21], are summarised and a figure based on these

correlations are given in Appendix C, and a discussion about these results are given in Section 5.4.

Among the correlations surveyed, ACRC and Pierre's correlations are most suitable ones for a domestic evaporator simulation work. Their experiments were performed for conditions (i.e. cooling capacity, refrigerant mass flowrate and tube geometry) similar to a refrigerator evaporator. Pierre's correlation is preferred in this study between two, for its simplicity and easiness.

2. MATHEMATICAL MODELLING

2.1. Governing Equations of 1-D Transient, Compressible Inviscid Flow

The governing equations can be obtained in various forms. In general theory, it is irrelevant whether one deals with one form or the other. Indeed through some simple manipulations, one can be obtained from the other. However, for computational fluid dynamics (CFD), the use of the equations in one form may lead to success whereas the use of an alternate form may result in oscillations in the numerical results, or instability.

The most suited form of the governing equations is the Conservation Form where the equations was obtained directly from a control volume that was fixed in space, rather than moving with the fluid. When the volume is fixed in space, we are concerned with the flux of mass, momentum and energy into and out of the volume. In this case, the fluxes become dependent variables in the equations.

Governing equations for an unsteady, one-dimensional, compressible flow are:

(Conservation form, with neglecting body forces)

continuity:
$$\frac{\partial \rho}{\partial t} + \frac{\partial (\rho u)}{\partial x} = 0 \qquad (2.1)$$

momentum
$$\frac{\partial (\rho u)}{\partial t} + \frac{\partial (\rho u^2)}{\partial x} = -\frac{\partial P}{\partial x} + \underbrace{\frac{\partial \tau_{xx}}{\partial x}}_{A} \qquad (2.2)$$

energy:
$$\frac{\partial}{\partial t}\left[\rho\left(e + \frac{u^2}{2}\right)\right] + \frac{\partial}{\partial x}\left[\rho u\left(e + \frac{u^2}{2}\right)\right] = -\frac{\partial (uP)}{\partial x} + \underbrace{\frac{\partial}{\partial x}\left(u\tau_{xx}\right)}_{B} + \underbrace{\frac{\partial}{\partial x}\left(k\frac{\partial T}{\partial x}\right)}_{C} \qquad (2.3)$$

The heat conduction term, "C", [the last term on the right-hand side of equation (2.3.)] is replaced by *heat flux term* which represents the heat exchange between fluid and heat exchanger wall.[22]

Viscosity terms appears in momentum and energy equations in the shear force terms, "A" and "B". The shear force term in the energy equation represents "frictional heating" and is usually neglected except for high velocity flows which is not our model case. In the momentum equation, the shear force represents the force required to overcome friction and it causes a pressure gradient. [10]

Due to the difficulty of analytical evaluation, the frictional pressure drop is predicted by correlations obtained using experimental pressure drop data. The frictional pressure gradient can be evaluated using either the momentum equation or the energy equation. However, the majority of the researchers have adopted the momentum balance as the basic equation and have defined the frictional component in terms of the wall shear force. The total wall shear force can be expressed in terms of a friction factor[10]. Evaluation of the friction factor has been explained in section 1.4.

Consequently, viscous term is dropped in the energy equation and is replaced by a *pressure drop term* in the momentum equation.

According to results obtained by evaluating various pressure drop correlations, (section 5.2.) it is found that pressure drop is only about 5-10 per cent of a typical saturation pressure value of an evaporator condition. Therefore, pressure drop effect is made optional in the developed program.

New form of the equations obtained by replacing some terms as discussed above and "ρu" term with "G", mass flow rate per area:

continuity:

$$\frac{\partial \rho}{\partial t} + \frac{\partial G}{\partial x} = 0 \qquad (2.4)$$

momentum:

$$\frac{\partial G}{\partial t} + \frac{\partial}{\partial x}\left(\frac{G^2}{\rho} + P\right) = friction\ term \qquad (2.5)$$

energy

$$\frac{\partial}{\partial t}\left[\rho e + \frac{G^2}{2\rho}\right] + \frac{\partial}{\partial x}\left[G\left(h + \frac{1}{2}\left(\frac{G}{\rho}\right)^2\right)\right] = heat\ flux\ term \qquad (2.6)$$

Some comments on the governing equations:

- They are coupled system of non-linear partial differential equations, hence are very difficult to solve analytically. There is no general closed-form solution to these equations.
- The system contains three equations in terms of four unknown variables; ρ, u, e, P therefore we need an additional equation. This equation is equation of state which relates the pressure, temperature and specific volume (or density). This provides a fourth equation, but it also introduces a fifth unknown, namely temperature, T. A fifth equation to close the entire system must be a thermodynamic relation between state variables. For example, $e = e(T, P)$

2.2. Two Phase Flow Equations

A simplified one-dimensional analysis of two phase liquid-vapor flow can be made by considering the system shown in Figure 2.1

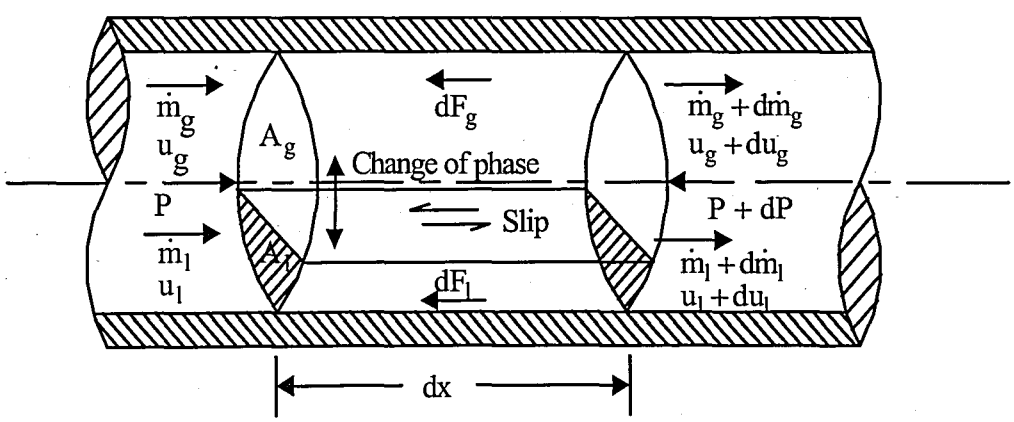

FIGURE 2.1. Schematic of horizontal two phase flow over element of tube[9]

Two phase flow obeys all of the basic laws of fluid mechanics. The equations are more complicated or more numerous than those of single phase flow. Single phase and two phase fluid flow are represented by the same system of non-linear, coupled partial differential equations representing the conservation laws of mass, momentum, and energy for a homogenous flow.

However, there exists slip between gas and liquid. The occurrence of slip between two phases can be modelled by a two fluid model with separate conservation equations for liquid and gas, and appropriate interphase coupling terms; but such an approach is computationally complicated and the interphase are often unknown.

A common practical approach is to allow only the velocity to differ for the two phase while the conservation equations are still written for the combined flow as in the case of homogenous flow model where equal gas and liquid velocities are assumed. The original homogenous form of the conservation equations can then be preserved by the introduction of the mixture variables.

In this way, the inclusion of slip in a two phase flow model can be made through minor modifications of terms in the single phase momentum and energy conservation equations. This approach also simplifies the modelling of fluid flow, as encountered in heat pump evaporators and condensers.

Dupont J.F. et. al.[23] state equations for an unsteady, 1-D, horizontal, compressible inviscid two-phase flow as:

mass:

$$\frac{\partial}{\partial t}\left\{\alpha\rho_g + (1-\alpha)\rho_l\right\} + \frac{\partial}{\partial x}\left\{\alpha\rho_g u_g + (1-\alpha)\rho_l u_l\right\} = 0 \qquad (2.7)$$

momentum:

$$\frac{\partial}{\partial t}\left\{\alpha\rho_g u_g + (1-\alpha)\rho_l u_l\right\} + \frac{\partial}{\partial x}\left\{\alpha\rho_g u_g^2 + (1-\alpha)\rho_l u_l^2 + P\right\} = \textit{friction pressure loss term} \qquad (2.8)$$

energy:

$$\frac{\partial}{\partial t}\left\{\alpha\left(\rho_g E_g\right) + (1-\alpha)\left(\rho_l E_l\right)\right\} + \frac{\partial}{\partial x}\left\{\alpha u_g\left(\rho_g E_g + P\right) + (1-\alpha)u_l\left(\rho_l E_l + P\right)\right\} = \textit{heat flux term} \qquad (2.9)$$

where: $E = e + \frac{u^2}{2}$: total energy

e (J/kg): spec. int. energy

u (m/s): velocity

ρ (kg/m^3): density

P (N/m^2): pressure

α (-): void fraction

t (s): time

x (m): space

and subscript l: liquid

g: vapour

Introducing mixture variables:[23]

$$\rho^* = \left\{\alpha\rho_g + (1-\alpha)\rho_l\right\} \tag{2.10}$$

$$G^* = \left\{\alpha\rho_g u_g + (1-\alpha)\rho_l u_l\right\} \tag{2.11}$$

$$e^* = \frac{1}{\rho^*}\left\{\alpha\rho_g e_g + (1-\alpha)\rho_l e_l\right\} \tag{2.12}$$

$$h^* = \frac{1}{\rho^*}\left\{\alpha\rho_g h_g + (1-\alpha)\rho_l h_l\right\} \tag{2.13}$$

we get,

continuity:

$$\frac{\partial\rho^*}{\partial t} + \frac{\partial G^*}{\partial x} = 0 \tag{2.14}$$

momentum:

$$\frac{\partial G^*}{\partial t} + \frac{\partial}{\partial x}\left(\frac{G^{*2}}{\rho^*} + P\right) = friction\ term \tag{2.15}$$

energy

$$\frac{\partial}{\partial t}\left[\rho^* e^* + \frac{G^{*2}}{2\rho^*}\right] + \frac{\partial}{\partial x}\left[G^*\left(h^* + \frac{1}{2}\left(\frac{G^*}{\rho^*}\right)^2\right)\right] = heat\ flux\ term \tag{2.16}$$

Therefore we get the original homogenous form of the conservation equations. This system of equations is closed with appropriate boundary conditions; constitutive equations for friction pressure loss, and heat input; as stated before. Pressure drop and heat transfer correlations explained in Chapter 1. are used to determine friction pressure loss and heat input. For simplicity , *'s of variables are dropped hereafter.

However, these mixture variables are different from the thermodynamic variables. Mixture variables show the instantaneous values of the variable at a cross section, whereas thermodynamic variables represent fluxes. Mixture and thermodynamic variables are equal if and only if the slip ratio is one, which means liquid and gas phases are travelling at the same velocity. Therefore, for homogeneous flow model, set of equations. (2.14), (2.15) and (2.16) are the same set of equations as (2.4), (2.5), (2.6).

Difference with these mixture variables with Dupont et al.'s work[23] is that they use "$\frac{\dot{m}}{A}$" instead of "G" in the mass equation, and they use three different mean velocity types in the momentum and energy equation.

Equations (2.14) to (2.16) are in the same form with Brasz, J and Koenig[24] work. For the mixture variables they also refer to Dupont et al.

The analytical investigation of the equations (2.11) to (2.13) shows that there are three characteristic velocities[24,25]: One characteristic is the actual fluid transport velocity and the other two correspond to a travelling pressure wave. The supersonic pressure wave does not represent a real physical phenomenon.[24]

2.2.1. Equations for a Simplified Model

Some other authors, MacArthur and Grald[25], Wang and Touber[17], Jia et. al.[26], and Sorensen et. al.[23] uses similar mass and momentum equations but a modified energy equation. They dotted the momentum equation with the velocity and subtract from the energy equations. (This process removes the kinetic energy terms from the left side of the energy equation.) Next, the term $\frac{\partial P}{\partial t}$ is added to both sides of the equation. Finally ignoring $\frac{\partial P}{\partial t}$ from the left side (which is pressure work), the energy equation becomes:

$$\frac{\partial}{\partial t}(\rho h) + \frac{\partial}{\partial x}(\rho u h) = heat\ flux\ term \qquad (2.17)$$

MacArthur and Grald[25], and Wang and Touber[17] neglect the pressure wave dynamics (therefore momentum equation), since their impact on energy interactions is very small. They used following refrigerant conservation equations for a simplified model:

$$\frac{\partial \rho}{\partial t} + \frac{\partial G}{\partial x} = 0 \qquad (2.18)$$

$$\frac{\partial}{\partial t}(\rho h) + \frac{\partial}{\partial x}(G h) = heat\ flux\ term \qquad (2.19)$$

Neglecting pressure dynamics in numerical solution have another advantage: with this approximation, the solution shows only one characteristic velocity: the fluid velocity. Therefore , larger time steps may be used.

The complete derivation of energy equation for the simplified model is given in Appendix D.

2.2.2. Conservation Equation for the Heat Exchanger Wall

The metal tube of the heat exchanger possess considerable heat and mass capacities. A drawing which shows the heat transfer process in the tube is given in Figure 2.2

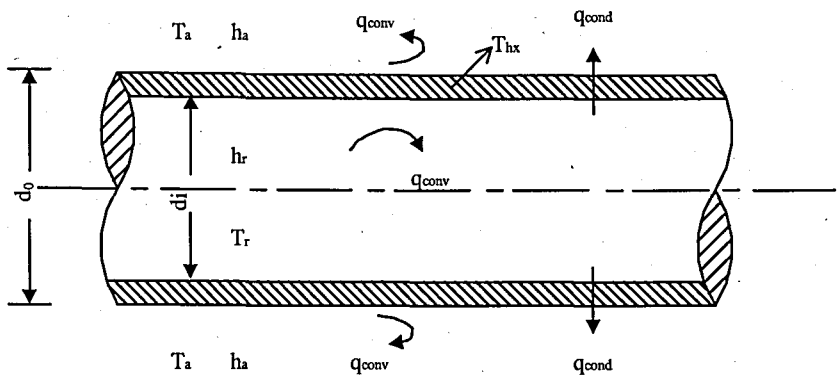

FIGURE 2.2. Heat transfer process in the heat exchanger tube.

The energy balance on the differential tube element gives:

Heat capacity rate of tube wall = Radial heat conduction + heat convection inside + heat convection outside

The radial heat conduction is neglected because the Biot number is small. Therefore the conservation energy equation is :

$$\left(\rho A c_p\right)_{hx} \frac{\partial T_{hx}}{\partial t} - h_r \pi d_i \left(T_r - T_{hx}\right) - h_a \pi d_o \left(T_a - T_{hx}\right) = 0 \qquad (2.20)$$

here

A : cross-sectional area of the heat exchanger tube: $\pi(d_o^2 - d_i^2) / 4$

h_a : heat transfer coefficient of the air side

h_r : refrigerant side heat transfer coefficient

T_a : temperature of the surrounding air, (assumed to be constant)

T_{hx} : heat exchanger wall local temperature

T_r : refrigerant local temperature

Finally, The heat flux term in equations (2.13) and (2.14) is

$$h_r \pi d_i \left(T_{hx} - T_r\right) \qquad (2.21)$$

3. NUMERICAL METHOD

Analytical solutions of partial differential equations, PDE, obtained by analytical methods give the variation of the dependent variables continuously the domain. In contrast, numerical methods give solutions at only discrete points in the domain.

The finite difference method, FDM, is widely used in solving PDE. The FDM replaces the partial derivatives appearing in the governing equations with algebraic terms. Then, a system of algebraic equations is left to solve.

The time dependent problems can be solved with finite difference methods explicitly or implicitly:

Explicit solutions involve time marching, in which the values of the unknowns at the next time level depend only on the values at the current time level. The stability of these methods limits the time step magnitude. The time step should be chosen as large as possible since each time level increment leads to error accumulation.

Implicit methods do not have stability problems. However, the non-linear system must first be linearised using eigenvalue decomposition and the equations must be uncoupled. Then the system can be converted into matrix form and solved using numerical techniques.

Some of these methods are listed below:

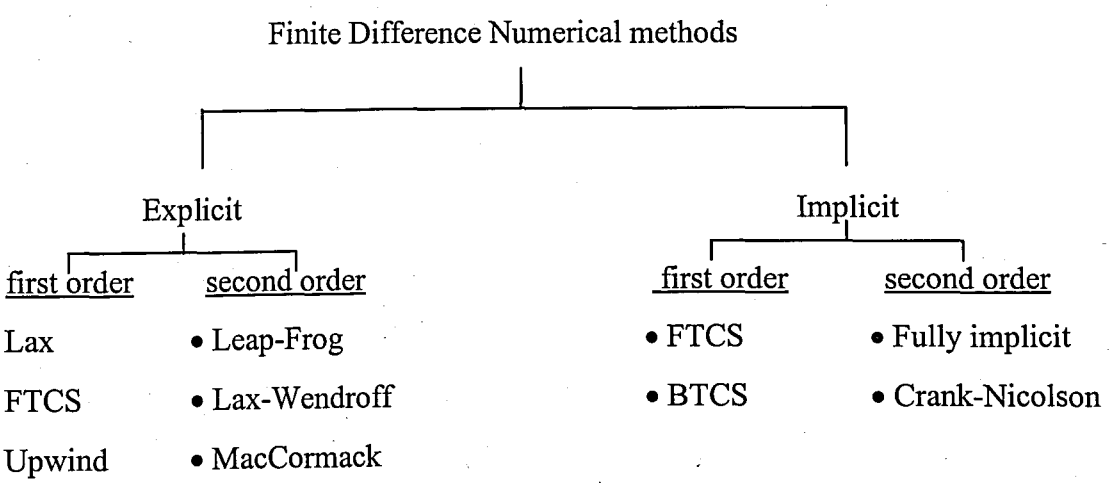

The relative major advantages and disadvantages of explicit and implicit approaches are: [27]

explicit approach:

Advantage.....Relatively simple to set up and program.

.....Convenient for parallel runs.

Disadvantage...For a given Δx, Δt must be less than some limit imposed by stability constraints. This can result in long computation time for a given time interval.

Implicit approaches:

Advantage.....Stability can be maintained over much larger values of Δt, hence fewer time steps is needed to make calculations over a given time interval. This results in less computation time.

Disadvantage...More complicated to set up and program.

...Since massive matrix manipulations are usually required at each time step, computation time per step is much larger than in the explicit approach.

...Since large Δt can be taken, the truncation error is larger, and the use of implicit methods to follow the exact transients may not be as accurate as an explicit approach. However, for a time dependent solution in which the steady state is the desired result, this relative time-wise inaccuracy is not important

It will be better to see accurately the dynamic behaviour of a two phase flow system as a first step of a modelling work. Hence an explicit method will be chosen. As discussed in Chapter 2., our governing equations are hyperbolic and non-linear. For non-linear hyperbolic equations, *multi-step methods* are suggested[28,29,30,31]

Multi step methods use the finite difference equations at split time levels, they may also be named as predictor-corrector methods. In the first step, a temporary value for the dependent variable is predicted, and in the second step, a corrected value is computed to provide the final value of the dependent variable. Multi-step methods are second order accurate both in time and space.

Among the multi-steps methods, the MacCormack method is widely used in solving partial differential equations, PDE. It is a variation of the two step Lax-Wendroff scheme, but it is more applicable. Hence it is mostly used in solving nonlinear PDE's.[29,30]

As it will be explained in the following chapter, a model problem for a nonlinear, transient, inviscid flow is inviscid Burger's equation:

$$\frac{\partial u}{\partial t} + \frac{\partial F}{\partial x} = 0 \qquad (3.1)$$

The first step is to "predict" temporary a new value of u at the time level $n+1$. This predicted value is shown as $\overline{u_i^{n+1}}$ and is equal to:

$$\overline{u_i^{n+1}} = u_i^n - \frac{\Delta t}{\Delta x}\left(F_{i+1}^n - F_i^n\right) \qquad (3.2)$$

It is simply forward difference scheme.

The final "corrected" value of u at the time level $n+1$ is calculated using backward differencing. The time discretisation is done between $n+1$ and $n+\frac{1}{2}$:

$$\frac{u_i^{n+1} - u_i^{n+\frac{1}{2}}}{\frac{1}{2}\Delta t} = -\frac{\overline{F_i^{n+1}} - \overline{F_{i-1}^{n+1}}}{\Delta x} \qquad (3.3)$$

reorganising, $$u_i^{n+1} = u_i^{n+\frac{1}{2}} - \frac{1}{2}\frac{\Delta t}{\Delta x}\left(\overline{F_i^{n+1}} + \overline{F_{i-1}^{n+1}}\right) \qquad (3.4)$$

The value of $n+\frac{1}{2}$ is replaced by an average, i.e.,

$$u_i^{n+\frac{1}{2}} = \frac{1}{2}\left(u_i^n + \overline{u_i^{n+1}}\right) \qquad (3.5)$$

Final form of the "predictor" step is:

$$u_i^{n+1} = \frac{1}{2}\left[u_i^n + \overline{u_i^{n+1}} - \frac{\Delta t}{\Delta x}\left(\overline{F_i^{n+1}} - \overline{F_{i-1}^{n+1}}\right)\right] \qquad (3.6)$$

Then the two-step MacCormack method is :

$$\overline{u_i^{n+1}} = u_i^n - \frac{\Delta t}{\Delta x}\left(F_{i+1}^n - F_i^n\right) \quad \textit{forward predictor step}$$

$$u_i^{n+1} = \frac{1}{2}\left[u_i^n + \overline{u_i^{n+1}} - \frac{\Delta t}{\Delta x}\left(\overline{F_i^{n+1}} - \overline{F_{i-1}^{n+1}}\right)\right] \quad \textit{backward corrector step} \qquad (3.7)$$

The stability requirement of the method is CFL ≤ 1, where the CFL number is defined as the ratio of the highest velocity in the system times time-step to space- step.

$$CFL = \left| u_{\max} \frac{\Delta t}{\Delta x} \right| \leq 1.0 \qquad (3.8)$$

Where u_{max} is the maximum velocity in the system. For a system with wave propagation, the fastest wave propagation velocity is the sum of the actual fluid velocity and sonic velocity, a. Therefore, for a fixed space discretisation, the upper limit for the time step size is:

$$\Delta t \leq \frac{\Delta x}{\left|\frac{G}{\rho}\right| + a} \qquad (3.9)$$

Another general comment on MacCormack method is that reversing the order of differencing for each time step, (i.e., forward / backward followed by backward / forward) provides the best result for non-linear problems.

4. COMPUTATIONAL MODELLING

4.1. A Model Equation for Fluid Equations

A single equation that could serve as a non-linear analog of the fluid mechanics equations would be very useful. This equation may be used as a model equation to investigate various solution procedures and parameters. This single equation must have terms which duplicate the physical properties of the fluid equations, i.e., the model equation should have a convective term, a diffusive or dissipative term and a time dependent term. In computational fluid dynamics textbooks Burgers equation is introduced as a simple non-linear equation which meets these requirements.

Referring to the discussion made in Section 2.2, dissipative terms can be disregarded. Hence, an inviscid model equation is chosen.

If the viscous term is neglected in the original Burgers equation, the remaining equation is composed of the unsteady term and a non-linear convective term. The resulting equation is named as inviscid Burgers equation and is hyperbolic:

$$\underbrace{\frac{\partial u}{\partial t}}_{\substack{unsteady\\ term}} + \underbrace{u\frac{\partial u}{\partial x}}_{\substack{convective\\ term}} = 0 \qquad (4.10)$$

which, in conservative form, may be expressed as

$$\frac{\partial u}{\partial t} + \frac{\partial}{\partial x}\left(\frac{u^2}{2}\right) = 0 \qquad (4.11)$$

or,

$$\frac{\partial u}{\partial t} + \frac{\partial H}{\partial x} = 0 \qquad (4.12)$$

where $H = \frac{u^2}{2}$

It may be viewed as a simple analog of the Euler equations for the flow of an inviscid fluid. Equation 4.11. can be interpreted as the propagation of a wave with each point on the wave front having different velocity and eventually forming a discontinuity in the domain.

Exact solution of the model equation: Anderson [29] shows that the discontinuity travels at the average value of the u function across the wave front, i.e., $\frac{u_1 + u_2}{2}$. Therefore a numerical solution of a similar problem for a discontinuity can be compared with the exact solution.

Anderson [29], and Hoffmann [30] examined applications and made discussions of various numerical schemes to non-linear, inviscid Burgers equation. Both agree that, the explicit methods provide better solutions at discontinuity. Among the explicit formulations, MacCormack's scheme yields the best solution.

To investigate effects of some parameters i.e., CFL number, Δx, and artificial viscosity, an example problem posed (same as Hoffmann [30]) as follows. A discontinuity described by the function:

$$u(x,0) = 1 \qquad 0 \le x \le 2.0$$

$$u(x,0) = 0 \qquad 2.0 \le x \le 4.0$$

shown in Figure 4.1. is to be used as initial data to investigate its propagation throughout the domain.

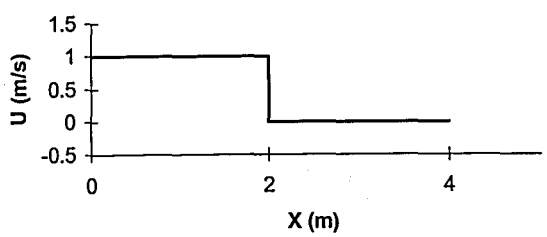

FIGURE 4.1. Discontinuity used as initial condition.

Since this problem is used as a model problem, the code will be validated if successful results will be obtained for model problem.

Code validation: Solution obtained at different time intervals with Δx=0.1, Δt=0.1 is shown in Figure 4.2

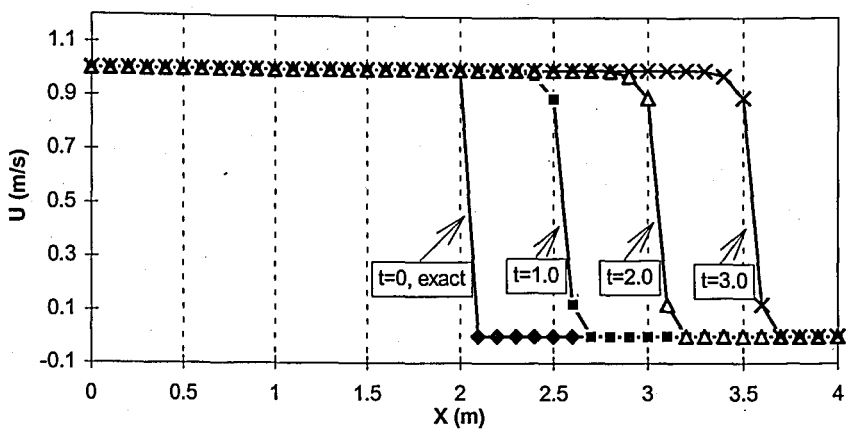

FIGURE 4.2. Solution of inviscid Burgers equation by the MacCormak method, Δx=0.1, Δt=0.1

The right moving discontinuity wave is correctly positioned and is well defined. Although the method is a second order one, the dispersion error is not seen for CFL=1.0. But when we look to the solution for CFL=0.5 the dispersion error become evident by the presence of oscillations in neighbourhood of the discontinuity. Two solutions obtained with various CFL numbers (and therefore, time step sizes) at t=2.0 are compared in Figure 4.3. In general, as the CFL number decreases, the solution degenerates, the best solution is obtained at a CFL number of one.

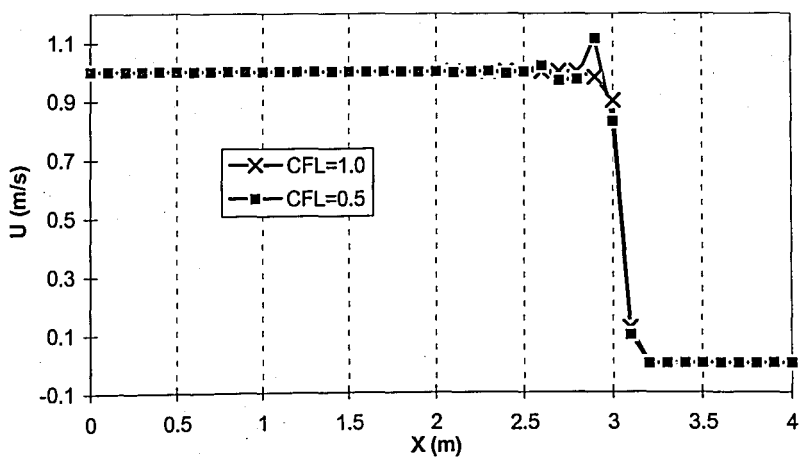

FIGURE 4.3. Effect of time step sizes on the solution of Burgers equation by the MacCormack method

The oscillations can be reduced by adding an artificial viscosity term. Two different artificial viscosity term suitable for second order methods are investigated. One is fourth order in space, other is second order both in space and time. The fourth order term has the form: Hoffman [30]

$$\frac{w}{8}\left(u_{i+2}^{n}-4u_{i+1}^{n}+6u_{i}^{n}-4u_{i-1}^{n}+u_{i-2}^{n}\right) \qquad (4.13)$$

Other term is [31],

$$\Delta u_{i}^{n}=\Delta u_{i}^{n}-av\left(\Delta u_{i+1}^{n}-2\Delta u_{i}^{n}+\Delta_{i-1}^{n}\right) \qquad (4.14)$$

where $$\Delta u_{i}^{n}=u_{i}^{n+1}-u_{i}^{n}$$

The resulting solutions with w=0.8 and av=0.25 (found to be best values after trial and error) is shown in Figure 4.4. The second term yields better solution.

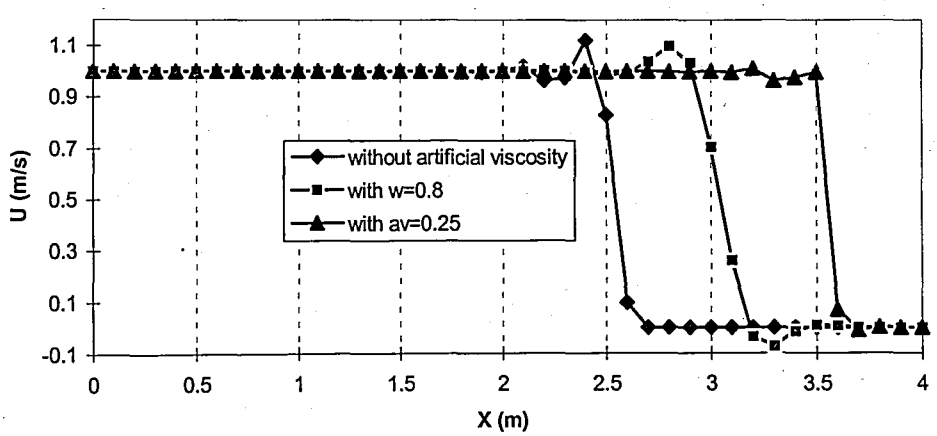

FIGURE 4.4. Solution of inviscid Burgers equation by the MacCormak method, with two different artificial viscosity term and $\Delta x=0.1$, $\Delta t=0.1$

Grid sensitivity analysis is done by changing node spacing: Decreasing the interval between two nodes, Δx, (by increasing node number) the solution approaches to the exact one as expected. Figure 4.5. shows the effect of Δx on the solution. The disadvantage of decreasing Δx is that the computation time is increasing.

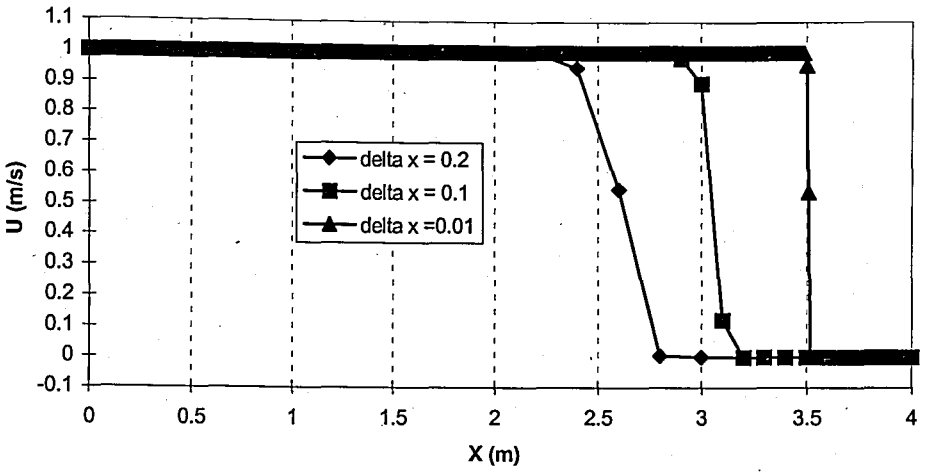

FIGURE 4.5. Effect of node spacing on the solution of Burgers equation by the MacCormack method

As a conclusion, The MacCormack scheme with CFL number one (or close to one) is the best choice for Burgers equations. Since Burgers equation was our model equation, to solve single phase fluid flow we apply MacCormack method. If dispersion error occurs a second order artificial viscosity term may be added with appropriate constant or a finer grid may be used.

4.2. Initial and Boundary Conditions

Although the governing equations are the same for all flow cases, the flow fields are quite different for different cases. The reason for this, is the boundary and initial conditions. The boundary and initial conditions dictate the particular solutions to be obtained from the governing equations.

Other than the physical boundary conditions, in computational fluid dynamics, we have an additional concern: numerical boundary conditions. In the same sense as the real flow field is dictated by the physical boundary conditions, the computed flow is driven by the numerical boundary conditions. The subject of proper and accurate boundary conditions in CFD is very important, and is the subject of current CFD research.[27]

The initial conditions of our problem are obtained from a steady state solution of equations (2.11.) to (2.13.) giving:

$$h_i^{n=0} = h\left(x = x_i,\ t = 0\right),$$
$$P_i^{n=0} = P\left(x = x_i,\ t = 0\right), \quad and$$
$$G_i^{n=0} = G(t = 0)$$

Boundary conditions for h and G are specified at the inlet:

$$h_{i=0}^{n} = h\left(x = 0,\ t = n\Delta t\right),$$
$$G_{i=0}^{n} = G\left(x = 0,\ t = n\Delta t\right)$$

and for P at the outlet:

$$P_{i=I}^{n} = P\left(x = X,\ t = n\Delta t\right).$$

4.3. Computer Model of the Governing Equations

As stated in section 4.1. the MacCormack method yields best results for a nonlinear equation, therefore we apply MacCormack method to our governing equations. We repeat here our three equations:

continuity:

$$\frac{\partial \rho}{\partial t} + \frac{\partial G}{\partial x} = 0$$

momentum:

$$\frac{\partial G}{\partial t} + \frac{\partial}{\partial x}\left(\frac{G^2}{\rho} + P\right) = friction\ term$$

energy:

$$\frac{\partial}{\partial t}\left[\rho e + \frac{G^2}{2\rho}\right] + \frac{\partial}{\partial x}\left[G\left(h + \frac{1}{2}\left(\frac{G}{\rho}\right)^2\right)\right] = heat\ \ flux\ term$$

It is convenient to represent these equations in a system of equations as:

$$\frac{\partial \mathbf{U}}{\partial t} + \frac{\partial \mathbf{F}}{\partial x} = \mathbf{C} \tag{4.15}$$

where,

$$\mathbf{U} = \begin{bmatrix} \rho \\ G \\ \rho e + \dfrac{G^2}{2\rho} \end{bmatrix}, \quad \mathbf{F} = \begin{bmatrix} G \\ \dfrac{G^2}{\rho} + P \\ G\left(h + \dfrac{1}{2}\left(\dfrac{G}{\rho}\right)^2\right) \end{bmatrix} \quad and \quad \mathbf{C} = \begin{bmatrix} 0 \\ pressure\ drop \\ heat\ flux \end{bmatrix} \tag{4.16}$$

Although ρ, G, P and *total energy* are the dependent variables, discretisation is applied directly to U and F. When applied to the system of equation, the MacCormack method becomes:

$$\overline{U_j^{n+1}} = U_j^n - \frac{\Delta t}{\Delta x}\left(F_{j+1}^n - F_j^n\right) + \Delta t\left(C_i^n\right) \quad forward\ predictor\ step$$

$$U_j^{n+1} = \frac{1}{2}\left[U_j^n + \overline{U_j^{n+1}} - \frac{\Delta t}{\Delta x}\left(\overline{F_j^{n+1}} - \overline{F_{j-1}^{n+1}}\right) + \Delta t\left(C_i^n\right)\right] \quad backward\ corrector\ step \tag{4.17}$$

At each stage of solution, ρ, G, P and e are evaluated from **U** (equation 4.16) so that the components of **F** can be determined.

The explicit solution of the system of equation (4.16) requires very small time-steps due to the numerical stability requirement of the MacCormack scheme. This restriction was explained in Chapter 3.

In our sample simulation cases the maximum available time step size found to be of the order of 0.001 sec.

First a simple code is developed for 1-D single phase flow. Runs are carried for single phase flow to understand the behaviour of the selected numerical scheme and some parameter for a system of equations. Runs for single phase flow are much faster than that

of two phase since it uses ideal gas equalities to find some thermodynamic variables. These equalities are :

$$\begin{aligned} P &= \rho RT \\ e &= c_v T \\ h &= c_p T \end{aligned} \qquad (4.18)$$

After seeing that the MacCormack scheme is still well behaved for the system of equations, another computer program is developed to simulate two phase flow with homogeneous flow model. Unfortunately, two phase flow refrigerant thermodynamic variables are not easy to calculate. A commercial software REFPROP [32] is used for this purpose. Several refrigerants and mixtures of refrigerants properties are available. Each refrigerant is represented by a file with extension "*.fld". Two refrigerants are chosen for the model developed, R134a and R22. For the rest of the refrigerant and mixture, the only thing to do is to copy related "*.fld" files into the project workspace of the FORTRAN code.

The algorithm of two phase flow code needs following thermodynamic relations.

Relation required	REFPROP supports
$\rho, T = f(P,h)$	✓
$speed\ of\ sound, cs = f(P,x)$	✓
$P, T = f(\rho,h)$	✗
$P, T = f(P,e)$	✗
$h, T = f(P,\rho)$	✗

For each relation, a number is assigned in the computer code to represent it. When REFPROP is called, this information is also send and related process are followed.

If REFPROP does not support a relation, related subroutines are modified to give desired values. The modification is done on available relation subroutine by introducing an iterative procedure to approximate the variable. For example, if P is needed as a function of ρ and h, the subroutine for $\rho, T = f(P,h)$ is called and P values are changed until ρ value of the $\rho = f(P,h)$ is equal to the known ρ.

Although the time step of two phase runs are larger than that of single phase runs, these subroutine calls and iterations increase significantly the total execution time of two phase flow runs.

5. RESULTS

5.1. Flow Patterns for an Evaporation in a Household Refrigerator

The flow patterns occurring in a typical household refrigerator evaporator is predicted with the aid of Figure 1.3. given in Section1.2.2. Points for refrigerant R134a at -25°C are evaluated using local flow parameters and plotted on this figure. It is seen that the flow is mostly wavy and stratified

5.2. Pressure Drop Calculations

Pressure drop due to gravity is very small comparing to pressure drop due to friction and pressure drop due to acceleration.. Therefore it is ignored in following discussions.

Results for an evaporator case obtained by evaluating correlations found in the surveyed literature are tabulated and given in Appendix A, Table A.1.

Summing the three pressure drop terms (friction, acceleration and bend) for L=15 m. and 25 bends, the resulting pressure drop is roughly 5-6 kPa. Which is approximately 5-10 per cent of the saturation pressure of a typical evaporator condition.

5.3. Void Fraction and Refrigerant Charge Prediction Calculations

Among the various void fraction models collected by Rice[16], homogenous (it is the simplest), Smith (it is an advanced slip-ratio correlated method), Lockhart-Martinelli (it is X_{tt} correlated and Domanski and Didion [10] used it in their simulation), Tandon, and Premoli (they are both mass-flux dependent methods) models are chosen for comparison. Hughmark method is skipped because of its complexity.

The conditions assumed for evaluation of the void fraction models are given in Table 5.1.

TABLE 5.1. Conditions assumed for evaluation of the void fraction models

	evaporator	**condenser**
$\dot{m}_r$	3.5 kg/hr	3.5 kg/hr
d_i	6.5×10^{-3} m	3.36×10^{-3} m
L	15 m	18 m
$A_{cross\ section}$	3.32×10^{-5} m^2	8.87×10^{-6} m^2
G	$\approx$ 30 kg/m^2.s	$\approx$ 110 kg/m^2.s
x_i / x_o	0.2 / 1.0	1.0 / 0.0

Calculations are done and graphics are prepared with Mathcad 6.0, which is a general purpose mathematical computing environment for numerical calculation and symbolic manipulation.

Examination of different models done for liquid fraction predictions and mass predictions. Conclusions of these studies are given in the following paragraphs, results and figures are given in Appendix B.

It is convenient to give the results in term of liquid fraction, $(1-\alpha)$, since the refrigerant liquid term is the major contributor to the total mass in the heat exchanger.

It is seen from the figures given in Appendix B, that the more involved models generally predict more liquid presence then the homogeneous baseline. At higher saturation pressures the heat exchanger mass quality range is occupied by more liquid. This is due to an increase in the gas to liquid density ratio which decreases void fraction at given quality level. Another conclusion is that the homogeneous method predicts very low void fraction at low saturation pressure.

The results to be shown for mass inventory predictions are given in general terms of average two phase refrigerant density, ρ_{tp} , which is directly proportional to the total refrigerant mass in the two phase section of the heat exchanger, i.e.,

$$\rho_{tp} = \frac{m_t}{V} \qquad (5.1)$$

Figure and tables of mass inventory predictions are given in Appendix B. Predicted mass in evaporators is in wide range, whereas is close to each other for different models.

The choice of two phase void fraction model is of major significance in determining the charge in the condensers and especially in the evaporators. Figure B.3 can be used as a guide to the inventory predictions of the various models.

Rice [16] concluded that the choice of heat flux assumption is insignificant for forced convection evaporators and of secondary importance after the choice of the void fraction model for condensers.

Literature comparisons with experimental data is also made by Rice[16].He concluded that the highest predicting void fraction models for condensers (where most charge is located), such as Hughmark, Premoli, Tandon, and Baroczy, will give closest agreement for total system charge. There are not sufficient data to recommend any one method. However, the Premoli method gives an approximate average of the above methods.

For a more accurate predictions, the solubility of refrigerant in the compressor oil must also be considered.

5.4. Heat Transfer Calculations

The correlations except ACRC and Pierre's works, are developed from data obtained for evaporators used in industrial cooling. Therefore, cooling capacities, refrigerant mass flowrate, and tube diameters of these evaporators are different than that of household refrigerators.

According to Pierre's correlation a typical value for the heat transfer coefficient of a domestic refrigeration evaporator is about 350 W/m^2C. The value is constant throughout the evaporation process since the correlation is independent of quality.

Table comparing the other correlations is given Appendix C.

5.5. Numerical Solutions

Following figures show some simulation results obtained with the MacCormack numerical scheme where, for clarity zero pressure drop was assumed.

5.5.1. Simulations for Single Phase Flow

Figure 5.2. and 5.3. shows pressure and mass flux profiles respectively for a 6 m. long evaporator with refrigerant R22 with initial conditions ($G = 244$ kg/m^2.s, $T = 400$ K, and $P = 1100.0$ kPa) at different times after a sudden disturbance (49 kg/m^2.s) in inlet mass flow rate at $t = 0$. These conditions are identical with Koenig's simulations except temperature, which is taken a high value to approach the ideal gas conditions.

Due to the compressibility of the medium, a wave propagates towards the outlet end. The fluid behind the wave front is at a high pressure and a high flow rate owing to the necessary pressure forces to accelerate the fluid. When the pressure wave reaches the exit of the tube where a fixed pressure boundary condition is defined, resulting pressure forces further accelerate the flow disturbance to twice its original value. As a consequence, a backward flowing pressure wave and a corresponding mass flow wave result. At the inlet side of the tube, the mass flux is prescribed, and the pressure is free which causes the wave reflections shown in the related chart.[24]

Figure 5.4. and 5.5. shows pressure and temperature profiles for the evaporator with identical initial conditions as above at different times after a 40 K step increase in inlet temperature at t=0. The sudden change in inlet temperature at constant inlet mass flow rate causes an increase in inlet pressure and accelerates the flow downstream of the inlet. Hence a similar situation as in Figure 5.2. arises: Pressure waves travelling at near sonic velocity from inlet to outlet. The temperature wave moves much slower at the fluid velocity. The numerical dispersion errors in Figure 5.4. and 5.5. is unacceptable. Therefore grid sensitivity and effect of CFL number are investigated since it was seen in Section 4.1. that they work well when numerical errors became significant These errors can be circumvented by decreasing the CFL number and increasing node number, Figure 5.6 and

5.7 gives simulation results with CFL=0.5 and increased node number ten times. Although some oscillations still exist, solutions are now acceptable.

Figure 5.8. shows wall temperature of the heat exchanger for adiabatic and non-adiabatic wall conditions. As seen on the Figure, when an adiabatic wall condition is applied, the heat exchanger wall temperature reached to the new refrigerant temperature at steady state. On the other hand, for the non-adiabatic wall condition, the wall temperature remained below the new refrigerant temperature by some degree (2-3 degree). Therefore, it can be concluded that a temperature measurement taking from the surface of the heat exchanger will not give the exact fluid temperature.

5.5.2. Simulations for Two Phase Flow

The programming logic of the two phase flow simulations are exactly the same as single phase flow. In two phase flow simulations, fluid thermodynamic properties are found by calling REFPROP. As stated in Section 4.3., these call procedures and iterations for converging some properties which are not supported directly by REFPROP slows the simulation, so that only limited number of runs are carried. Heat transfer and pressure drop effects are neglected in these simulations

Figure 5.9. and 5.10. shows mass flux and pressure profiles respectively for a 6 m. long evaporator with refrigerant R22 with initial conditions identical as Koenig's work (G=244 $kg/m^2.s$, h=167.472 kJ/kg and P=1093.515 kPa) at different times after a sudden disturbance (49 $kg/m^2.s$) in inlet mass flow rate at t = 0.

Figure 5.11. and 5.12. shows pressure and enthalpy profiles for the evaporator with identical initial conditions as above at different times after a 23.26 kj/kg step increase in inlet enthalpy at t=0. The dotted square waves in Figure 5.12. indicate where the enthalpy wave should be according to the average fluid particle velocity. [24].

5.5.3. Discussion and Comparison with The Surveyed Literature

Among the surveyed literature, there are two studies which worked with three conservation equations without ignoring kinetic energy terms in the energy equations.

Dupont et al.[23] made a numerical comparison between a reference and simplified two phase flow models. They preserved the homogeneous form of the conservation equations by introducing the mixture variable concept. A model taking into account the complete three equations is used as a reference. They concluded that two phase flow dynamics can be simplified from three to one differential equation namely energy equation. This transient solution can be named as thermal transient. However for a true simulation of transients involving sonic effects, that is rapid variation of mass flow rate and pressure, three equations remain necessary. They used a first order implicit method based on the trapezoidal rule.

The idea of mixture variable is used by all other researchers, Koenig and Brasz [24] first modelled complete system of equation using a θ differencing scheme. Even with implicit case of the scheme the method is found to be too slow. Then they neglected both dynamic and static acceleration terms in the momentum equation. They concluded that their simplified model is useful and practical for overall system simulation.

Simulation results obtained with the model presented in this study are compared with Koenig's simulation results for similar disturbance in boundary conditions. Except the excessive computer time required, the presented model showed similar characteristics and better accuracy to simulate transient behaviour.

Other studies in the literature are directly used a simplified model which is explained in Section 2.3.1. MacArthur and Grald [25], and Wang and Touber [17], considered the momentum equation as time independent and ignored kinetic and potential energy terms in the energy equation. MacArthur and Grald included accumulator in their model. They used an implicit upwind scheme with variable time steps and they used Zivi void fraction model. Wang and Touber assumed a constant evaporator temperature in their model. The pressure drop was taken into account at the end of the two phase flow region. (However, Jia et. al. [26], did not agreed with this assumption.) They also presented a simplified void fraction equation by numerically solving the momentum equation. They used an implicit finite difference method, and they suggested to use variable time steps in order to save computational costs.

Some researches used three conservation equations but ignored the kinetic and potential energies in the energy equations. Jia et. al., accepted the two phase flow as a homogeneous flow to calculate void fraction. They used an implicit discretisation and

Newton-Raphson algorithm for the iteration processes. Sorenson et al. [22], applied a software originating in the aerospace industry, and made with the purpose of modelling and simulating general thermo-fluid systems to a domestic refrigerator. The software used same equations with Jia et al. and solved them using finite difference approximation. The authors reported long execution time.

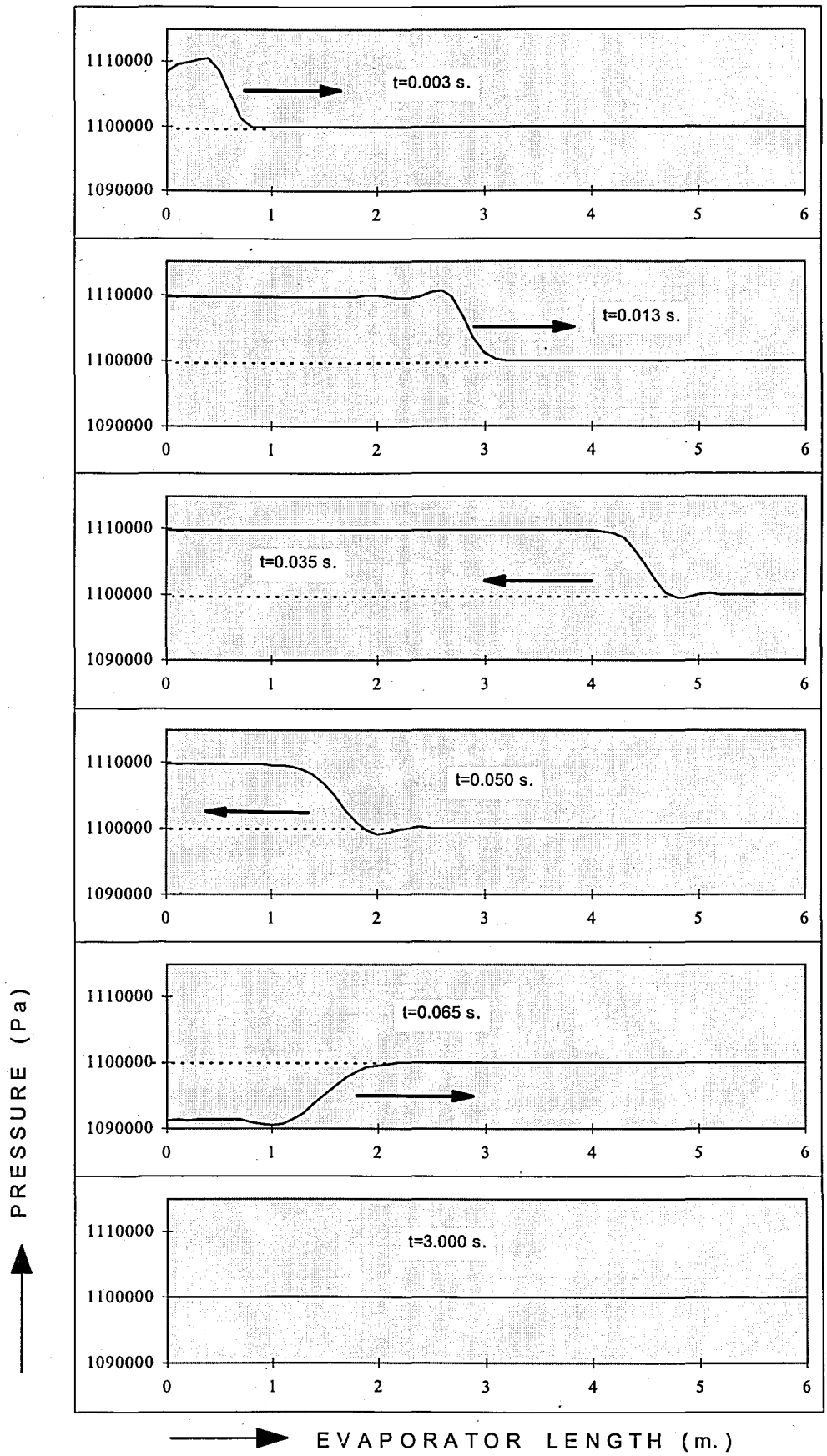

FIGURE 5.2. Pressure profiles at various moments after an inlet disturbance in mass flow rate

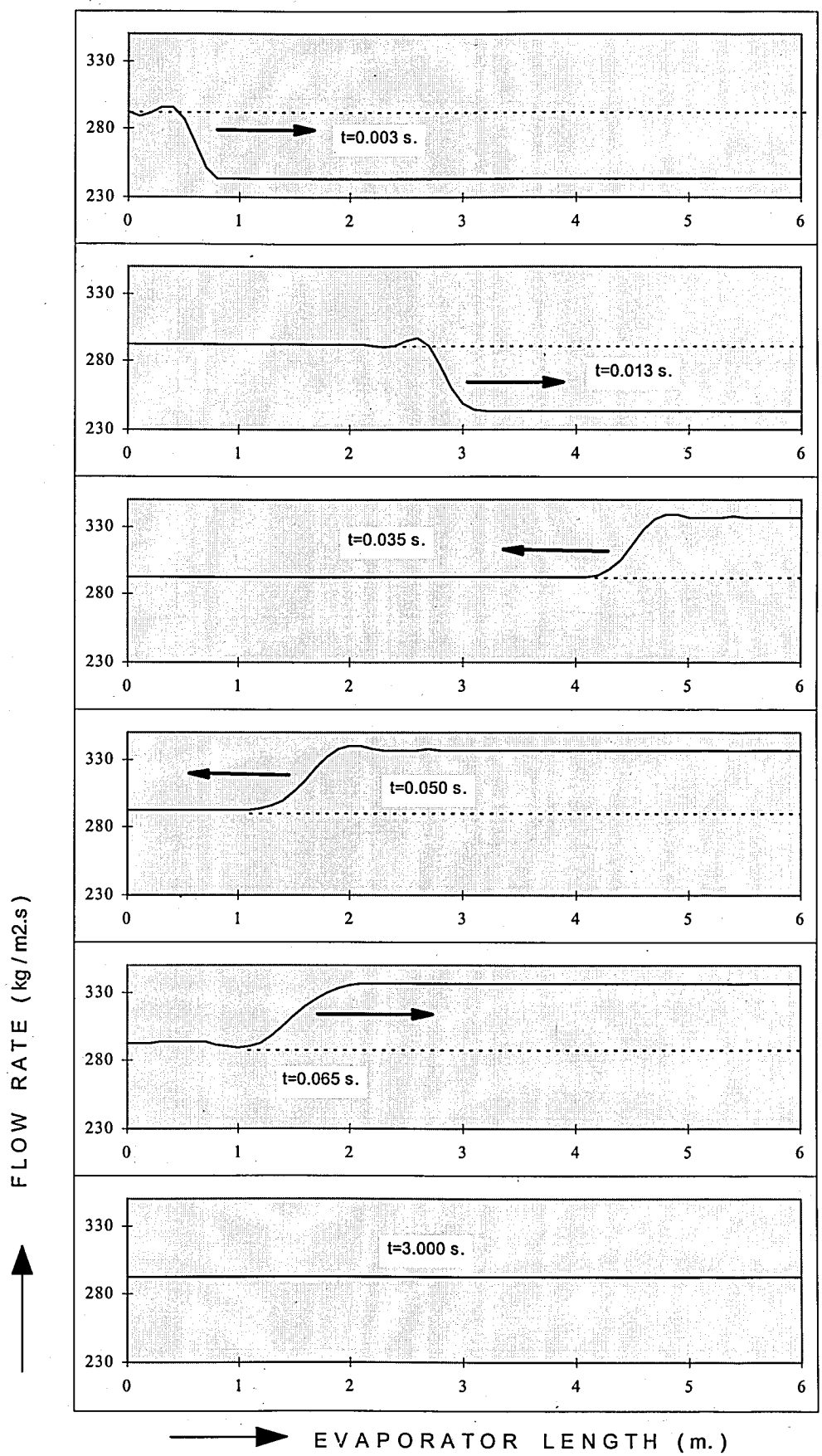

FIGURE 5.3. Flow profiles at various moments after an inlet disturbance in mass flow rate

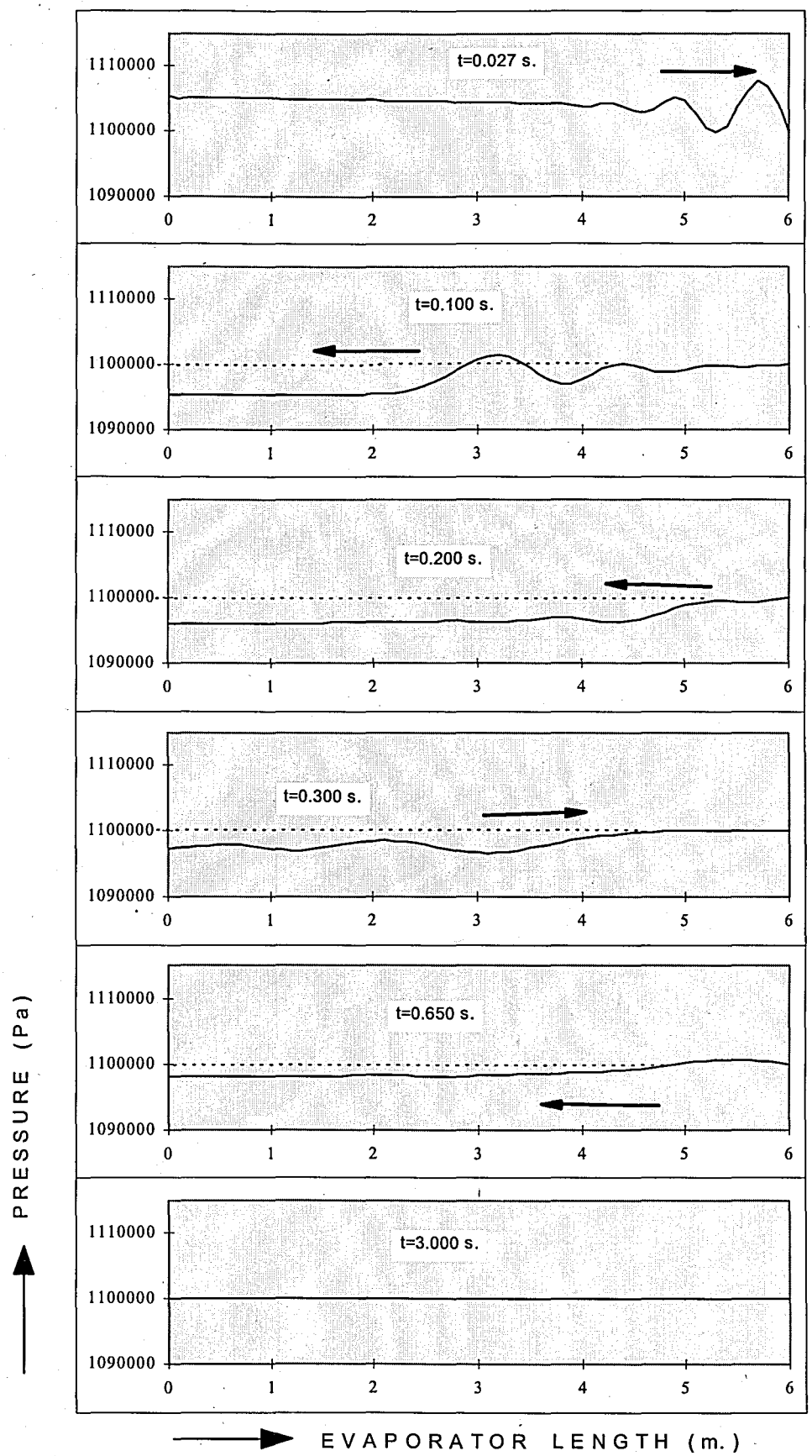

FIGURE 5.4. Pressure profiles at various moments after a disturbance in temperature (coarse grid and CFL=0.9)

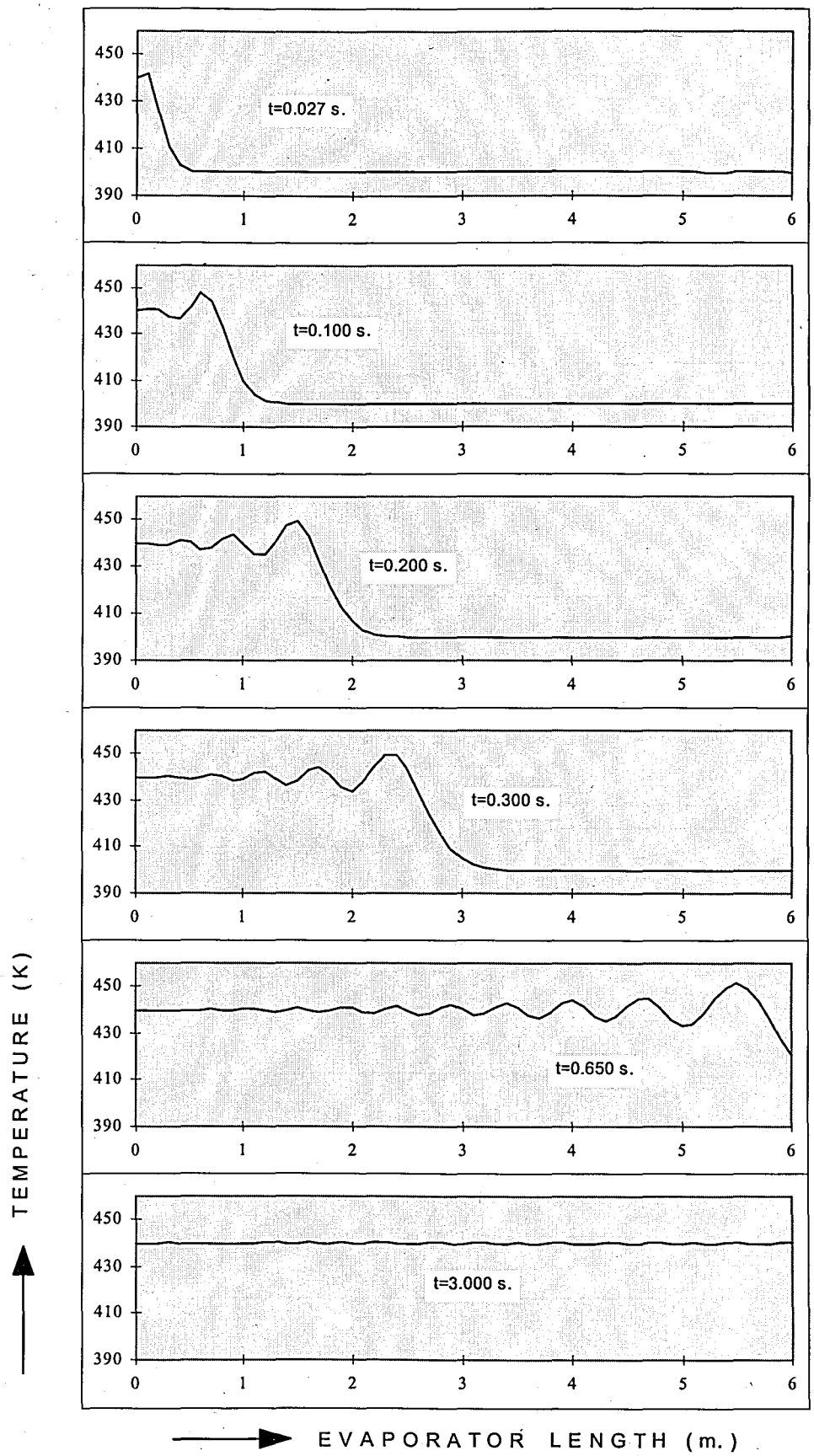

FIGURE 5.5. Temperature profiles at various moments after a disturbance in temperature (coarse grid and CFL=0.9)

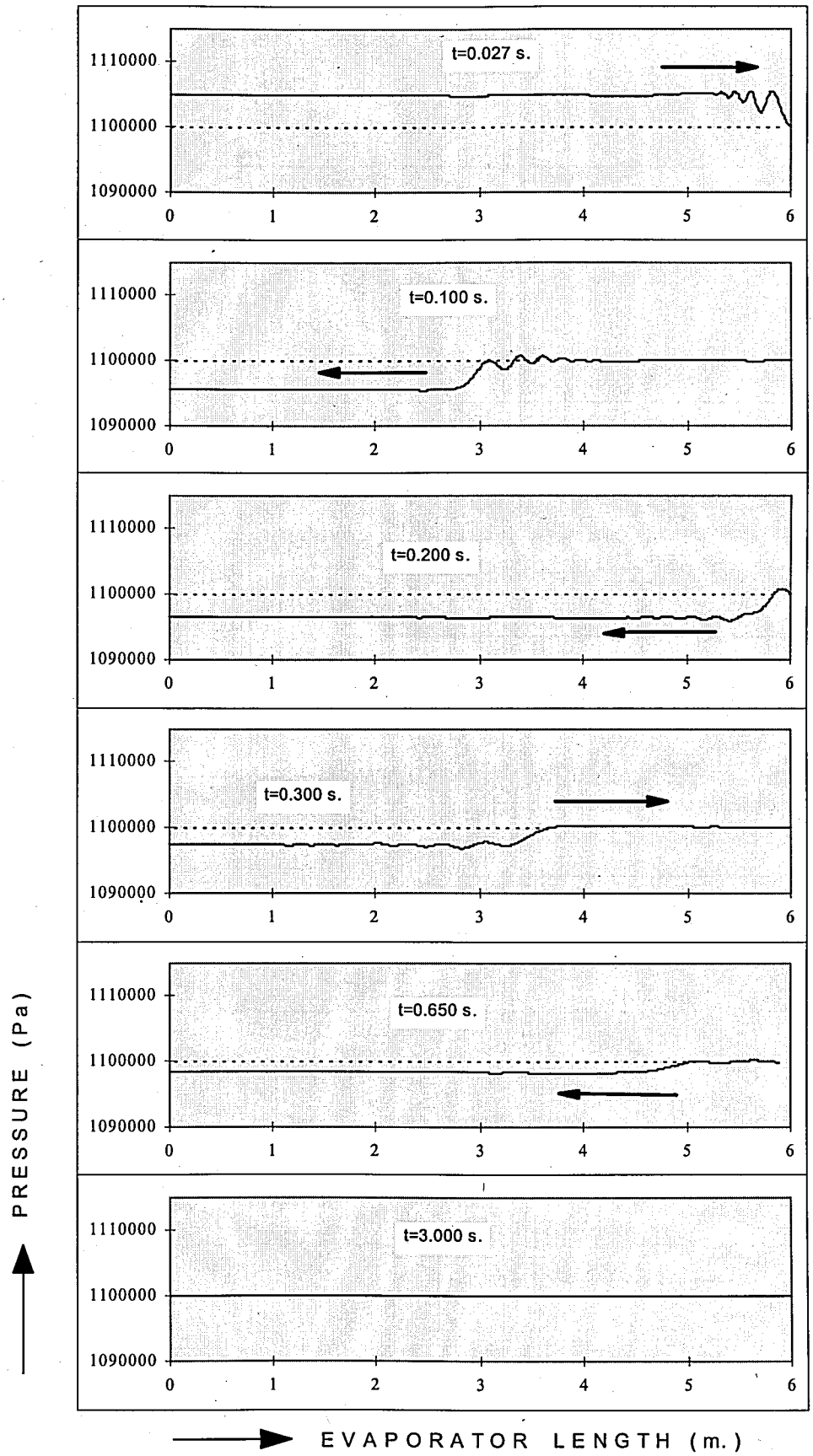

FIGURE 5.6. Pressure profiles at various moments after a disturbance in temperature (fine grid and CFL=0.5)

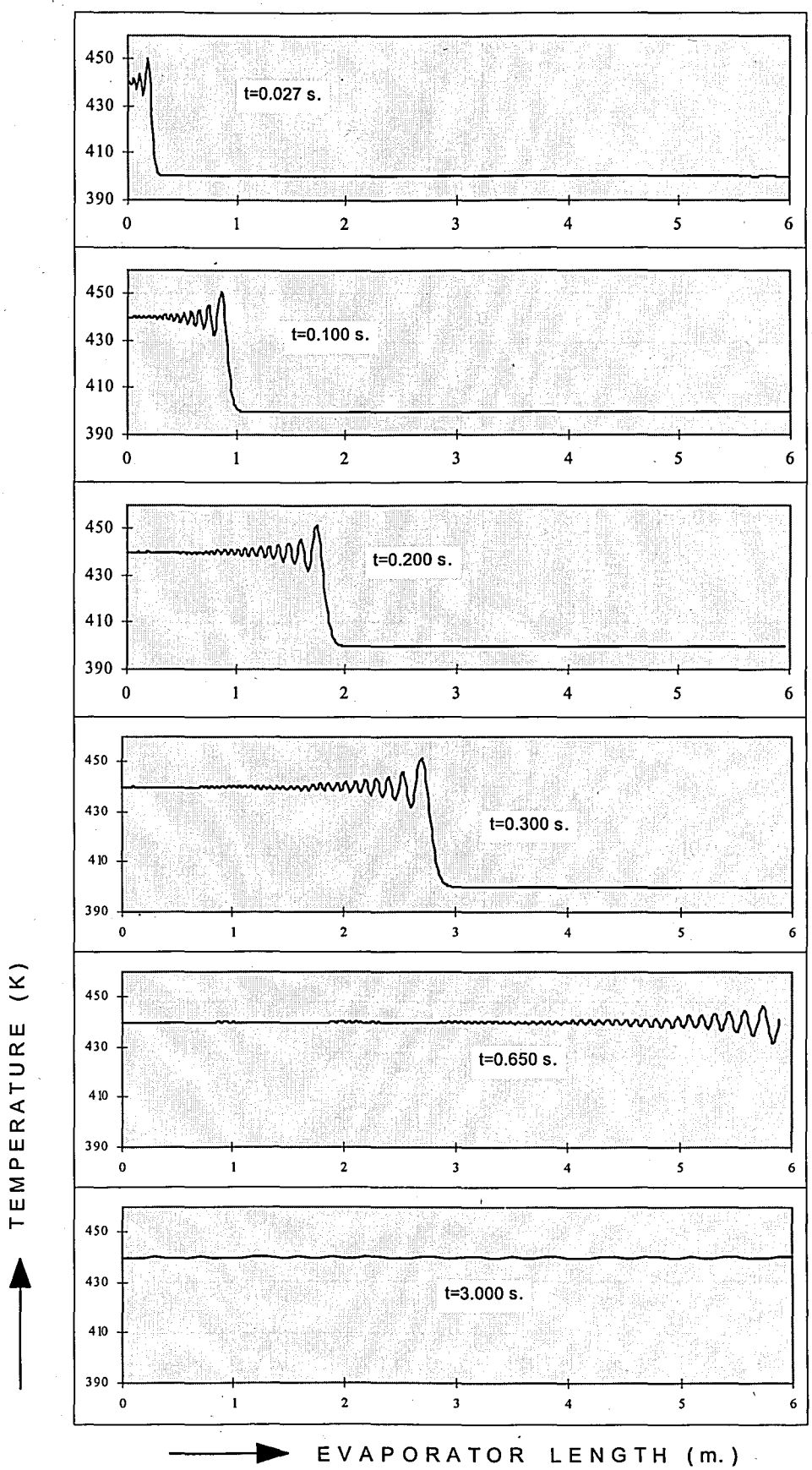

FIGURE 5.7. Temperature profiles at various moments after a disturbance in temperature (fine grid and CFL=0.5)

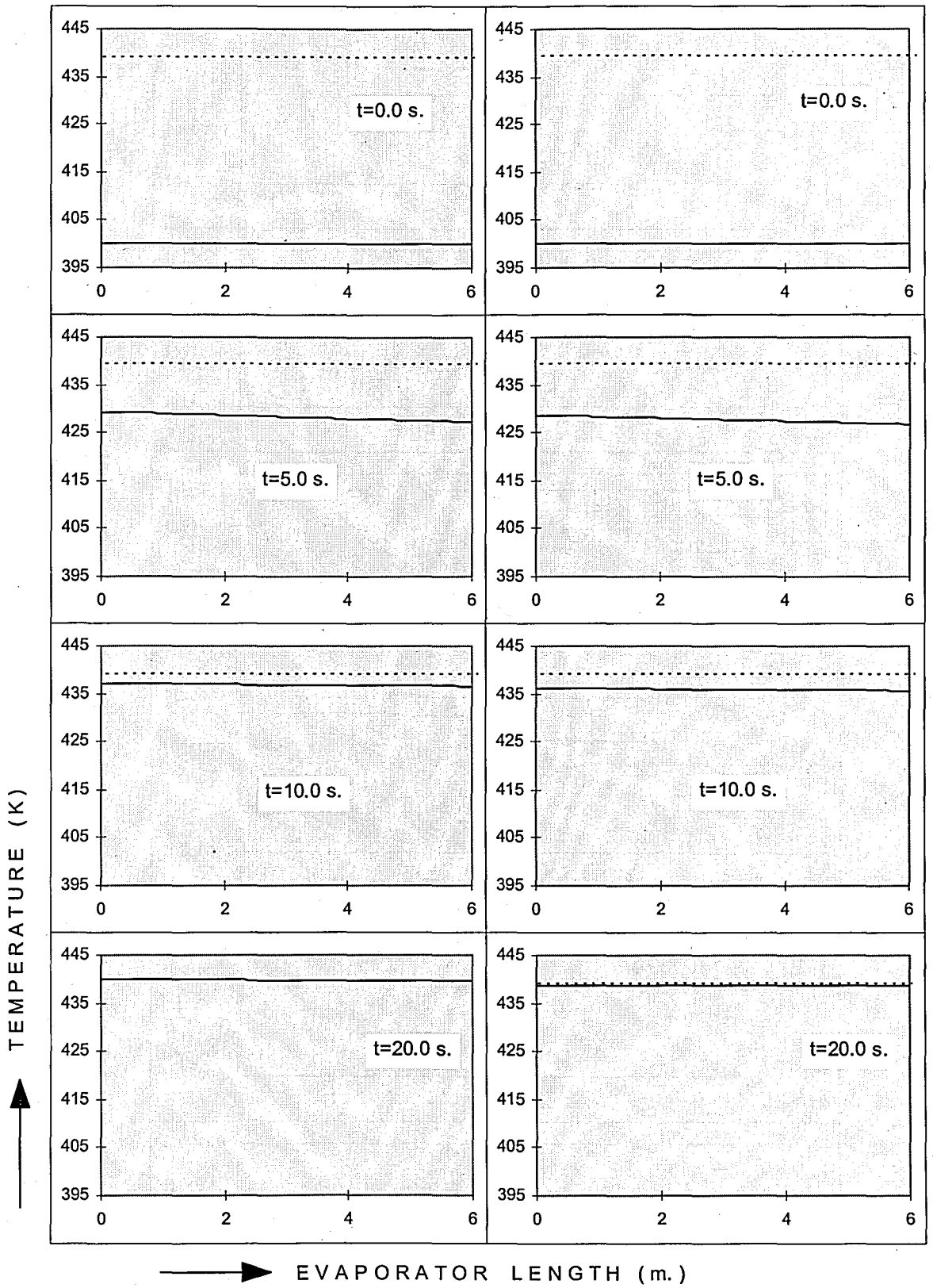

FIGURE 5.8. Heat exchanger wall temperature profiles for adiabatic (h_a=0.0) and non-adiabatic (h_a=9.0) wall conditions

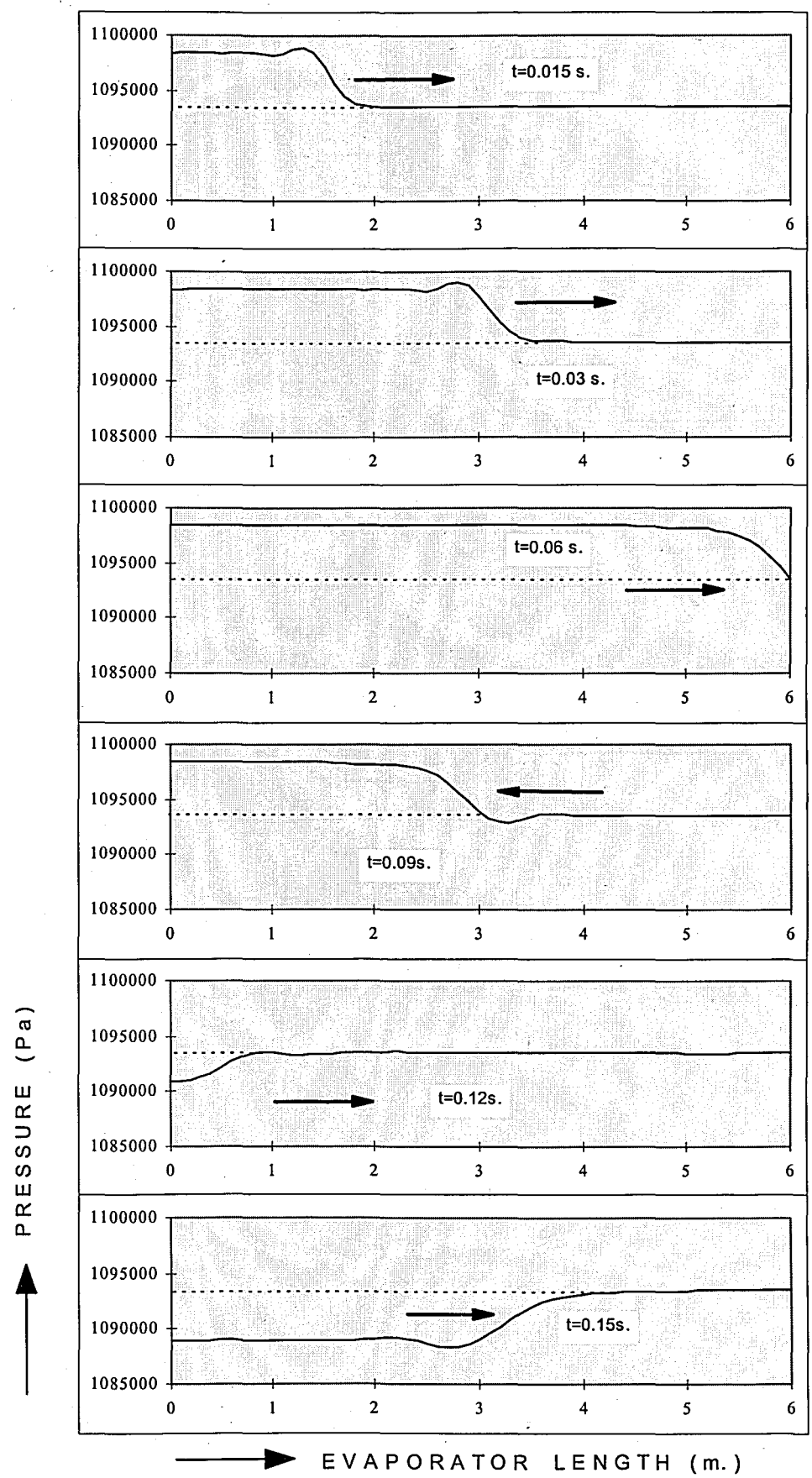

FIGURE 5.9. Pressure profiles at various moments after an inlet disturbance in mass flow rate

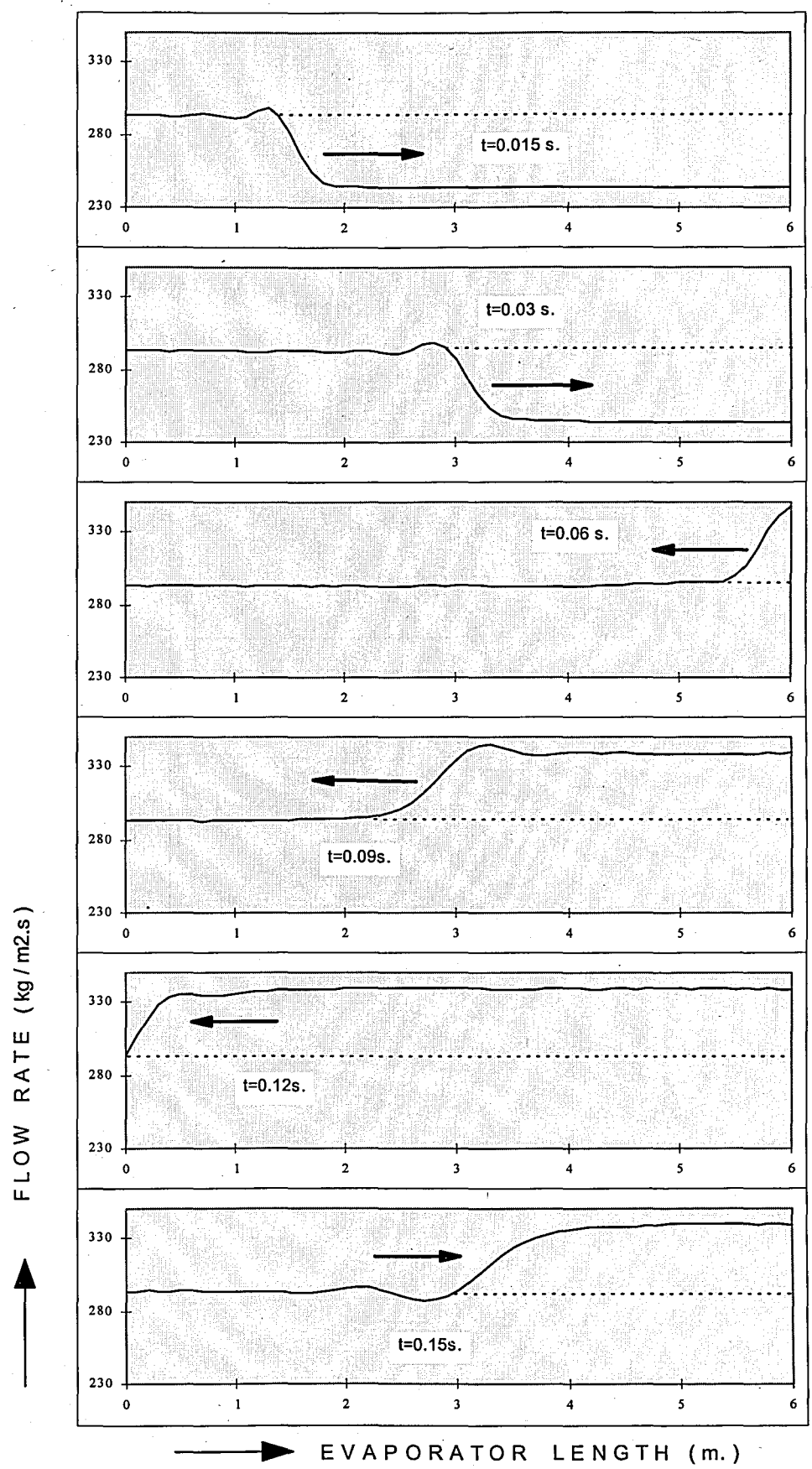

FIGURE 5.10. Flow profiles at various moments after an inlet disturbance in mass flow rate

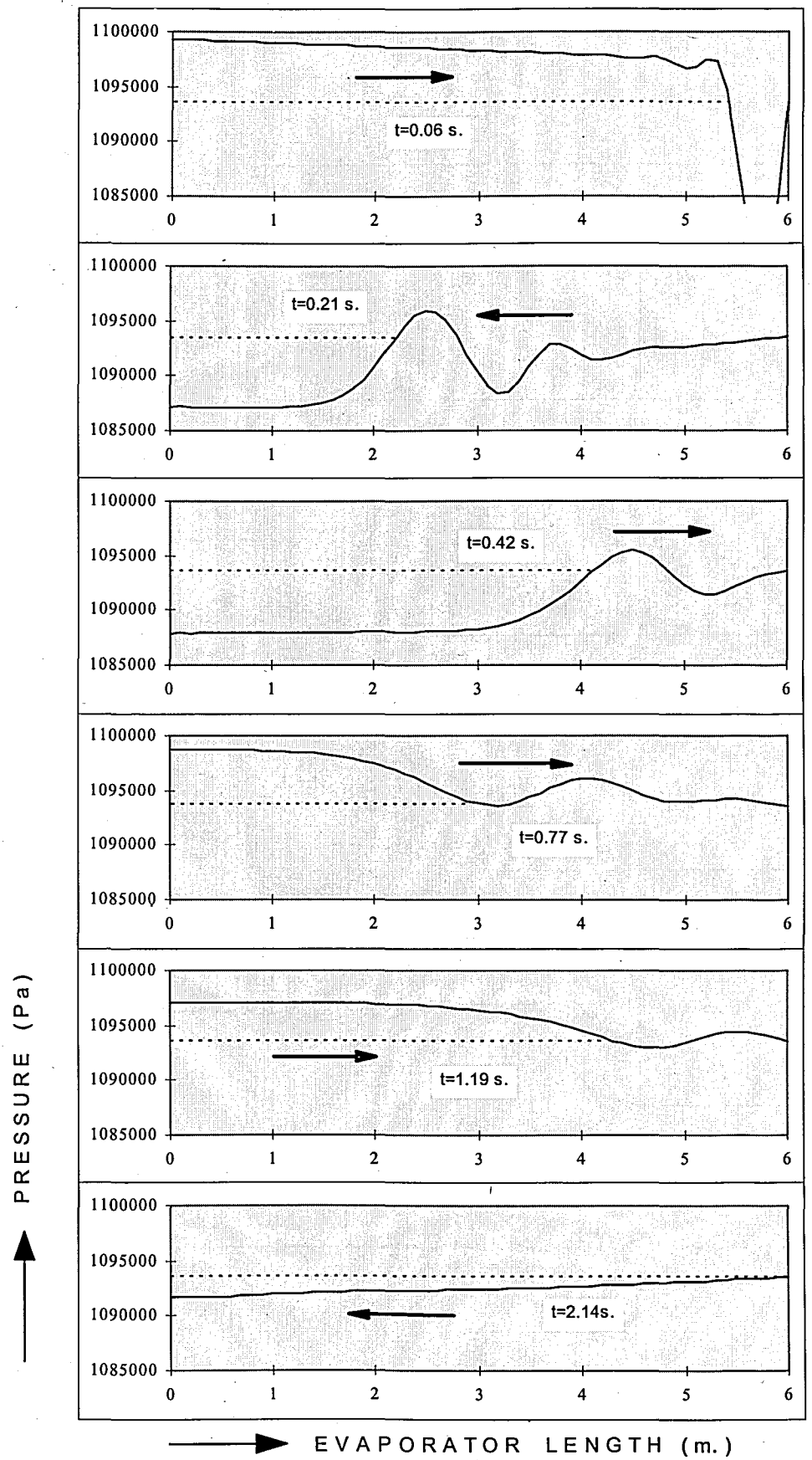

FIGURE 5.11. Pressure profiles at various moments after an inlet disturbance in enthalpy

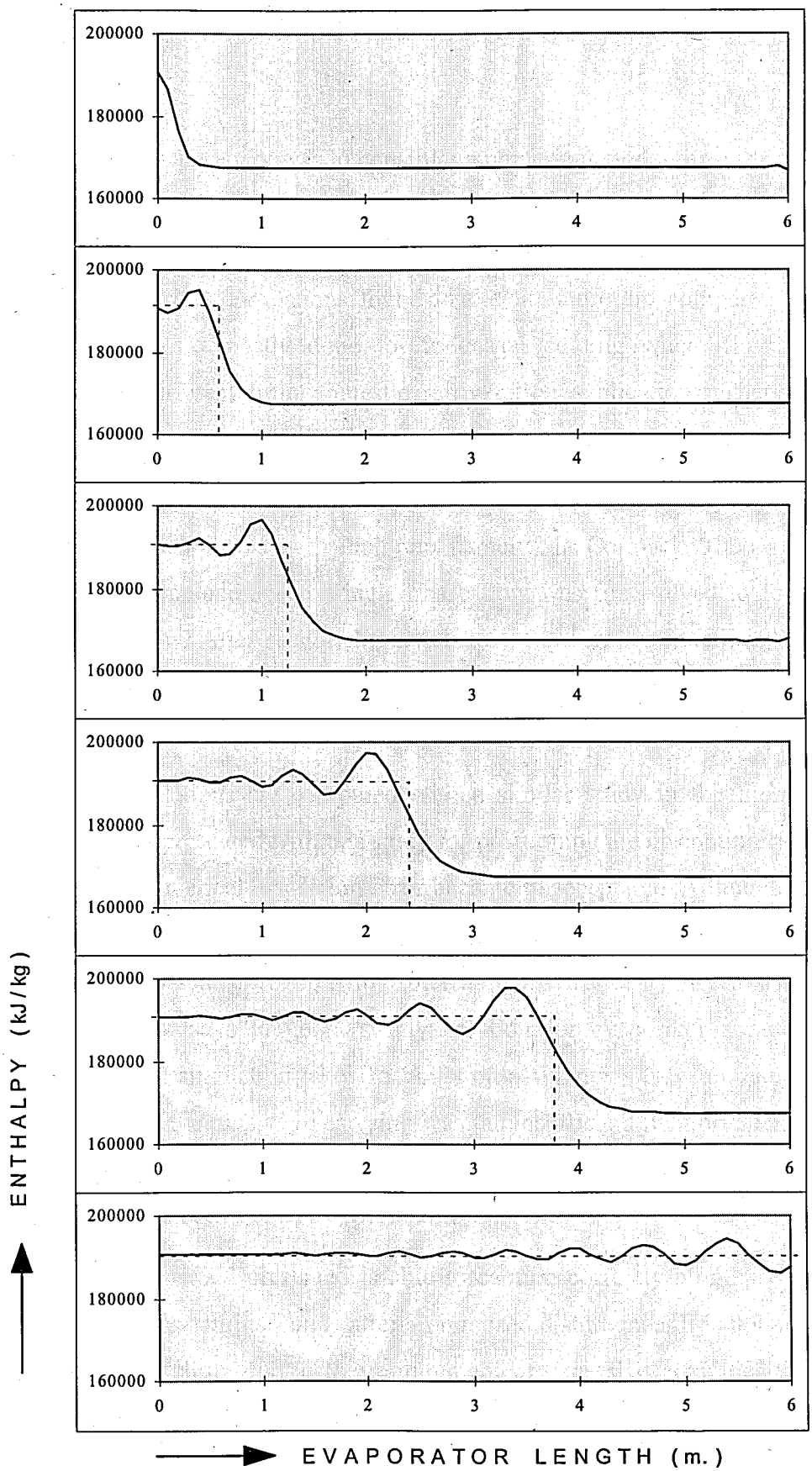

FIGURE 5.12. Enthalpy profiles at various moments after an inlet disturbance in enthalpy

6. CONCLUSIONS

The objective of this study was to construct a numerical model for one dimensional two phase flow occurring in the heat exchangers used in domestic refrigeration. A detailed literature review is performed on physical characteristics of two phase flow and heat transfer in tubes. Empirical correlations found in the literature are compared with each other. Related studies are mostly done for industrial cooling where flow rates and geometries are quite different from domestic refrigeration applications. Therefore for a study like this one, it is not worthwhile to take advanced correlations.

A computer program is developed to numerically model 1-D two phase flow in tubes. The numerical method was an explicit one, namely MacCormack. The accuracy was second order both in time and space. Single phase flow was first solved to form a base study for two phase flow. After seeing characteristics of governing equations, two phase flow model was constructed. Pressure drop and heat transfer mechanisms are made optional in the developed program.

Results of simulations are compared with a similar study in the literature. The accuracy of the method presented with this study for positioning the discontinuity is better. In some applications numerical dispersion error became unacceptable. Although the errors can be circumvented in some degree with smaller CFL number and using very fine grid, another disadvantage arised: execution time increased tremendously. Even with today's fast computers, it costs days to get a steady solution for evaporator simulation. For example, a three second simulation takes 15 hours on a Windows NT computer. Another problem occurred when the runs were carrying was the insufficient memory. This was due to a execution error of the FORTRAN PowerStation 4.0. This problem is solved by installing a patch program developed by Microsoft.

The numerical method presented is able to capture correctly high speed pressure waves occurred in the few milliseconds after an imposed disturbance. It is not suitable for a complete system modelling due to the requirement of excessive computer time. Even with today's high speed personal computers, it costs about 10-15 hours to simulate 3 seconds of an evaporator.

Following future works are recommended:

On the modelling side: Inlet and outlet boundary conditions may be modified as functions of time. To improve computation time a reduced model may be used. This reduced model will neglect pressure wave dynamics, therefore uses only two equations; continuity and a modified energy conservations (Section 2.3.1). Spatial variations of pressure may be replaced by an empirical correlation for calculation the pressure drop in the two phase flow region. The accumulator which is placed at the end of the evaporator before the compressor inlet can be added to the model.

On the numerical side: An implicit method may be used with variable time stepping. Implicit method must be applied to the reduced model equations. If pressure wave dynamic is required, parallel computing tools may be used to reduce computer time. Effects of using control-volume formulation with upwind scheme and staggered grid arrangement may be investigated.

Finally, the model presented in this study can be taken as a base and reference model for future simplified model and for other numerical methods

APPENDIX A : Pressure Drop Correlations

Mixture viscosity relations for homogeneous flow assumption given in Collier and Thom, [10] in their textbook are summarised below:

McAdams et al. proposed following equation:

$$\frac{1}{\bar{\mu}} = \frac{x}{\mu_g} + \frac{1-x}{\mu_f} \qquad (A.1)$$

Cicchitti et al. chose another equation:

$$\bar{\mu} = x\mu_g + (1-x)\mu_f \qquad (A.2)$$

Dukler et al. suggested:

$$\bar{\mu} = \bar{\rho}\left[x\upsilon_g\mu_g + (1-x)\upsilon_f\mu_f\right] \qquad (A.3)$$

$$\bar{\rho} = \frac{1}{(1-x)\upsilon_f + x\upsilon_g} \qquad (A.4)$$

Other correlations for separated flow (Friedel's, Paliwoda's, and Wattelet's correlations) are summarised below for reference:

Friedel using a large data base of two phase pressure drop measurements, gives following correlation for frictional multiplier[10] :

$$\phi_{lo}^2 = A_1 + \frac{3.24\,A_2\,A_3}{Fr^{0.045}We^{0.035}} \qquad (A.5)$$

where

$$A_1 = (1-x)^2 + x^2\left(\frac{\rho_l f_{lo}}{\rho_g f_o}\right)$$

$$A_2 = x^{0.78}(1-x)^{0.224}$$

$$A_3 = \left(\frac{\rho_l}{\rho_g}\right)^{0.91}\left(\frac{\mu_g}{\pi_l}\right)^{0.19}\left(1-\frac{\mu_g}{\mu_l}\right)^{0.7}$$

$$Fr = \frac{G^2}{gD\bar{\rho}^2}$$

$$We = \frac{G^2 D}{\bar{\rho}^2 \sigma} \quad ,$$

$$and \qquad \bar{\rho} = \frac{1}{\frac{x}{\rho_g} + \frac{1-x}{\rho_l}}$$

Standard deviations of the correlation are found to be 40-50 per cent which is large with respect to single phase flows, but quite good for two phase flows.[10]

Collier and Thom also mentioned that Whalley has evaluated separated flow models against a large proprietary data bank and gives the following recommendation:

a) For $(\mu_l / \mu_g) < 1000$: Utilise the Friedel correlation;

b) For $(\mu_l / \mu_g) > 1000$ and G > 100 kg/m^2.s : Utilise the Chisholm correlation;

c) For $(\mu_l / \mu_g) > 1000$ and G < 100 kg/m^2.s : Utilise the correlations of Lockhart Martinelli.

For most fluids and operating conditions, (μ_l / μ_g) is less than 1000 and the Friedel correlation will be the preferred method.

Paliwoda[12] proposed a relatively simple correlation:

$$\frac{\partial p}{\partial z} = \frac{0.3164}{2} G^{1.75} \frac{\mu_g^{0.25}}{\rho_g} d_i \beta_m' \qquad (A.6)$$

here β_m is a two phase flow factor given in reference [12] in a tabulated form which change with liquid / vapour pressure gradient ratio, θ :

$$\theta = \begin{cases} \dfrac{64}{0.3164}\dfrac{\mu_f}{\mu_g^{0.25}}\dfrac{\rho_g}{\rho_f}\left(G.d_i\right)^{-0.75} & \textit{for laminar liquid and turbulent vapour flow.} \\ \dfrac{\rho_g}{\rho_f}\left(\dfrac{\mu_f}{\mu_g}\right)^{0.25} & \textit{for turbulent liquid and turbulent vapour flow.} \end{cases} \qquad (A.7)$$

Wattelet et al. [6] used the correlation for the two phase multiplier which was developed for horizontal, evaporating flow in smooth, straight tubes and was presented in ACRC Technical Report 25. It was defined as :

$$\phi_l^2 = 1.376 + C_1 X_{tt}^{\ C_2} \qquad (A.8)$$

Where C_1 and C_2 are functions of mass flux. The mass flux dependence of the coefficients was accounted for using the Froude number as :

For $0<Fr_l\leq 0.7$,

$$\begin{aligned} C_1 &= 4.172 + 5.48 Fr_l - 1.564 Fr_l^2 \\ C_2 &= 1.773 - 0.169 Fr_l \end{aligned} \qquad (A.9)$$

For $Fr_l>0.7$,

$$\begin{aligned} C_1 &= 7.242 \\ C_2 &= 1.655 \end{aligned} \qquad (A.10)$$

This correlation was tested for all of the refrigerants used in their study[6], and they found the mean deviation under ±20 per cent for all tests conducted in both annular and wavy flows.

The pressure drop due to momentum change for two phase flow can be estimated by the following equation: [6,13]

$$\left(\frac{dp}{dz}\right) = -G^2 \frac{d}{dz}\left[\frac{x^2}{\rho_g \alpha} + \frac{(1-x)^2}{\rho_l (1-\alpha)}\right] \qquad (A.11)$$

For two phase pressure drop in tees and bends Paliwoda developed a model.[14].

$$\Delta P_{bend} = N_b \left(\frac{G^2}{2\rho_g} \right) \xi \beta_c \qquad (A.12)$$

where :

N_b : number of bends,

ξ : coefficient of local resistance in single phase flow, and

β_c : two phase multiplier.

ξ values are given in table form by Paliwoda, Karatas [15] in his master thesis summarise Paliwoda's model and develop a function for local pressure drop coefficient :

$$\xi = 0.276 - 0.687 \log\left(\frac{R_b}{d_i}\right) + 1.229 \log^2\left(\frac{R_b}{d}\right) - 0.868 \log^3\left(\frac{R_b}{d_i}\right) \qquad (A.13)$$

This equation is valid for $1.0 \leq R_b/d_i \leq 4.0$. Here R_b is the radius of bend.

The two phase multiplier β_c, is :

$$\beta_c = \left[\theta + 3.0(1-\theta)x\right](1-x)^{0.333} x^{2.276} \qquad (A.14)$$

where

$$\theta = \frac{\rho_g}{\rho_l} \left(\frac{\mu_l}{\mu_g} \right)^{0.25} \qquad (A.15)$$

Another correlation for pressure losses in bends given by Chisholm is reported in some literature.[10,11]

$$\Delta P_{bend} = \Delta P_f \left(1 + \frac{C}{T} + \frac{C}{T^2} \right) \qquad (A.16)$$

where

$$T = \left(\frac{1-x}{x} \right) \left(\frac{\upsilon_f}{\upsilon_g} \right)^{0.5} \qquad (A.17)$$

$$\Delta P_f = \frac{1}{2} C_0 \upsilon_f (1-x)^2 G^2 \qquad (A.18)$$

$$C=\left[0.682+\left(C_2-0.682\right)\left(\frac{\upsilon_{fg}}{\upsilon g}\right)^{0.5}\right]\left[\left(\frac{\upsilon_g}{\upsilon_f}\right)^{0.5}+\left(\frac{\upsilon_f}{\upsilon_g}\right)^{0.5}\right] \qquad (A.19)$$

$$C_0=\frac{1}{16}\left(0.67-0.1\left(\frac{S}{r_i}\right)+6*10^{-3}\left(\frac{S}{r_i}\right)^2-10^{-4}\left(\frac{S}{r_i}\right)^3\right) \qquad (A.20)$$

$$S=\frac{1}{2}\left(S_l+S_m\right) \qquad (A.21)$$

For the coefficient C_2 , Wakeland used

$$C_2=1+\frac{20d_i}{S} \qquad (A.22)$$

Later a general expression for C_2 is given by Chisholm [10] :

$$C_2=1+\frac{2.2}{f\left(2+R/d\right)} \qquad (A.23)$$

S_l : distance between tube centers in neighbouring rows,

S_m : distance between tube centers in the same row,

r_i, d_i : inside tube radius, diameter,

f: single phase pressure drop coefficient,

R : radius of bend,

A correlation developed for return bend pressure drop was given in ACRC Technical Report 55 written by Wattelet et al.[6].

$$\Delta P_{bend}=\frac{6.93*10^{-5}}{4}X_{tt}^{-0.712}\left(\frac{r_i}{R_b}\right)^{0.5}\frac{Gd_i(1-x)}{\mu_f}G^2\left[(1-x)\upsilon_f+x\upsilon_g\right] \qquad (A.24)$$

To make comparison some of the correlations are evaluated and the results are given in Table A.1.

TABLE A.1. Pressure drop prediction by different models

Flow Approach	Source	Predicted Pressure Drop (Pa / m) or (Pa / bend)	
		Friction	bend
homogeneous	McAdams et. al.	172	–
	Cicchitti et. al.	308	–
	Dukler et. al.	158	–
separated	Chisholm	259	38
	Friedel	318	–
	Paliwoda	342	17

The acceleration pressure drop is estimated as 0.055 kPa per meter according to equation (A.12)

Summing the three pressure drop terms (friction, acceleration and bend)for L=15 m. and 25 bends, the resulting pressure drop is roughly 5-6 kPa. Which is approximately 5-10 per cent of the saturation pressure of a typical evaporator condition.

APPENDIX B : Void Fraction Models

Correlations listed below are taken from Rice's study[16] where he was collected various void fraction models.

A slightly more involved approach than homogeneous model is to assume that the liquid, $_f$ and vapour, $_g$ phases are separated into two streams that flow through the tubes with different velocities, u_g and u_f, the ratio of which is given by the slip ratio $S = u_g / u_f$. Including this effect to the original homogeneous form:

$$\alpha = \frac{1}{1 + \left[\frac{1-x}{x}\right]\frac{\rho_g}{\rho_f} * S} \qquad \text{(B.1)}$$

Rigot and Ahrens/Thom suggested using an average value of two for slip ratio for his intended application. Ahrens recommended use of the steam /water data of suitably generalised by the property index P.I. given by:

$$P.I. = \left[\frac{\mu_f}{\mu_g}\right]^{0.2} \frac{\rho_g}{\rho_f} \qquad \text{(B.2)}$$

with the data tabulated below:

P.I.	0.00116	0.0154	0.0375	0.0878	0.187	0.446	1.0
S	6.45	2.48	1.92	1.57	1.35	1.15	1.00

Zivi developed a void fraction equation similar in form to Equation (B.1) where S is given by:

$$S = \left(\frac{\rho_g}{\rho_f}\right)^{-1/3} \qquad \text{(B.3)}$$

This relationship was developed for annular flow based on principles of minimum entropy production under conditions of zero wall friction and zero liquid entrainment (100 per cent liquid entrainment gives a slip ratio of one).

Smith developed a correlation based on equal velocity heads of a homogeneous mixture center and an annular liquid phase. He obtained an equation for slip ratio S, dependent on the density ratio, mass quality, and entrainment ratio K given by:

$$S = K + (1-K)\left[\frac{\frac{1}{\frac{\rho_g}{\rho_f}} + K\left(\frac{1-x}{x}\right)}{1 + K\left(\frac{1-x}{x}\right)}\right]^{1/2} \qquad (B.4)$$

and where K = 0.4 was found to correlate well with the three sets of experimental data considered.

Another group of correlations avoids the use of a form of the homogeneous equation by employing the Lockhart-Martinelli (L-M) correlating parameter X_{tt} defined as:

$$X_{tt} = \left[\frac{1-x}{x}\right]^{0.9}\left[\frac{\mu_f}{\mu_g}\right]^{0.1}\left[\frac{\rho_g}{\rho_f}\right]^{0.5} \qquad (B.5)$$

The well known early L-M pressure drop work presented void fraction data as function of X_{tt} on two phase/two component adiabatic flows near atmospheric conditions. These data were approximated by equations developed by and refined by Domanski and Didion [13] for $X_{tt}>10$. The equations are:

for $X_{tt}\leq 10$

$$\alpha = f(X_{tt}) = \left(1 + X_{tt}^{0.8}\right)^{-0.378} = 0.823 - 0.157 \ln X_{tt} \qquad (B.6)$$

for $X_{tt}>10$

$$\alpha = f(X_{tt}) = 0.823 - 0.157 \ln X_{tt} \qquad (B.7)$$

The model developed by Tandon et al is an improvement for annular flow over the Zivi method in that the effect of wall friction is included. The Tandon method predicts void fraction results close to those of Smith yet does include a small mass flux effect. The correlation is of the form

$$\alpha = f\left(\mathrm{Re}_L, X_{tt}\right) \tag{B.8}$$

where Re_L is the liquid Reynolds number.

For $50<\mathrm{Re}_L<1125$

$$\alpha = \left[1 - \frac{1.928\,\mathrm{Re}_L^{-0.315}}{F\left(X_{tt}\right)} + \frac{0.9293\,\mathrm{Re}_L^{-0.63}}{F\left(X_{tt}\right)^2}\right] \tag{B.9}$$

or for $\mathrm{Re}_L>1125$

$$\alpha = \left[1 - \frac{0.38\,\mathrm{Re}_L^{-0.088}}{F\left(X_{tt}\right)} + \frac{0.0361\,\mathrm{Re}_L^{-0.176}}{F\left(X_{tt}\right)^2}\right] \tag{B.10}$$

where

$$F\left(X_{tt}\right) = 0.15\left(\frac{1}{X_{tt}} + \frac{2.85}{X_{tt}^{0.476}}\right) \tag{B.11}$$

$$\mathrm{Re}_L = \frac{G_r D_i}{\mu_f} \tag{B.12}$$

Premoli developed an empirical correlation to minimise liquid density prediction errors with the slip ratio, S, represented by,

$$S = f\left(x, \rho_g / \rho_f, \mathrm{Re}_L, We\right) \tag{B.13}$$

$$S = 1 + F_1\left(\frac{y}{1+yF_2} - yF_2\right)^{1/2} \tag{B.14}$$

where

$$F_1 = 1.578\,\mathrm{Re}_L^{-0.19}\left(\frac{\rho_f}{\rho_g}\right)^{0.22} \tag{B.15}$$

$$F_2 = 0.0273 We_L \, \mathrm{Re}_L^{-0.51} \left(\frac{\rho_f}{\rho_g} \right)^{-0.08} \qquad \text{(B.16)}$$

$$y = \frac{\beta}{1-\beta} \qquad \text{(B.17)}$$

and

$\mathrm{Re_L}$ = liquid Reynolds number, $\frac{GD_i}{\mu_f}$

$\mathrm{We_L}$ = liquid Weber number, $\frac{G^2 D_i}{\sigma \rho_f g_c}$

σ = surface tension,

g_c = gravitational constant,

β = volumetric quality, $\frac{1}{1+\left(\frac{1-x}{x}\right)\left(\frac{\rho_g}{\rho_f}\right)}$

Hughmark's empirical correlation is a generalisation of the work of Banoff, which assumed a bubble flow regime with a radial gradient of bubbles across the channel. Although developed for vertical upward flow with air liquid systems near atmospheric pressure, the correlation was found by Hughmark to do equally well for horizontal flow, for much higher pressures, and for other flow regimes.

In the correlation , void fraction is given by a correction factor K_H to the homogeneous equation ie.

$$\alpha = \frac{K_H}{1+\left[\frac{1-x}{x}\right]\left(\frac{\rho_g}{\rho_f}\right)} \qquad \text{(B.18)}$$

where $K_H = f(Z)$ and Z is dependent on viscosity-averaged Reynolds number, the Froude number, and the liquid volume fraction, ie

$$Z = f\left(x, \rho_g/\rho_f, G, D_i, \mu_f, \mu_g, \alpha\right) \quad \text{(B.19)}$$

where

G = mass flux,

D_i = tube inside diameter,

μ = kinematic viscosity.

Since Z contains a dependence on void fraction α, equation (B.18) must be iteratively evaluated to obtain the void fraction at each refrigerant quality. Because of the need for iteration, Hughmark method is the most difficult method to use.

Results obtained by evaluating void fraction models explained above and discussions are given in the following paragraphs.

Liquid Fraction Predictions

It is convenient to give the results in term of liquid fraction, (1-α), since the refrigerant liquid term is the major contributor to the total mass in the heat exchanger. The results for refrigerant saturation temperature representing evaporator condition (-25°C) and condenser condition (58°C), are shown in Figure B.1. and Figure B.2. as a function of refrigerant quality.

From the comparisons, it is seen that the more involved models generally predict more liquid presence then the homogeneous baseline. Comparing Figure B.1. and Figure B.2., at higher saturation pressures the heat exchanger mass quality range is occupied by more liquid. This is due to an increase in the gas to liquid density ratio which decreases void fraction at given quality level. Another conclusion is that the homogeneous method predicts very low void fraction at low saturation pressure.

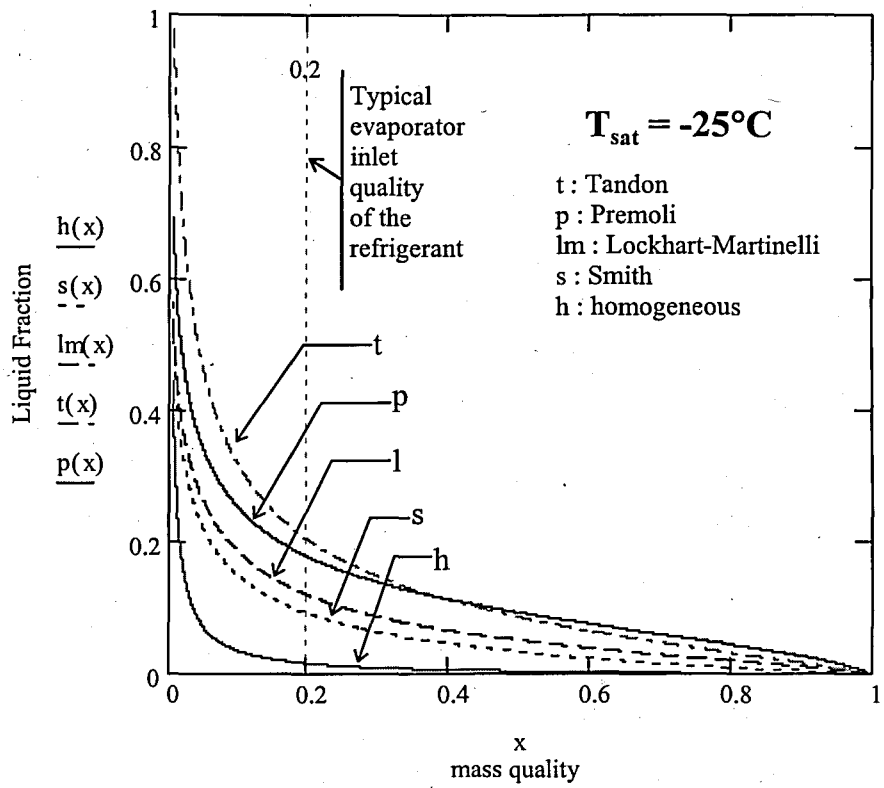

FIGURE B.1. Comparison of local R134a liquid fraction predictions at *evaporator* condition

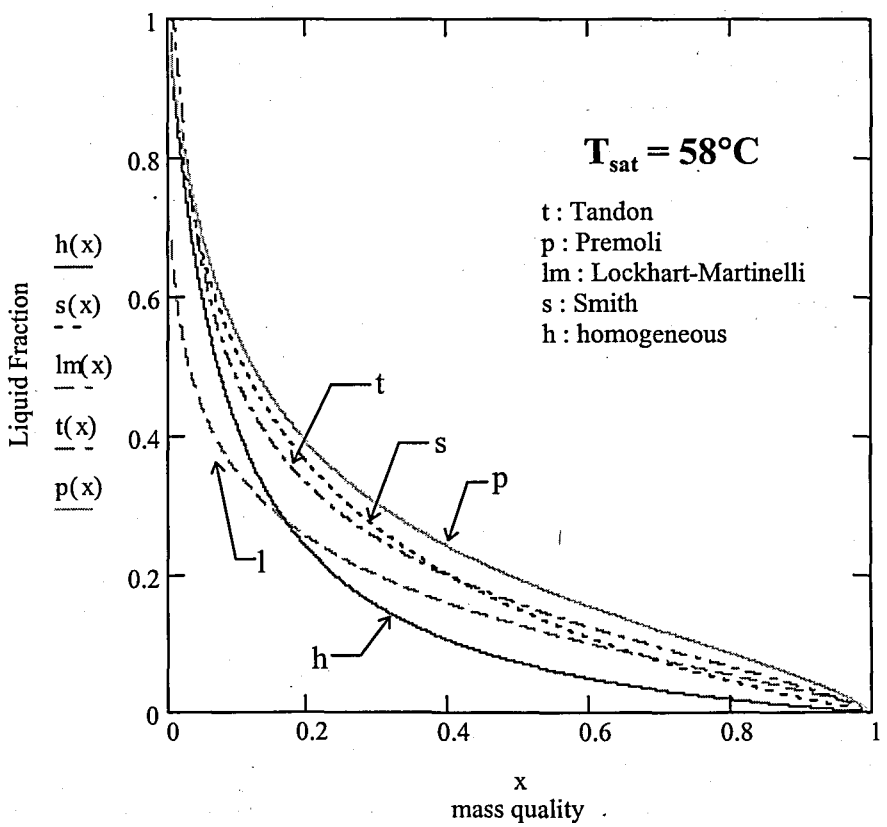

FIGURE B.2. Comparison of local R134a liquid fraction predictions at *condenser* condition

Mass Inventory Predictions

The results to be shown for mass inventory predictions are given in general terms of average two phase refrigerant density, ρ_{tp}, which is directly proportional to the total refrigerant mass in the two phase section of the heat exchanger, i.e.,

$$\rho_{tp} = \frac{m_t}{V} \qquad \text{(B.20)}$$

Calculations are done for four different evaporator / condenser conditions:

-25°C / 58°C, -15°C / 30°C, -5°C / 45°C, and 5°C / 15°C

Results are shown in table B.1. :

TABLE B.1. Results for mass inventory predictions for different conditions

	-25°C / 58°C		**-15°C / 30°C**	
	m_t (g.)	ρ_{ave} (kg/m^3)	m_t (g.)	ρ_{ave} (kg/m^3)
homogeneous	4.4 / 36.5	8.8 / 228.9	6.6 / 21.4	13.2 / 133.9
Smith	18.3 / 46.9	36.8 / 294.2	22.8 / 33.7	45.8 / 211.3
L - M	26.6 / 38.7	53.5 / 242.7	30.7 / 30.6	61.7 / 191.7
Tandon	43.3 / 42.9	86.9 / 268.6	47.6 / 35.8	95.7 / 224.1
Premoli	45.6 / 52.4	91.6 / 328.2	50.7 / 40.4	101.8 / 253.4

	-5°C / 45°C		**5°C / 15°C**	
	m_t (g.)	ρ_{ave} (kg/m^3)	m_t (g.)	ρ_{ave} (kg/m^3)
homogeneous	9.6 / 28.8	19.2 / 180.5	13.5 / 15.3	27.0 / 95.9
Smith	28.0 / 40.5	56.3 / 253.5	34.0 / 27.7	68.3 / 173.3
L - M	35.1 / 34.6	70.5 / 217.1	39.8 / 27.0	80.0 / 169.2
Tandon	52.0 / 39.3	104.5 / 246.5	56.4 / 32.4	113.4 / 203.3
Premoli	56.0 / 46.5	112.4 / 291.4	61.6 / 34.9	123.7 / 218.9

The evaporator inlet quality, rather than 0.0, is typically around 0.2 after isenthalpic expansion from condenser exit conditions. Therefore it is taken as 0.2 in our calculations.

The various two phase density predictions for the case of constant heat flux and a quality range of 0.2 to 1.0 for evaporator conditions and 0.0 to 1.0 for condenser conditions are summarised in Figure B.3. The curve representing pure R134a vapour density is included in the Figure B.3. as lower boundary. At low evaporator conditions, the density prediction difference become higher.

Another way of comparing the results is the ratio of the predicted condenser density to the predicted evaporator density, i.e.,

$$\frac{\rho_{tp,\,cond.}}{\rho_{tp,\,evap.}} \qquad \text{(B.21)}$$

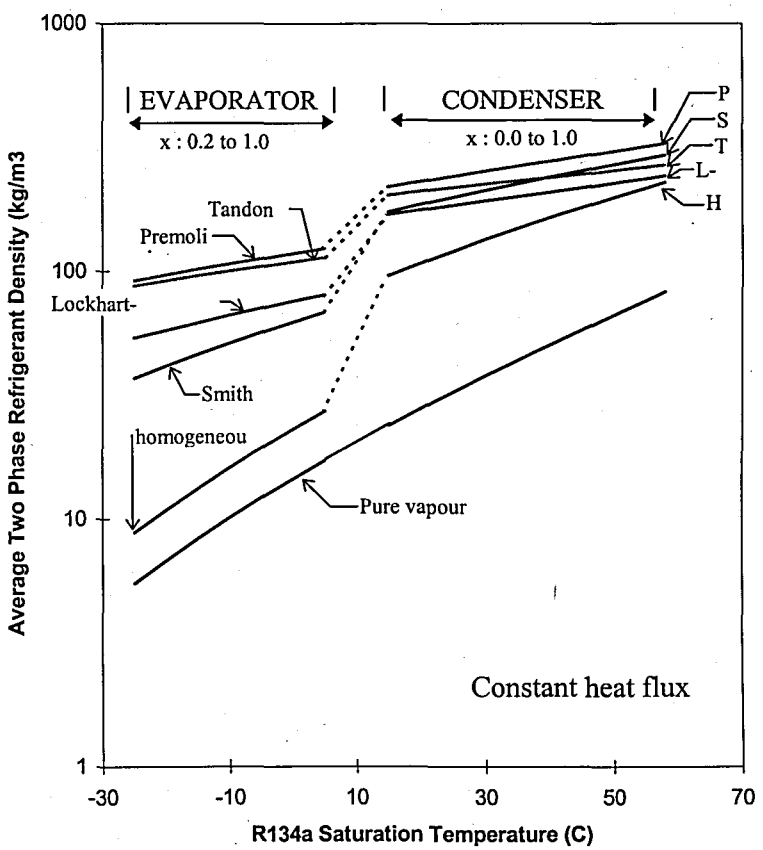

FIGURE B.3. Summary of R134a two phase density predictions

These ratios for different evaporator / condenser conditions are given in Table B.2.

TABLE B.2. Comparison of predicted condenser to evaporator two phase ratios for different conditions

	Evaporator / Condenser Temperatures		
	-25°C / 58°C	-15°C / 30°C	-5°C / 45°C
	$\rho_{tp,\,cond} / \rho_{tp,\,evap}$		
homogeneous	26.0	10.1	9.4
Smith	8.0	4.6	4.5
Lockhart-Martinelli	4.5	3.1	3.1
Tandon	3.1	2.3	2.4
Premoli	3.6	2.5	2.6

The wide range of predicted evaporator densities shown in Figure B.3. results in a similar variations in the predicted proportions of mass to be found in the condenser relative to the evaporator, as seen in Table B.2. The two mass flux dependent method and L-M method show the least change in ratio with change in operating conditions.

Conclusions :

- The choice of two phase void fraction model is of major significance in determining the charge in the condensers and especially in the evaporators. Figure B.3. can be used as a guide to the inventory predictions of the various models.
- Rice [16] concluded that the choice of heat flux assumption is insignificant for forced convection evaporators and of secondary importance after the choice of the void fraction model for condensers.
- Literature comparisons with experimental data is also made by Rice[16].He concluded that the highest predicting void fraction models for condensers (where most charge is located), such as Hughmark, Premoli, Tandon, and Baroczy, will give closest agreement for total system charge. There are not sufficient data to recommend any one method. However, the Premoli method gives an approximate average of the above methods.
- For a more accurate predictions, the solubility of refrigerant in the compressor oil must also be considered.

APPENDIX C : Heat Transfer Correlations

Berghmans [4] and Wattelet et al. [6] give correlations developed by several researchers for forced-convective evaporation in both vertical and horizontal tubes using the form below

$$\frac{h_{TP}}{h_l} = f\left(\frac{1}{X_{tt}}\right) \qquad (C.1)$$

Some of these correlations are shown in Table C.1.[4,6]

TABLE C.1. Two phase flow early convective correlations [4,6]

SOURCE	CORRELATION
Denglor and Addoms	$\frac{h_{TP}}{h_l} = 3.5\left[\frac{1}{X_{tt}}\right]^{0.5}$
Guerrieri and Talty	$\frac{h_{TP}}{h_l} = 3.4\left[\frac{1}{X_{tt}}\right]^{0.45}$
Chaddock and Noerager	$\frac{h_{TP}}{h_l} = 3.0\left[\frac{1}{X_{tt}}\right]^{0.67}$
Shrock and Grossman	$\frac{h_{TP}}{h_l} = 2.5\left[\frac{1}{X_{tt}}\right]^{0.75}$
Collier and Pulling	$\frac{h_{TP}}{h_l} = 2.167\left[\frac{1}{X_{tt}}\right]^{0.699}$

Wakeland [11] uses the Shrock-Grossmann correlation, and Wang and Touber [17] uses the Guerreri and Talty correlation for the refrigerant side film coefficient in their evaporator simulation work.

Some more involved correlations mentioned in Wattelet et al.'s study [6] are summarised below:

Rohsenov first proposed an addictive model of the nucleate and convective boiling heat transfer coefficients, and Chen utilised this, based on the superposition of heat transfer coefficients, as follows:

$$h_{TP} = Sh_{nb} + Fh_l \qquad (C.2)$$

where S is a suppression factor for nucleate boiling and F is the two phase convective multiplier for heat transfer as defined on the right side of Equation (1.84). Fh_l represents the macroconvective component and is obtained with a two-phase Reynolds number factor, F, which accounts for an increase in velocity due to increased quality and a single-phase heat transfer coefficient, h_l, calculated as if the liquid flows alone. The microconvective component, Sh_{nb}, is determined by a suppression factor S and a nucleate pool boiling heat transfer coefficient, h_{nb}. The suppression factor was dependent on the liquid Reynolds number. Collier later curve fitted the suppression factor curves developed by Chen as follows:

$$S = \frac{1}{1 + 2.53 \cdot 10^{-6} \,\mathrm{Re}_l \, F^{1.25}} \qquad (C.3)$$

F was curve fitted by Kenning and Cooper for $1/X_{tt} > 1.0$ as follows:

$$F = 1 + 1.8\left(\frac{1}{X_{tt}}\right)^{0.79} \qquad (C.4)$$

The nucleate boiling heat transfer coefficient was evaluated using the Forster Zuber correlation defined as:

$$h_{nb} = 0.00122\left[\frac{k_l^{0.79} C_{pl}^{0.45} \rho_l^{0.49}}{\sigma^{0.5} \mu_l^{0.29} i_{lv}^{0.24} \rho_v^{0.24}}\right] \Delta T_{sat}^{0.24} \Delta P_{sat}^{0.75} \qquad (C.5)$$

The heat transfer coefficient's dependency on mass flux and heat flux is illustrated by introducing a boiling number, Bo, (dimensionless) which is defined as:

$$Bo = \frac{q''}{G * h_{fg}} \qquad (C.6)$$

where

q'' heat flux

G mass flowrate

h_{fg} enthalpy of evaporation

VDI Heat Atlas [3], gives Shah's generalised correlation for two phase heat transfer coefficients in flow boiling. In his convective term, he defines a convection number, Co, which is only a function of quality and vapour to liquid density ratio as follows, since the viscosity ratio was found to have no significant influence. A total of 800 data points was used in the correlation development for vertical and horizontal flow for water , R11, R12, R22, R-113, Cyclohexane. Convection number is defined as:

$$Co = \left(\frac{1-x}{x}\right)^{0.8}\left(\frac{\rho_g}{\rho_f}\right)^{0.5} \qquad (C.7)$$

and the correlation is:

$$\frac{h_{tp}}{h_l} = \left[1+\left(\frac{2}{Co}\right)^{1.6}\left(\frac{0.04}{Fr}\right)^{-0.4608}\right]^{1/2} \qquad (C.8)$$

Recognising that the boiling number could not accurately model the nucleate boiling term alone, Kandlikar [20] developed a similar correlation that multiplied the boiling number by a fluid specific term which accounted for the different nucleate boiling effects that occurred from fluid to fluid. Kandlikar gives the following correlation by expanding the data base to 5246 data points from twenty four experimental investigations with ten fluids. The two phase boiling heat transfer coefficient, h_{TP}, was expressed as the sum of the convective and the nucleate boiling terms by using an additive model and a fluid dependent parameter F_{fl}. It results in a mean deviation of 15.9 per cent with water data, and 18.8 per cent with all refrigerant data combined.

$$\frac{h_{TP}}{h_l} = C_1 Co^{C_2}\left(25Fr_l\right)^{C_5} + C_3 Bo^{C_4} F_{fl} \qquad (C.9)$$

where the single phase liquid only heat transfer coefficient h_l is given by:

$$h_l = 0.023\,\mathrm{Re}_l^{0.8}\,\mathrm{Pr}_l^{0.4}\left(k_l/D\right) \qquad (C.10)$$

h_l: single phase heat transfer coefficient with only liquid fraction flowing in the tube where Dittus-Boelter Equation is used to calculate h_l.

The data was divided into two regions as follows:

Co<0.65 convective boiling region

Co>0.65 nucleate boiling region

TABLE C.2. Constants in the Kandlikar correlation [20]

	CO<0.65 CONVECTIVE REGION	CO>0.65 NUCLEATE BOILING REGION
C1	1.1360	0.6683
C2	-0.9	-0.2
C3	667.2	1058.0
C4	0.7	0.7
C5	0.3	0.3

C5 = 0 for vertical tubes, and for horizontal tubes with Fr_l>0.04

TABLE C.3. Fluid dependent parameter F_{fl} in the Kandlikar correlation [20]

FLUID	F_{FL}
Water	1.00
R-134a [6]	1.63
R-12	1.5
R-11	1.3
R-22	2.2
R113	3.0
Nitrogen	4.7
Neon	3.5

Güngör and Winterton [21], considering pool boiling effect, with the aid for over 4300 data points for several fluids, gives the following correlation:

$$h_{tp} = Eh_l + Sh_{pool} \qquad (C.11)$$

h_l is given by Dittus-Boelter equation for liquid only flowing in the tube

$$h_{pool} = 55P_r^{0.12}\left(-\log_{10} P_r\right)^{-0.55} M^{-0.5} q''^{0.67} \qquad (C.12)$$

where :

P_r : reduced pressure i.e., $\frac{P_{sat}}{P_{crit}}$,

M : molecular weight

Using all of the saturated boiling tube data available at that time, the expression for E and S were:

$$E = 1 + 24{,}000 Bo^{1.16} + 1.37\left(1/X_{tt}\right)^{0.86} \qquad (C.13)$$

and

$$S = \frac{1}{1 + 1.15 * 10^{-6} E^2 \,\mathrm{Re}_l^{\,1.17}} \qquad (C.14)$$

All properties are calculated at the saturation temperature. If the tube is horizontal and the Froude number is less than 0.05 then E should be multiplied by:

$$E_2 = Fr^{(0.1-2Fr)} \qquad (C.15)$$

and S should be multiplied by:

$$S_2 = \sqrt{Fr} \qquad (C.16)$$

Air Conditioning and Refrigeration Center at University of Illinois develops the following overall heat transfer correlation for horizontal tube evaporator in ACRC TR-55 Report [6].

$$h_{TP} = \left[h_{nb}{}^n + h_{cb}{}^n\right]^{1/n} \qquad (C.17)$$

with n=2.5

$$h_{nb} = 55q''^{0.67} M^{-0.5} P_r^{0.12} \left[-\log_{10} P_r \right]^{-0.55} \quad (C.18)$$

$$h_{cb} = F * h_l * R \quad (C.19)$$

$$F = 1 + 1.925 X_{tt}^{-0.83} \quad (C.20)$$

$$h_l = 0.023 \frac{k_l}{D} \mathrm{Re}_l^{0.8} \mathrm{Pr}_l^{0.4} \quad (C.21)$$

$R = 1.32 Fr_l^{0.2}$ for $\mathrm{Fr_l} < 0.25$

$R = 1$, for $\mathrm{Fr_l} \geq 0.25$

Figure C.1. shows the heat transfer calculations based on correlations found in the literature for following evaporator conditions:

Refrigerant : R-134a

Evaporation temperature : -25°C

Refrigerant mass flowrate : 3.5 kg/h

tube inner diameter : 6.5 mm

tube length : 15 m

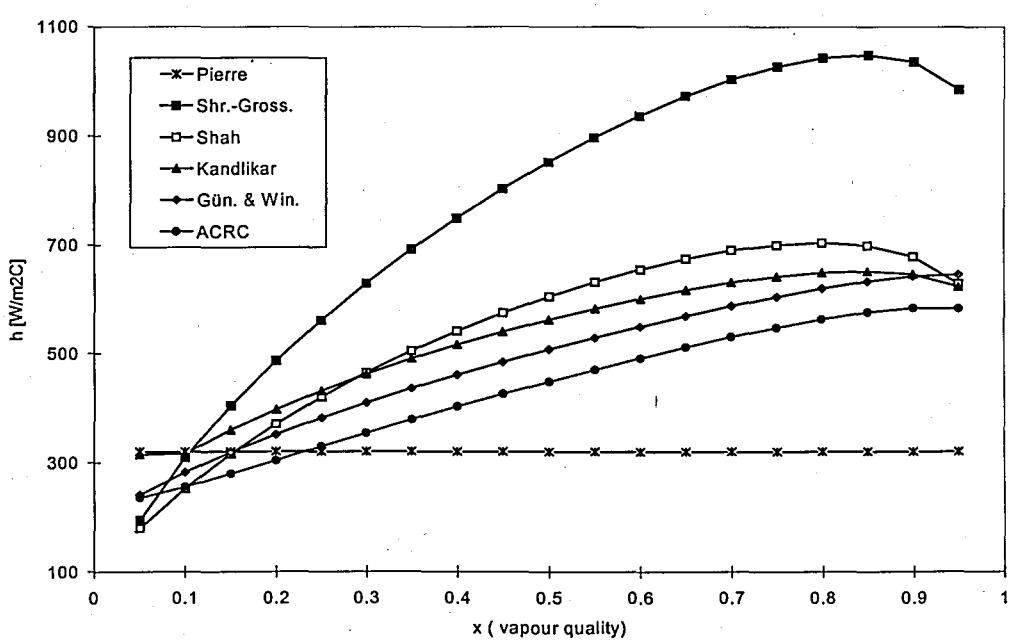

FIGURE C.1. Comparison of the correlations for refrigerant side heat transfer coefficient.

The correlations of ACRC, Kandlikar, Güngör - Winterton, and Shah shows similar behaviours. The Shrock and Grossmann correlation shows the maximum deviation. All correlations are invalid between 0.95 and 1.0

Above correlations, except ACRC and Pierre's works, are developed from data obtained for evaporators used in industrial cooling. Therefore, cooling capacities, refrigerant mass flowrate, and tube diameters of these evaporators are different than that of household refrigerators.

The correlations of ACRC, Kandlikar, Güngör - Winterton, and Shah shows similar behaviours. The Shrock and Grossmann correlation shows the maximum deviation. All correlations are invalid between 0.95 and 1.0

APPENDIX D : Derivation of The Energy Equation for a Simplified Model

Remembering the conservation equations used for the complete model:

Continuity:

$$\frac{\partial \rho}{\partial t} + \frac{\partial (\rho u)}{\partial t} = 0 \qquad (D.1)$$

Momentum:

$$\frac{\partial (\rho u)}{\partial t} + \frac{\partial (\rho u^2)}{\partial x} + \frac{\partial P}{\partial x} = 0 \qquad (D.2)$$

Energy :

$$\frac{\partial}{\partial t}(\rho e) + \frac{\partial}{\partial t}(\rho u^2) + \frac{\partial}{\partial x}(\rho u h) + \frac{\partial}{\partial x}\left(\frac{1}{2}\rho u^3\right) = 0 \qquad (D.3)$$

Multiplying the momentum equation with velocity, u:

$$u\frac{\partial (\rho u)}{\partial t} + u\frac{\partial (\rho u^2)}{\partial x} + u\frac{\partial P}{\partial x} = 0 \qquad (D.4)$$

Subtracting (D.4) from (D.3)

$$\frac{\partial}{\partial t}(\rho e) + \underbrace{\left[\frac{\partial}{\partial t}(\rho u^2) - u\frac{\partial}{\partial t}(\rho u)\right]}_{A} + \frac{\partial}{\partial x}(\rho u h) + \underbrace{\left[\frac{\partial}{\partial x}\left(\frac{1}{2}\rho u^3\right) - u\frac{\partial}{\partial x}(\rho u^2)\right]}_{B} - u\frac{\partial P}{\partial x} = 0 \qquad (D.5)$$

$$A = \frac{\partial}{\partial t}\left(\frac{\rho u^2}{2}\right) - u\frac{\partial}{\partial t}(\rho u)$$

$$= \rho\frac{\partial}{\partial t}\left(\frac{u^2}{2}\right) + \frac{u^2}{2}\frac{\partial \rho}{\partial t} - u^2\frac{\partial \rho}{\partial t} - \rho u\frac{\partial u}{\partial t}$$

$$= \rho\frac{\partial}{\partial t}\left(\frac{u^2}{2}\right) + \frac{u^2}{2}\frac{\partial \rho}{\partial t} - u^2\frac{\partial \rho}{\partial t} - \rho\frac{\partial}{\partial t}\left(\frac{u^2}{2}\right)$$

$$= -\frac{1}{2}u^2\frac{\partial \rho}{\partial t}$$

$$\mathrm{B} = \frac{\partial}{\partial x}\left(\frac{1}{2}\rho u^3\right) - u\frac{\partial}{\partial x}\left(\rho u^2\right)$$

$$= \frac{\rho}{2}\frac{\partial}{\partial x}\left(u^3\right) + \frac{u^3}{2}\frac{\partial \rho}{\partial x} - u^3\frac{\partial \rho}{\partial x} - \rho u\frac{\partial}{\partial x}u^2$$

$$= 3u^2\frac{\rho}{2}\frac{\partial u}{\partial x} + \frac{u^3}{2}\frac{\partial \rho}{\partial x} - u^3\frac{\partial \rho}{\partial x} - 2\rho u^2\frac{\partial u}{\partial x}$$

$$= -\frac{1}{2}\rho u^2\frac{\partial u}{\partial x} - \frac{u^3}{2}\frac{\partial \rho}{\partial x}$$

$$\mathrm{A+B} = -\frac{1}{2}u^2\frac{\partial \rho}{\partial t} - \frac{1}{2}\rho u^2\frac{\partial u}{\partial x} - \frac{u^3}{2}\frac{\partial \rho}{\partial x}$$

$$= -\frac{u^2}{2}\left(\frac{\partial \rho}{\partial t} + \rho\frac{\partial u}{\partial x} + u\frac{\partial \rho}{\partial x}\right)$$

$$= -\frac{u^2}{2}\left(\frac{\partial \rho}{\partial t} + \frac{\partial \rho u}{\partial x}\right)$$

$= 0$,using continuity equation (D.1)

Therefore equation (D.5) becomes:

$$\Rightarrow \qquad \frac{\partial}{\partial t}\left(\rho e\right) + \frac{\partial}{\partial x}\left(\rho u h\right) - u\frac{\partial P}{\partial x} = 0 \qquad \text{(D.6)}$$

adding $\frac{\partial P}{\partial t}$ to both sides of equation (D.6)

$$\frac{\partial}{\partial t}(\rho e) + \frac{\partial P}{\partial t} + \frac{\partial}{\partial x}(\rho u h) - u\frac{\partial P}{\partial x} = \frac{\partial P}{\partial t} \qquad (D.7)$$

Using the relation $h = e + \frac{P}{\rho}$,

$$\frac{\partial}{\partial t}(\rho h) + \frac{\partial}{\partial x}(\rho u h) - u\frac{\partial P}{\partial x} = \frac{\partial P}{\partial t} \qquad (D.8)$$

Finally, neglecting spatial variations of pressure and the work associated with he rate of change of pressure with respect to time, the energy equation becomes:

$$\frac{\partial}{\partial t}(\rho h) + \frac{\partial}{\partial x}(\rho u h) = heat\ \ flux\ \ term \qquad (D.9)$$

APPENDIX E : Flow Chart

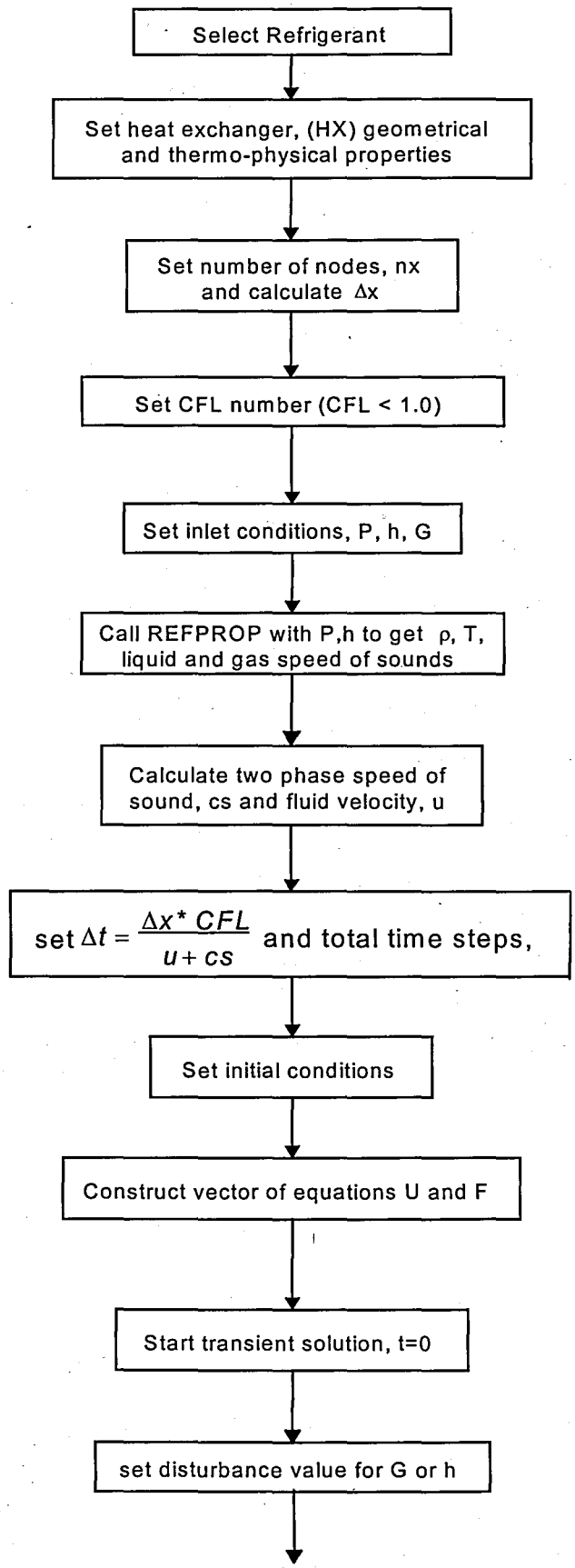

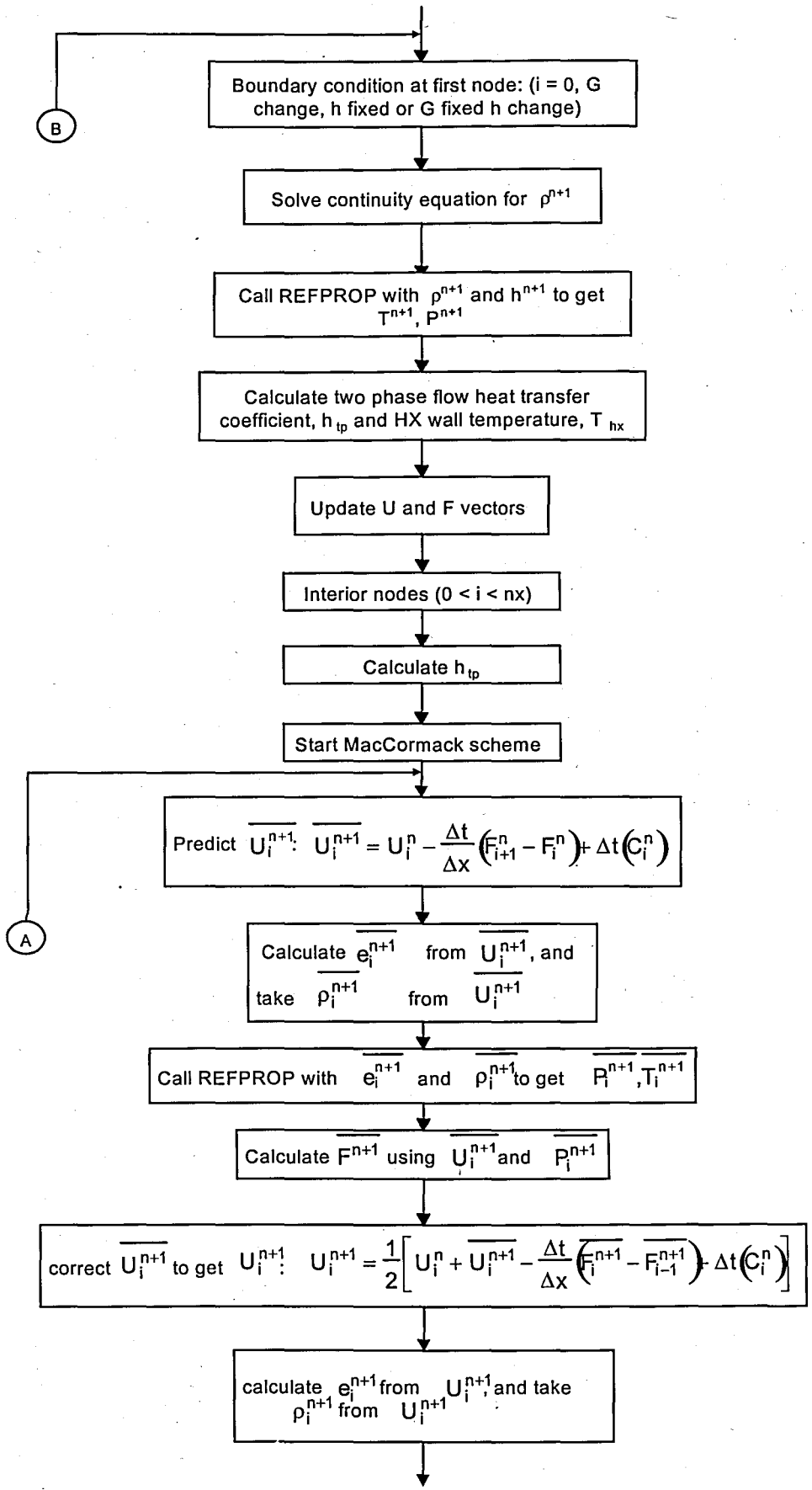
B
Boundary condition at first node: (i = 0, G change, h fixed or G fixed h change)
Solve continuity equation for ρ^{n+1}
Call REFPROP with ρ^{n+1} and h^{n+1} to get T^{n+1}, P^{n+1}
Calculate two phase flow heat transfer coefficient, h_{tp} and HX wall temperature, T_{hx}
Update U and F vectors
Interior nodes (0 < i < nx)
Calculate h_{tp}
Start MacCormack scheme
A
Predict $\overline{U_i^{n+1}}$: $\overline{U_i^{n+1}} = U_i^n - \frac{\Delta t}{\Delta x}\left(F_{i+1}^n - F_i^n\right) + \Delta t\left(C_i^n\right)$
Calculate $\overline{e_i^{n+1}}$ from $\overline{U_i^{n+1}}$, and take $\overline{\rho_i^{n+1}}$ from $\overline{U_i^{n+1}}$
Call REFPROP with $\overline{e_i^{n+1}}$ and $\overline{\rho_i^{n+1}}$ to get $\overline{P_i^{n+1}}$, $\overline{T_i^{n+1}}$
Calculate $\overline{F^{n+1}}$ using $\overline{U_i^{n+1}}$ and $\overline{P_i^{n+1}}$
correct $\overline{U_i^{n+1}}$ to get U_i^{n+1}: $U_i^{n+1} = \frac{1}{2}\left[U_i^n + \overline{U_i^{n+1}} - \frac{\Delta t}{\Delta x}\left(\overline{F_i^{n+1}} - \overline{F_{i-1}^{n+1}}\right) + \Delta t\left(C_i^n\right)\right]$
calculate e_i^{n+1} from U_i^{n+1}, and take ρ_i^{n+1} from U_i^{n+1}

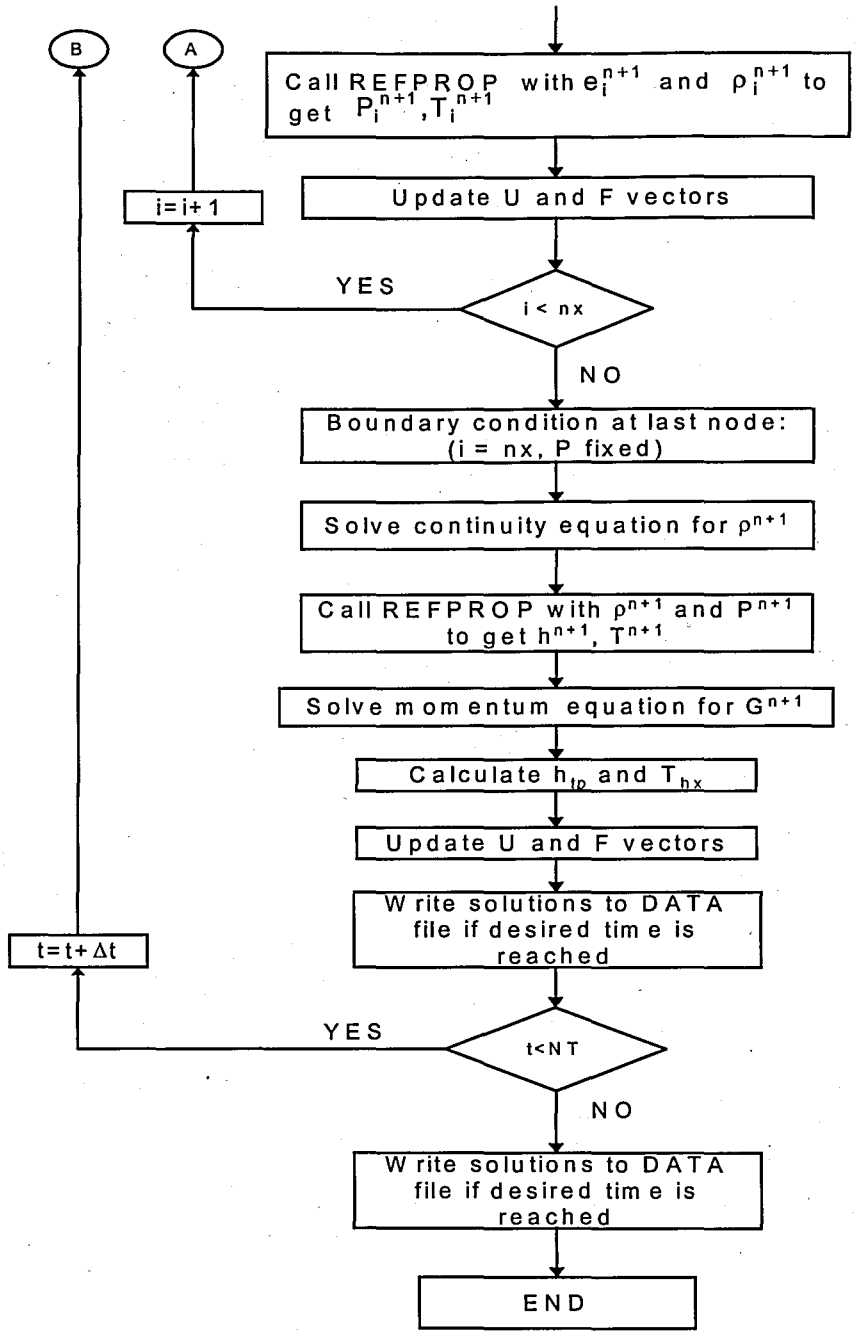
B
A
Call REFPROP with e_i^{n+1} and ρ_i^{n+1} to get P_i^{n+1}, T_i^{n+1}
Update U and F vectors
i=i+1
YES
i < nx
NO
Boundary condition at last node: (i = nx, P fixed)
Solve continuity equation for ρ^{n+1}
Call REFPROP with ρ^{n+1} and P^{n+1} to get h^{n+1}, T^{n+1}
Solve momentum equation for G^{n+1}
Calculate h_{tp} and T_{hx}
Update U and F vectors
Write solutions to DATA file if desired time is reached
t=t+Δt
YES
t<NT
NO
Write solutions to DATA file if desired time is reached
END

APPENDIX F : COMPUTER PROGRAM

The main program:

```
      Program MACCORMACK_void
      USE PORTLIB
      implicit double precision (A-H,O-Z)
      implicit integer (i-n)
      character*80 refrigerant
      parameter (NX=60)

     REAL(8) elapsed_time

      dimension U(0:NX,3),X(0:NX),UP(0:NX,3),UC(0:NX,3),V(0:NX)
      dimension G(0:NX),RH0(0:NX),P(0:NX),T(0:NX),THX(0:NX),H(0:NX)
      dimension E(0:NX,3),DELU(0:NX,3),EI(0:NX),C(3),XV(0:NX)

     CHARACTER TIMEO*12
      CHARACTER TIMEO1*8
      DATA TT/3.0/
      DATA CFL/0.9/
      COMMON /PROP/ RHOG, RHOL
      HXL=6.0
      DX=HXL/NX
      AV=0.00
      refrigerant=''
      PI=4*ATAN(1.0)

3     PRINT*, 'REFRIGERANT ? '
      PRINT*, '  1- R134a  '
      PRINT*, '  2- R22    '
      READ*, REFR
      IF (REFR.EQ.1) THEN
      refrigerant='R134a.fld'
      ELSEIF (REFR.EQ.2) THEN
      refrigerant='R22.fld'
      ENDIF
      IF (refrigerant.EQ.'')THEN
      PRINT*, 'PLEASE ENTER 1 OR 2  !'
      PRINT*
      GOTO 3
      ENDIF

      PRINT*, 'INCLUDE PRESSURE DROP 1-YES / 2-NO ? '
      READ*,PR
      PRINT*, 'INCLUDE HEAT TRANSFER 1-YES / 2-NO ? '
      READ*,HT

      TA=310.0

      IF (HT.EQ.1) THEN
     HTA= 0.9
      ELSEIF (HT.EQ.2) THEN
      HTA=0.0
      ENDIF


      CMAX=0.0
      CTOT=0.0

!     Exchanger properties (Al)
      CPHX=890
      DINNHX=0.0065
```

```
      DOUTHX=0.008
      RH0HX=2720
      AHX=1.7E-5


    5 PRINT*,' REFRIGERANT : ',refrigerant
      PRINT*,' CROSS-SECTION AREA 33.2e-6 m2:  '
      AC=33.18307E-6
      PRINT*,' PRESSURE : 1093.5 Kpa'
      PR0=1093515
      PRINT*,' ENTHALPY : 167.47 kj/kg'
      H0=167472
      PRINT*,' MASS FLOW RATE : 244 kg/hr  '
      GM0=244*AC
      PRINT*,' DISTURBANCE MASS FLOW RATE: 293 kg/hr '
      GM1=293*AC

      call refprop (0.0d0,refrigerant,PR0/1000,h0,0.0d0,1,RHO,RHOG,RHOL,
      +E0,px,T0,X0,0.0D0,0.0D0,0.0D0)

      RH0(0)=RHO
      ALPHA=(RH0(0)-RHOL) / (RHOG-RHOL)
      U1=GM1/AC/RHO
      PRINT*
      PRINT*,'REPORT TYPE:'
      PRINT*,'             1- SEPARATE FILES'
      PRINT*,'          2- SINGLE FILE'

      REPORT=2

      call refprop(0.0d0,refrigerant,PR0/1000,0.0D0,0.0d0,0
      +           ,RHO,RHOg,RHOl,EI(0),P(0),T(0),1.0D0,SS,0.0D0,0.0D0)
      SSG=SS
      call refprop(0.0d0,refrigerant,PR0/1000,H(0),0.0d0,0
      +           ,RHO,RHOg,RHOl,EI(0),P(0),T(0),0.0D0,SS,0.0D0,0.0D0)
      SSL=SS

!     SPEED OF SOUND
      CS=1 / SQRT( (ALPHA*RHOG+(1-ALPHA)*RHOL)*
      +  (ALPHA/(RHOG*SSG**2)+(1-ALPHA)/(RHOL*SSL**2) ))

      DT=DX*CFL/(U1+CS)

      PRINT*,'U=',U1,'  CS=',CS
      NT=INT(TT/DT)+1
      PRINT*
    7 FORMAT(/"    TOTAL TIME                : ",F6.2,' s')
      WRITE(*,7)TT
    9 FORMAT("    TOTAL TIME STEP           : "I6)
      WRITE(*,9)NT
   10 FORMAT("    TIME INCREMENT (DELTA T)  : ",F8.7//)
      WRITE(*,10)DT
      ITI=0

      elapsed_time = TIMEF()
      time0=0.0

!      SET INITIAL CONDITIONS

      TM=0.0
      do  I=0,NX
      X(I)=I*DX
      P(I)=PR0
      G(I)=GM0/AC
      T(I)=T0
      THX(I)=T0
      RH0(I)= RHO
```

```
      XV(I)=X0
      H(I) = H0
      EI(I)= E0

      U(I,1)=RH0(I)
      U(I,2)=G(I)
      U(I,3)=U(I,1)*EI(I)+U(I,2)**2/2/U(I,1)
      E(I,1)=U(I,2)
      E(I,2)=U(I,2)**2/U(I,1) + P(I)
      E(I,3)=U(I,2)*(H(I)+1/2*(U(I,2)/U(I,1))**2)
     END DO
      DO I=0,NX
      DO J=1,3
      DELU(I,J)=0
      ENDDO
      ENDDO


!     advance solution in time
!
      do  IT=1,NT
      TM=TM+DT

!     IF (IT.EQ.1) THEN
!     H(0)=190732
!     ENDIF

!     Boundary Condition (x=0)

     X(0)=0
      G1=GM1/AC

      OLDR=RH0(0)
      RH0(0)=OLDR-DT/DX/2*(-3*G(0)+4*G(1)-G(2))

      ALPHA=(RH0(0)-RHOL) / (RHOG-RHOL)
      XV(0)=ROOT(ALPHA,XV(0))

      call RefProp (0.0d0,refrigerant,P(0)/1000,H(0),0.0d0,4,RH0(0),
     +      RHO1,RHO2,EI(0),PX,T(0),XV(0),0.0D0,0.0D0,0.0D0)

      IF (HT.EQ.1) THEN
     HTP= HTCOEFF (G1)
      ELSEIF (HT.EQ.2) THEN
      HTP=0.0
      ENDIF
      THX(0)=1/(AHX*RH0HX*CPHX)*(THX(0)*(AHX*RH0HX*CPHX-DT*(PI*DINNHX*
     +    HTP+PI*DOUTHX*HTA))+DT*(PI*DINNHX*HTP*T(0)+PI*DOUTHX*HTA*TA))

      P(0)=PX
      U(0,1)=RH0(0)
      U(0,2)=G1
      U(0,3)=RH0(0)*EI(0)+G1**2/2/RH0(0)
      G(0)=G1


      E(0,1)=G1
      E(0,2)=G1**2/RH0(0) + P(0)
      E(0,3)=G1*(H(0)+1/2*(G1/RH0(0))**2)


     do  I=1,NX-1

      C(1)=0

      IF (PR.EQ.1) THEN
      FPR= PRDROP (G(I),XV(I))
```

```
      C(2)=DX*FPR*G(I)**2*(1-XV(I))**2/DINNHX/RHOL
      ELSEIF (PR.NE.1)THEN
      C(2)=0.0
      ENDIF

      IF (HT.EQ.1) THEN
      HTP= HTCOEFF (G(I))
      C(3)= HTP*DINNHX*PI*(THX(I)-T(I))
      ELSEIF (HT.NE.1) THEN
      C(3)=0.0
      ENDIF


!     Predictor Step (MACCORMACK)
      DO  J=1,3
      UP(I,J)=U(I,J)-DT/DX*(E(I+1,J)-E(I,J))-DT*C(J)
      END DO
      ALPH=(UP(I,1)-RHOL) / (RHOG-RHOL)
      XV(I)=ROOT(ALPH,XV(I))
      EI(I)=( UP(I,3)-UP(I,2)**2/2/UP(I,1) ) / UP(I,1)

      call RefProp (T(I),refrigerant,0.0d0,0.0d0,0.0d0,2,UP(I,1),RHO1,
     +      RHO2,EI(I),P(I),TI,XV(I),0.0D0,0.0D0,0.0D0)

      T(I)=TI
      H(I)=EI(I)+P(I)/UP(I,1)

     E(I,1)=UP(I,2)
      E(I,2)=UP(I,2)**2/UP(I,1)+P(I)
      E(I,3)=( UP(I,2)* (H(I)+1/2*(UP(I,2)/UP(I,1))**2) )

      C(1)=0

      IF (PR.EQ.1) THEN
      FPR= PRDROP (UP(I,2),XV(I))
      C(2)=DX*FPR*UP(I,2)**2*(1-XV(I))**2/DINNHX/RHOL
      ELSEIF (PR.NE.1)THEN
      C(2)=0.0
      ENDIF

      IF (HT.EQ.1) THEN
      HTP= HTCOEFF (UP(I,2))
      C(3)= HTP*DINNHX*PI*(THX(I)-T(I))
      ELSEIF (HT.NE.1) THEN
      C(3)=0.0
      ENDIF


!  Corrector Step (MACCORMACK)
      DO J=1,3
      UC(I,J)=(U(I,J)+UP(I,J)-DT/DX*(E(I,J)-E(I-1,J))-DT*C(J) )/2
      DELU(I,J)=UC(I,J)-U(I,J)
      END DO

      end do


      DO I=1,NX-1
      DO J=1,3
      DELU(I,J)=DELU(I,J)-AV*(DELU(I+1,J)-2.0*DELU(I,J)+DELU(I-1,J))
      UC(I,J)=U(I,J)+DELU(I,J)
      ENDDO
      ENDDO


     DO I=1,NX-1
      X(I)=I*DX
```

```
 ALPH=(UC(I,1)-RHOL) / (RHOG-RHOL)

 XV(I)=ROOT(ALPH,XV(I))
 EI(I)=( UC(I,3)-UC(I,2)**2/2/UC(I,1) ) / UC(I,1)
 G(I)=UC(I,2)

 call RefProp (T(I),refrigerant,0.0d0,0.0d0,0.0d0,2,UC(I,1),RHO1,
 +      RHO2,EI(I),P(I),TI,XV(I),0.0D0,0.0D0,0.0D0)
 T(I)=TI
 H(I)=EI(I)+P(I)/UC(I,1)

 IF (HT.EQ.1) THEN
HTP= HTCOEFF (G(I))
 ELSEIF (HT.NE.1) THEN
 HTP=0.0
 ENDIF

 HTP= HTCOEFF (G(I))
 THX(I)=1/(AHX*RH0HX*CPHX)*(THX(I)*(AHX*RH0HX*CPHX-DT*(PI*DINNHX*
 +     HTP+PI*DOUTHX*HTA))+DT*(PI*DINNHX*HTP*T(I)+PI*DOUTHX*HTA*TA))

 ENDDO

 DO  I=1,NX-1
 RH0(I)=UC(I,1)
 U(I,1)=UC(I,1)
U(I,2)=G(I)
 V(I)=G(I)/RH0(I)
 U(I,3)=U(I,1)*EI(I)+U(I,2)**2/2/U(I,1)
 E(I,1)=U(I,2)
 E(I,2)=U(I,2)**2/U(I,1) + P(I)
 E(I,3)=U(I,2)*(H(I)+1/2*(U(I,2)/U(I,1))**2)
END DO

  !     Boundary Condition (x=NX)

 X(NX)=NX*DX
 OLDR=RH0(NX)
RH0(NX)=OLDR-DT/DX/2*(3*G(NX)-4*U(NX-1,2)+U(NX-2,2))
G(NX)=U(NX,2)-DT/DX/2*( 3*(U(NX,2)**2/OLDR+PR0)
 +                        -4*(U(NX-1,2)**2 /U(NX-1,1)+P(NX-1))
+                           +(U(NX-2,2)**2 /U(NX-2,1)+P(NX-2))       )

 call RefProp (0.0d0,refrigerant,PR0/1000,H(NX),0.0d0,3,RH0(NX),
 +      RHOg,RHOl,EI(NX),b,T(NX),XV(NX),0.0D0,0.0D0,0.0D0)

 H(NX)=EI(NX)+PR0/RH0(NX)

 IF (HT.EQ.1) THEN
HTP= HTCOEFF (G(NX))
 ELSEIF (HT.NE.1) THEN
 HTP=0.0
 ENDIF


THX(NX)=1/(AHX*RH0HX*CPHX)*(THX(NX)*(AHX*RH0HX*CPHX-DT*(PI*DINNHX
 +   *HTP+PI*DOUTHX*HTA))+DT*(PI*DINNHX*HTP*T(NX)+PI*DOUTHX*HTA*TA))

 U(NX,1)=RH0(NX)
 U(NX,2)=G(NX)
 U(NX,3)=RH0(NX)*EI(NX)+G(NX)**2/2/RH0(NX)

 E(NX,1)=U(NX,2)
 E(NX,2)=U(NX,2)**2/U(NX,1) + PR0
 E(NX,3)=U(NX,2)*(H(NX)+1/2*(U(NX,2)/U(NX,1))**2)
```

```
!     PRINTING SOLUTIONS
      TIMEO1='DAT      '
      IF ((IT.EQ.(INT(0.015/DT)))
      +.OR.(IT.EQ.(INT(0.03/DT)))
      +.OR.(IT.EQ.(INT(0.06/DT)))
     +.OR.(IT.EQ.(INT(0.09/DT)))
      +.OR.(IT.EQ.(INT(0.12/DT)))
      +.OR.(IT.EQ.(INT(0.15/DT)))
     +.OR.(IT.EQ.NT) )THEN
      WRITE(*,15)DT*IT,IT,NT-IT
15    FORMAT ("   CURRENT TIME: ",F8.3,4X,"CURRENT TIME STEP: "I6,4X,
     +"TIME STEP LEFT: "I6,5X)

      ITI=ITI+1

      IF (REPORT.EQ.1) THEN
      WRITE (TIMEO,'(I3.3,A1,A3)') ITI,'.',TIMEO1
      OPEN (6,FILE=TIMEO)
      ELSE IF  (REPORT.EQ.2) THEN
     OPEN (6,FILE='VOID.DAT')
      ENDIF
20    FORMAT(8(F15.5,2X))
      DO I=0,NX
     WRITE(6,20 ) X(I),G(I),P(I),RH0(I),XV(I),H(I),T(I),THX(I)
      END DO
      ENDIF

      elapsed_time = TIMEF()

      PRINT*, IT,elapsed_time-time0
      time0=elapsed_time
     END DO

       elapsed_time = TIMEF()
     PRINT *, elapsed_time
      STOP
      END


      DOUBLE PRECISION FUNCTION PRDROP(G,X)
      implicit double precision (A-H,O-Z)
      implicit integer (i-n)
      COMMON /PROP/ RHOG, RHOL

!     The transport properties are for R22 for the sample case

      viscl=162.6*1e-6
      viscg=12.77*1e-6
      DINNHX=0.0065

      Rel=abs(G)*DINNHX*(1-X)/viscl
      Reg=abs(G)*DINNHX*X/viscg

!      for laminar liquid and turbulent vapor flow
      C=12

      PDROPL=32*abs(G)/DINNHX**2*viscl/RHOL*(1-X)
      PDROPG=0.1582/(abs(G)*DINNHX/viscg*X)**.25*abs(G)**2/DINNHX/RHOG*X**2
      XX=(PDROPL/PDROPG)**0.5
      FISQ=(1+C/XX+1/XX**2)

      PRDROP=FISQ*32/abs(G)/DINNHX*viscl/(1-X)

      END FUNCTION
```

```
      DOUBLE PRECISION FUNCTION HTCOEFF(G)
      implicit double precision (A-H,O-Z)
      implicit integer (i-n)

      viscl=162.6*1e-6
      condl=0.08287
      hfg=181000
      hxl=6.0

      HTCOEFF=.0011*condl*G/viscl*(0.5*hfg/9.81/hxl)**0.5

      END FUNCTION

      DOUBLE PRECISION FUNCTION SLIPR(X)
      implicit double precision (A-H,O-Z)
      implicit integer (i-n)
      COMMON /PROP/ RHOG, RHOL
      SLIPR=1.0
      END FUNCTION

      DOUBLE PRECISION FUNCTION ALPHA(X)
      implicit double precision (A-H,O-Z)
      implicit integer (i-n)
      COMMON /PROP/ RHOG, RHOL
      ALPHA=1 / (1+(1-X)/X*RHOG/RHOL*SLIPR(X))
      END FUNCTION

      DOUBLE PRECISION FUNCTION ROOT(ALPH,XX)
      implicit double precision (A-H,O-Z)
      implicit integer (i-n)
      P0=XX-0.04
      P12=XX+0.04
      Y0=ALPH-ALPHA(P0)
      Y1=ALPH-ALPHA(P12)
      ERR=1.0
      Y2=1.0
      DO WHILE  ((ERR.GT.1E-7).AND.(ABS(Y2).GT.1E-7))
      DF=(Y1-Y0) / (P12 - P0)
      DP=Y1/DF
      P2=P12-DP
      Y2=ALPH-ALPHA(P2)
      ERR=2*ABS(DP)/(ABS(P2)+1E-9)
      P0=P12
      P12=P2
      Y0=Y1
      Y1=Y2
      ENDDO
      ROOT=P12
      END FUNCTION
```

The modified section of the REFPROP subroutine:

```
if (iflag.eq.0) then
      call PQFLSH  (PSG,q1,X,kq,t,D,Dl,Dv,x,y,e,h,s,cv,cp,w,ierr,herr)
      ss=w
      elseif (iflag.eq.1) then
      ha=HE(h1)
      AP1=Psg
      call PHFLSH(AP1,ha,x,Tger,RHO,RHOl,RHOv,xliquid,xvapor,q,
      +en,s,cv,cp,w,ierr,herr)
      en=HU(en)*1000.0
      RHO1=RHO*wmm
```

```
RHOv=RHOv*wmm
RHOl1=RHOl*wmm
RHOgas=RHOv
q1=q

elseif (iflag.eq.2) then
DELTAT=1.
OFACT=-1.
FACT=0.0
EN=HE(EN)
E=0.0

DO WHILE (ABS(EN-E)/EN*100.GT.1E-3)
TSG=TSG+FACT*DELTAT
call TDFLSH (tsg,D,x,p,Dl,Dv,xl,vl,q,e,h,s,cv,cp,w,ierr,herr)
call ERRMSG (ierr,herr)
OFACT=FACT
IF (EN.GT.E) THEN
FACT=+1.
ELSEIF (EN.LT.E) THEN
FACT=-1.
 IF (OFACT*FACT.LT.0.0) THEN
  DELTAT=DELTAT/2.
 ENDIF
ENDIF
ENDDO
TGER=TSG
PGER=P*1000.0
EN=HU(e)*1000.0
q1=q
RHOgas=Dv*wmm
RHOl1=Dl*wmm

elseif (iflag.eq.3) then
HA=HE(h1)
DELTAH=H1/1E6
OFACT=-1.
FACT=0.0
RHO1=DE(RHO1)
RHOF=0.0
DO WHILE (ABS(RHO1-RHOF)/RHO1*100.GT.1E-3)
HA=HA+FACT*DELTAH
call PHFLSH (PSG,HA,x,TGER,RHOF,RHOl,RHOv,xliquid,xvapor,q,
+en,s,cv,cp,w,ierr,herr)
call ERRMSG (ierr,herr)
OFACT=FACT
IF (RHO1.GT.RHOF) THEN
FACT=-1.
ELSEIF (RHO1.LT.RHOF) THEN
FACT=+1.
 IF (OFACT*FACT.LT.0.0) THEN
  DELTAH=DELTAH/2.
 ENDIF

ENDIF
ENDDO
RHO1=RHOF*WMM
q1=q
EN=HU(en)*1000.0

elseif (iflag.eq.4) then
ha=HE(h1)
DELTAP=0.3
OFACT=-1.
FACT=0.0
RHO1=DE(RHO1)
RHOF=0.0
```

```
DO WHILE (ABS(RHO1-RHOF)/RHO1*100.GT.1E-3)
PSG=PSG+FACT*DELTAP
call PHFLSH (PSG,HA,x,TGER,RHOF,RHOl,RHOv,xliquid,xvapor,q,
+en,s,cv,cp,w,ierr,herr)
call ERRMSG (ierr,herr)
OFACT=FACT
IF (RHO1.GT.RHOF) THEN
FACT=+1.
ELSEIF (RHO1.LT.RHOF) THEN
FACT=-1.
 IF (OFACT*FACT.LT.0.0) THEN
  DELTAP=DELTAP/2.
 ENDIF
ENDIF
ENDDO
PGER=PSG*1000
RHO1=RHOF*WMM
ql=q
EN=HU(en)*1000.0

elseif (iflag.eq.5) then
RHO1=DE(RHO1)
CALL TRNPRP(TSG,RHO1,1,VI,CO,ierr,herr)
RHO1=RHOF*WMM

endif
```

REFERENCES

1. Wallis, G., *One Dimensional Two Phase Flow*, McGraw-Hill, New York, 1969.

2. Yılmaz, T., *Process Technologies in Multiphase Flows*, Çeşme-İzmir, 16th to 29th August 1997.

3. VDI Heat Atlas, Association of German Engineers, VDI, Düsseldorf, 1993.

4. Berghmans, J., "Two-Phase Flows in Heat Exchanger Tubes", *Two Phase Flows With Phase Transition*, Belgium, 29 May - 1 June 1995, VKI Lecture Series, 1995.

5. ASHRAE Handbook of Fundamentals, 1993.

6. Wattelet, J.P., J.C Chato, B.R. Christoffersen, J.A. Gaibel, M. Ponchner, P.J. Kenney, R.L. Shimon, T.C. Villaneuva, N.L. Rhines, K.A. Sweeney, D.G. Allen, and T.T. Hershberger, Heat Transfer Flow Regimes of Refrigerants in a Horizontal-Tube Evaporator, ACRC TR-55, University of Illinois, Urbana, May 1994.

7. Jones, JR., and, N. Zuber, " The Interrelation Between Void Fraction Fluctuations and Flow Patterns in Two Phase Flow," *International Journal of Multiphase Flow*, Vol. 2, No. 3, pp. 273-306, December 1975.

8. Kakaç, S., and F. Mayinger, "Two Phase Flows and Heat Transfer," *Proceedings of NATO Advanced Study Institute*, Istanbul- Turkey, 16-27 August, 1976, Vol. 1,

9. Collier, J. G., *Convective Boiling and Condensation*, McGraw-Hill, London,1985

10. Collier, J. G., and R.J. Thome., *Convective Boiling and Condensation*, Oxford University Press, New York, 1994.

11. Wakeland, J.F., "Evaporator Simulation", MS. Thesis, Purdue University, 1988

12.Paliwoda, A., "Generalised Method of Pressure Drop and Tube Length Calculation With Boiling and Condensing Refrigerants within the Entire Zone of Saturation," *International Journal of Refrigeration,* Vol. 12, pp. 314-322, November 1989.

13.Domanski, P., and D. Didion., Computer Modeling of the Vapour Compression Cycle With Constant Flow Area Expansion Device, US Department of Commerce National Bureau of Standards, NBS Building Science Series No.155, May 1983.

14.Paliwoda A., "Generalised Method of Pressure Drop Calculation Across Pipe Components Containing Two Phase Flow of Refrigerants," *International. Journal of Refrigeration,* Vol. 15, No.2, pp. 119-125, 1992.

15.Karataş, H., "Bir Buzdolabı Buharlaştırıcısının Teorik ve Deneysel İncelenmesi," MS. Thesis, İstanbul Technical University, 1996.

16.Rice, C. K., "The Effect of Void Fraction Correlation and Heat Flux Assumption on Refrigerant Charge Inventory Predictions," *ASHRAE Transactions*, Vol. 93, pp.341-367, 1987.

17.Wang, H., and S. Touber. "Distributed and Non-Steady-State Modeling of an Air Cooler," *International. Journal of Refrigeration,* Vol. 14, pp. 98-111, 1991

18.Incropera, F. and D. DeWitt., *Introduction to Heat Transfer*, John Wiley & Sons, Singapore, 1990.

19.Hambraeus, K., "Heat Transfer Coefficient During Two Phase Flow Boiling of HFC-134a," *International Journal of Refrigeration,* Vol. 14, pp. 357-362, 1991.

20.Kandlikar, S.G., "A General Correlation for Saturated Two Phase Boiling Heat Transfer Inside Horizontal and Vertical Tubes," *Journal of Heat Transfer*, pp. 219-228, 1990.

21.Güngor, K.E., and H.S. Winterton., "A general Correlation for Flow Boiling in Tubes and Annuli," *International Journal of Heat and Mass Transfer*, Vol. 29, No. 3, pp. 351-358, 1986.

22.Sorensen, L.P., J.P. Fredsted, M. Willatzen, "Improvements in The Modeling and Simulation of Refrigeration Systems: Aerospace Tools Applied to A Domestic Refrigerator," *HVAC&R Research,* Vol. 3, pp. 387-403,1997.

23.Dupont, J.F., G. Sarlos, and D.M. Le Febve, "Numerical Comparison Between a Reference and Simplified Two Phase Flow Models as Applied to Steam Generator Dynamics," *Proceedings of the Second International BNES Conference on Boiler Dynamics and Control in Nuclear Power Stations 2* pp. 223-232, Bournemouth-U.K., 23-25 October, 1979.

24.Brasz, J.J, and K. Koenig., "Numerical Methods for the Transient Behaviour of Two Phase Flow Heat Transfer in Evaporators and Condensers," *Proceedings of the Second National Symposium on Numerical Properties and Technologies for Heat Transfer,* Hemisphere Publishing, pp. 461-476, New York, USA 1993.

25.MacArthur, J.W., and E.W. Grald., "Unsteady Compressible Two Phase Flow Model for Predicting Cyclic Heat Pump Performance and A Comparison With Experimental Data," *International Journal of Refrigeration,* Vol. 12, pp. 29-41, 1989.

26.Jia, X., C.P. Tso, P.K. Chia, "A Distributed Model for Prediction of The Transient Response of An Evaporator," *International Journal of Refrigeration,* Vol. 18, pp. 336-342, 1995.

27.Anderson, J.D., "*Introduction*," Introduction to Computational Fluid Dynamics, 19-23 January 1998, VKI Lecture Series, 1995.

28.Pozrikidis, C., *Introduction to Theoretical and Computational Fluid Dynamics,*, Oxford, New York, 1997.

29.Anderson, D.A., J.C.Tannehill, R.H. Pletcher, *Computational Fluid Mechanics and Heat Transfer*, McGraw-Hill, New York, 1984.

30.Hoffmann, K.A., *Computational Fluid Dynamics for Engineers*, Engineering Education System Publication, Texas, 1989

31.Peyret, R., T.D. Taylor., *Computational Methods for Fluid Flow*, Springer-Verlag, New York, 1983.

32. NIST Thermodynamic and Transport Properties of Refrigerants and Refrigerant mixtures - REFPROP, version 6.0, USA, 1998